Evaluation of the effect of polyethylene glycol incorporation on the performance of poly(lactic-co-glycolic acid) nanoparticles

Tendai Samkange

UNIVERSITY *of the*
WESTERN CAPE

A thesis submitted in fulfilment of the requirements for the degree of *Magister Scientiae* (Pharmaceutical Sciences) in the Discipline of Pharmaceutics at the University of the Western Cape, Bellville, South Africa.

Supervisor: Dr. Admire Dube

Co-supervisor: Dr. Kenechukwu Obikeze

November 2016

List of abbreviations and units

°C	Degrees Celsius
µg	Micrograms
µl	Microliters
^{125}I	Radioactive Iodine
^{1}H	Proton (Hydrogen atom)
ANOVA	Analysis of variance
AUC	Area under curve
$CDCl_3$	Deuterated chloroform
DDS	Drug delivery system
D_H	Hydrodynamic diameter
DL	Drug loading
DLS	Dynamic light scattering
DSPE	1,2-distearoyl-sn-glycero-3-phosphatidylethanolamine
EE	Encapsulation efficiency
FDA	Food and drug administration
g	G-force
GRAS	Generally regarded as safe
h	Hour
HSA	Human serum albumin
IgM	Immunoglobin M
ISO	International Organization for Standardization
kDa	Kilo Daltons
mA	Milliamps
mg	Milligrams
MHz	Mega-Hertz
min	Minute
ml	Milliliters
mm	Millimeters
MPS	Mononuclear phagocytic system
mV	Millivolts

Mw	Molecular weight
NDDS	Nanoparticulate drug delivery systems
nm	Nanometers
NMR	Nuclear magnetic resonance
PBS	Phosphate buffered saline
PDI	Polydispersity index
PEG	Polyethylene glycol
PEG-PBLA	PEG-b-poly(β-benzyl L-aspartate) block copolymer
PEG-PLGA	A co-polymer of polyethylene glycol and poly(lactic-co-glycolic acid)
PET	Poly(ethylene terephthalate)
PHDCA	Poly cyanoacrylate-co-n-hexadecyl cyanoacrylate
PLA	Poly(lactic acid)
PLGA	Poly(lactic-co-glycolic acid)
ppm	parts per million
rpm	Revolutions per minute
RSD	Relative standard deviation
SD	Standard deviation
SEM	Scanning electron microscopy
SLN	Solid lipid nanoparticles
SPIONs	Superparamagnetic iron oxide nanoparticles
TB	Tuberculosis
TEM	Transmission electron microscopy
TMS	Tetramethylsilane
UK	United Kingdom
USA	United States of America
UV-VIS	Ultraviolet visible spectra
v/v	Volume per volume
w/v	Weight per volume
w/w	Weight per weight

List of Figures

List of Tables

Peer-reviewed conference presentations

The findings reported in this thesis have been presented at the following national and international conferences:

Oral presentation at international conference:

SAMKANGE T*, OBIKEZE K & DUBE A (2016). PEGylation of Rifampicin Loaded PLGA Nanoparticles Delays Protein Binding and Modulates Drug Release. Presented at the **All Africa Congress on Pharmacology and Pharmacy** (The Congress was: the 50th anniversary of the South African Society for Basic and Clinical Pharmacology, the 6th All Africa Congress of Basic and Clinical Pharmacology, the 10th anniversary of Pharmacology for Africa, and the 37th annual meeting of the Academy of Pharmaceutical Sciences of South Africa), 5 – 8 October, Johannesburg, Gauteng, South Africa.

Poster presentation at national conference:

SAMKANGE T*, BHAWANIEPERSAD S.A, RAMA P.P, BAMBIES S, SULEMAN Y, BAKACO S, DYSON S.N, NDUMISO M, OBIKEZE K & DUBE A (2015). Size Tailoring of PLGA Nanoparticles using Composition Ratios and Stability Assessment in Human Serum Albumin. Presented at the **36th Academy of Pharmaceutical Sciences of South Africa Annual Conference and Annual Conference of the South African Association of Pharmacists in Industry**, 17 – 19 September, Johannesburg, Gauteng, South Africa.

* Indicates presenting author.

CHAPTER 1
INTRODUCTION

A drug delivery system (DDS) is defined as a formulation or a device that enables the introduction of a therapeutic substance into the body and improves its therapeutic efficacy and safety by controlling the rate and place of release in the body [1]. Nanoparticles are sub-micron sized structures and have shown great potential when applied in drug delivery [2]. This has resulted in the coining of the term: nanoparticulate drug delivery systems (NDDS). NDDS include formulations of liposomes, polymeric nanoparticles, solid lipid nanoparticles and even metallic nanoparticles.

The process of drug delivery includes the administration of NDDS, circulation and distribution of NDDS in blood, and the release of drug during circulation or at the target site. Throughout this process NDDS face the challenge of interacting with proteins, cells and other components of blood. For example, in 2013 Tenzer and co-workers observed about 300 plasma proteins rapidly binding to silica nanoparticles within 30 seconds of exposure to human plasma [3]. One of the goals of NDDS is to prolong the residence time of the drug in the body. However, it has been noticed that when proteins bind to NDDS, the nanoparticle-protein interactions contribute towards the rapid clearance of the delivery systems from systemic circulation. This clearance is facilitated by phagocytic cells of the mononuclear phagocytic system (MPS), which take up these NDDS [4].

To overcome the challenge of NDDS rapid clearance, researchers have modified the surfaces of NDDS to make them resist protein binding and therefore delay uptake by MPS cells. This strategy has worked and the systemic circulation times of NDDS have significantly improved [5, 6]. The most common technique used to modify surfaces of NDDS is the attachment of polyethylene glycol (PEG). This technique is referred to as PEGylation and NDDS that have undergone this process are referred to as PEGylated NDDS. PEGylation has proved to be successful in prolonging the circulation of drugs in the body, as there are already some PEGylated NDDS currently in clinical use. One example is Doxil®, which is a PEGylated liposomal formulation of doxorubicin, an anti-cancer drug [2, 7].

Though success has been realized with PEGylated liposomes, a lot of work still needs to be done on PEGylated polymeric nanoparticles before there is successful translation to clinical use. One of the challenges facing researchers is not knowing the optimal PEG content required for polymeric NDDS to resist protein binding. How much of the PEG is enough? This question has not yet been answered. Gref and co-workers tried to address this question and they concluded that 5% (w/w) PEG content on poly(lactic acid) (PLA) nanoparticles was sufficient for resistance of protein binding [8]. The danger with this conclusion is that it cannot be applied to all NDDS even amongst polymeric NDDS, as it has been shown that the effect of PEGylation on protein resistance depends on the nanoparticle material [9]. As a result, there is still uncertainty regarding “the optimal PEG content” of NDDS.

It is logical to assume that since the material which forms the core of the nanoparticle influences nanoparticle-protein interactions, then there might not be any universal “optimal nanoparticle PEG content”. The optimal PEG content is nanoparticle-specific; therefore, researchers have to conduct investigations on a case-by-case basis. It is also notable that most research on PEGylated NDDS focuses on nanoparticle-protein interactions, and often neglects drug release studies. In cases were drug release studies are performed, little attention has been paid to the effect of PEGylation on the release of drug payload from NDDS. Yet a holistic understanding of the *in vitro* effects of PEGylation on both NDDS-protein interactions and drug release is needed before translation to *in vivo* assessments. Despite the attempts to address this concern, the effect of PEGylation on drug release is still under studied and the few available results are contradicting. Avgoustakis and co-workers investigated the release of cisplatin from PEGylated PLGA nanoparticles and concluded that an increase in PEG content increases drug release [10]. However, Luo and co-workers recently demonstrated that PEGylation reduces the release rate of doxorubicin from PEGylated liposomes [11]. In both scenarios the focus was on anti-cancer drugs. These findings also suggest that different drugs and materials might result in differing effects of PEGylation on drug release, thus justifying the call for case-by-case investigations.

This study addressed the issues raised above. The optimal PEG content for PLGA nanoparticle protein binding resistance was investigated, as well as the effect of PEGylation on the release of a hydrophobic drug used in tuberculosis therapy

(rifampicin). Having observed that most successful research on PEGylated NDDS is focused on cancer, this study instead focused on tuberculosis (TB), another global health threat. PEGylated anti-TB NDDS can contribute towards improved formulations of current TB treatment. Rifampicin was the model drug of choice as it is one of the pillars of the currently recommended first line treatment for tuberculosis. It has been known to have a short plasma half-life and poor solubility in biological milieu, hence it would be prudent to deliver it in PEGylated nanoparticles.

Biodegradable PLGA nanoparticles with a range of PEG content were prepared. The interaction of nanoparticles with proteins in human serum was assessed, as well as the influence of PEGylation on the release kinetics of rifampicin from PLGA nanoparticles.

CHAPTER 2
LITERATURE REVIEW

In this chapter a review of the challenges encountered *in vivo* by NDDS is presented with particular emphasis on the role played by nanoparticle-protein interactions in the undesired rapid clearance of NDDS from the body. The technique of attaching polyethylene glycol on to NDDS (PEGylation) to control nanoparticle-protein interactions is discussed as a solution to this challenge. This is followed by a review on the effect of PEGylation on drug release from NDDS. Current issues with respect to nanoparticle delivery of anti-TB drugs are also discussed.

2.1 Nanotechnology and medicine

The International Organization for Standardization (ISO) defines nanotechnology as: the application of scientific knowledge to manipulate and control matter predominantly in the nanoscale to make use of size- and structure-dependent properties and phenomena distinct from those associated with individual atoms or molecules, or extrapolation from larger sizes of the same material [12].

The definition of nanoparticle comes with some nuances even amongst experts in standardization authorities. For example, On one hand, ISO defines a nanoparticle as a discrete piece of material with all external dimensions within the range of 1 – 100 nm [13]. On the other hand, ASTM International defines nanoparticles as materials with at least 2 of the dimensions ranging from 1 – 100 nm and a third dimension which can be more than 100 nm. This definition caters for nanotubes [14]. The European Commission Scientific Committees further expand the definition and state that any material is a nanomaterial when >0.15% of the material, based on number concentration, has a size below 100 nm [15]. They subdivide nanoparticles into three categories, where Category 1 are samples with a median size > 500 nm in which the lower size distribution is less likely to be below 100 nm (that is less than 0.15% of the particles are below 100 nm, if any). These are generally not considered as nanomaterials unless otherwise proven. Category 2 are samples with a median particle size between 500 nm -100 nm and are generally considered as nanomaterials as > 0.15% of the particle size distribution is most likely below 100 nm. Category 3 are

samples with a median particle size between 100 nm - 1 nm [15]. The European Commission Scientific Committees advise that particle size results factoring in particle size distribution are the most applicable [15]. The absence of consensus amongst experts indicates that the characterization of nanoparticles depends on the sample.

Particle size, particle size distribution or polydispersity index (PDI) and zeta potential (surface charge) are the three basic physicochemical properties of nanoparticles which most researchers rely on to characterize nanoparticle formulations. Particle size and PDI can be measured using the dynamic light scattering (DLS) technique. This technique measures the diffusion of particles moving under Brownian motion, and converts this to size and a size distribution using the Stokes-Einstein relationship [16]. A light from a predetermined angle is transmitted through the sample and is scattered at different intensities as particles move in a sample. This movement relies on particle size and therefore can be used to determine size and PDI [16]. The zeta potential of nanoparticles can be measured by a micro-electrophoresis technique. Upon applying an electric field to a nanoparticle dispersion, the particles will then move with a velocity related to their zeta potential. The technique enables the calculation of electrophoretic mobility from which the zeta potential can be accurately measured [16].

The application of nanotechnology in the medical field has led to the creation of the new field called nanomedicine, which like conventional medicine has a therapeutic and diagnostic side. The therapeutic part of this field focuses on the delivery of therapeutic agents as NDDS [17]. The conventional nanoparticulate drug delivery systems are liposomes, polymeric nanoparticles, micelles and dendrimers. New NDDS like inorganic nanoparticles with both therapeutic and diagnostic functions have also emerged [18-20]. Drug molecules are loaded into NDDS by adsorption, chemical conjugation or encapsulation. The desired advantages associated with NDDS include prolonged systemic circulation of the drug, sustained release, targeting of sites of infection as well as improved therapeutic and pharmacokinetic profiles of drugs [20].

2.1.1 Nanoparticulate drug delivery systems (NDDS)

NDDS research is no longer a mere academic quest, as some NDDS have reached clinical trials and others are now in clinical use [2]. Liposomal formulations of

doxorubicin (Doxil®) have been approved for clinical use by pharmaceutical regulatory authorities around the world [2, 18, 21]. A poly(lactic-co-glycolic acid) nanoparticle formulation of leuprolide (Eligard®), a drug for prostate cancer is an example of polymeric NDDS currently on the market [2, 22]. Polymeric micelles of paclitaxel are in phase II clinical trials, whilst gold nanoparticles for the delivery of recombinant human tumor necrosis factor are also in phase II clinical trials [19]. **Figure 2.1** illustrates the major NDDS and their general stages of development.

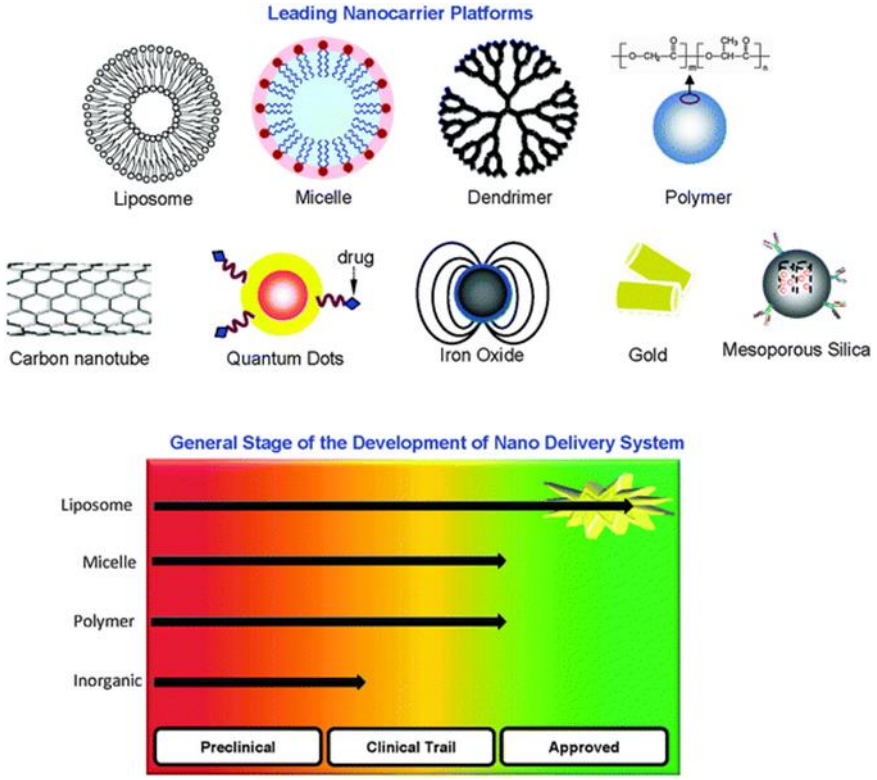

Figure 2.1 *The main nanoparticulate drug delivery systems (NDDS). The first row represents the conventional NDDS and the second row represents inorganic NDDS [19].*

Each of the conventional NDDS has its own set of challenges. Liposomes require special storage conditions and are known to be unstable under *in vivo* conditions, hence regarded as too leaky. Dendrimers are said to be expensive and the synthesis involves numerous steps which make scaling up difficult. For these reasons, polymeric nanoparticles are preferred since they are relatively easy to synthesize and have tunable drug release [19].

The use of Food and Drug Administration (FDA) approved polymers has become common in designing of polymeric NDDS as this guarantees safety and ease of registration. Polymers used for nanoparticulate drug delivery can be classified as natural, synthetic or semi synthetic polymers [23]. Synthetic polymers like poly(lactic-co-glycolic acid) (PLGA) are biodegradable and biocompatible, hence widely used in pharmaceutical applications [24-26]. On breakdown PLGA yields lactic and glycolic acid molecules. On one hand, this is makes the polymer desirable for human use as lactic acid and glycolic acid are molecules that are inherently found *in vivo*. On the other hand, this has also been identified as a limitation in cases were acid labile drugs are encapsulated by PLGA, as the acidic molecules might facilitate drug degradation [27].

However, the greatest challenge faced by all NDDS is the body itself. The physiological responses of the body to the introduction of NDDS make it difficult to achieve the ideals of nanoparticulate drug delivery.

2.1.2 Challenges in nanoparticle drug delivery

The mononuclear phagocyte system (MPS) is the greatest challenge NDDS face *in vivo*, as its role is to clear any xenobiotic material which enters the body. The MPS is made up of phagocytic cells like blood monocytes, granulocytes, dendritic cells and macrophages resident in the spleen, liver and lymph nodes [4, 8]. Inasmuch as the MPS is an excellent defence mechanism which protects the body from “perceived” danger which might come from foreign materials, it is also a hindrance to drug delivery as it causes the rapid clearance of NDDS. This clearance process is facilitated by the adsorption of proteins onto nanoparticle surfaces; in the process making nanoparticles susceptible to phagocytosis by MPS cells [4, 28-30].

The adsorption of proteins on to nanoparticle surfaces is a result of hydrophobic interactions, electrostatic interactions as well as hydrogen bonding. The outcome of these interactions is the formation of a protein corona around nanoparticles. The protein corona forms the biological identity of NDDS, which facilitates their easy

identification and engulfment by MPS cells. The protein corona is implicated in undermining the circulation time of NDDS; nanoparticle aggregation [31], loss of targeting function [32], and there have been reports of amyloidosis, a condition in which hard complexes of proteins and polysaccharides are deposited in tissues [33]. **Figure 2.2** summarises the challenge faced by NDDS *in vivo*.

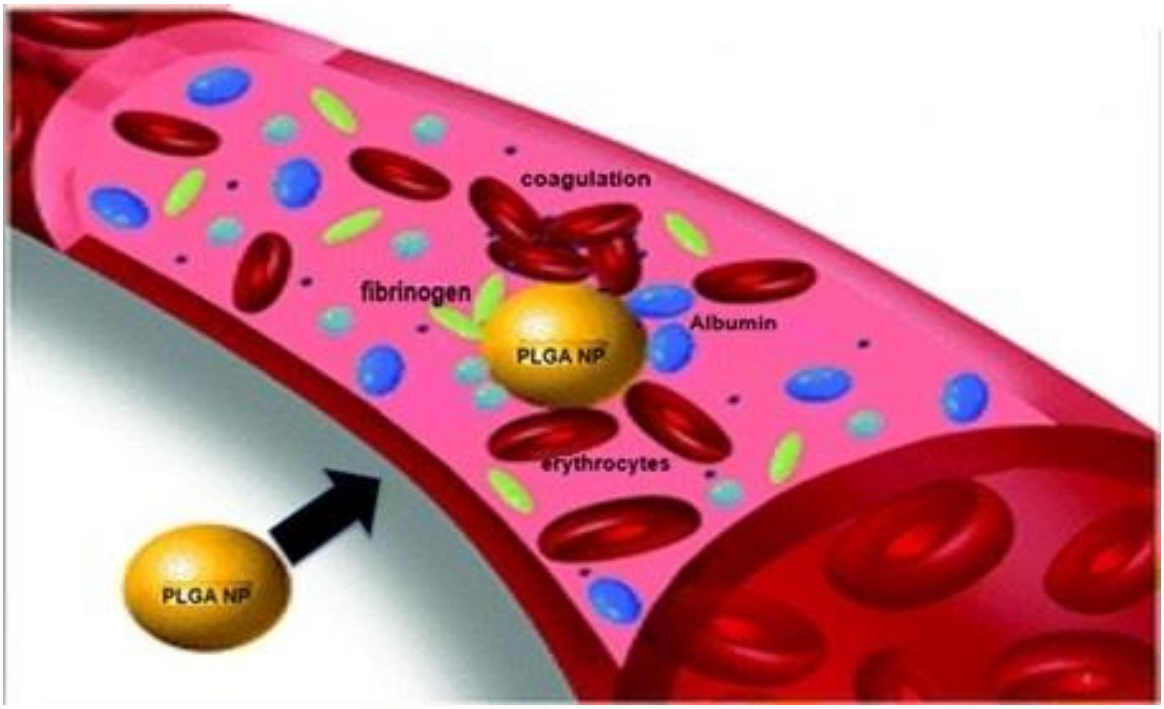

Figure 2.2 *Schematic of a PLGA NDDS in a blood vessel. Proteins, cells and other biomolecules bind to the NDDS resulting in their rapid clearance from the circulatory system [34].*

To add on to the above-mentioned problems, upon systemic administration nanoparticles can reach any organ which has a well-developed vasculature [31]. This has raised toxicity concerns and questions over the efficiency of NDDS. Some schools of thought have proven that in cases were targeted delivery of the drug payload is desired only 5 – 10% of nanoparticles reach the target destination [18, 31]. This means 90 – 95% of nanoparticles are misdirected to other destinations within the body. On the other hand, other schools of thought argue that the fraction which reaches the target site is therapeutically sufficient. To back this argument some have proven that therapeutic concentrations of the drug at the target site can be achieved by merely prolonging the blood circulation time of NDDS without the need for active targeting

[35]. For that reason prolongation of nanoparticle circulation in blood is still the frontline strategy in nanoparticle drug delivery [31].

2.2 Nanoparticle-protein interactions

2.2.1 Understanding the nanoparticle-biological interface

When a nanoparticle is in a biological medium like blood, the interface of the nanoparticle and medium is known as the nano-bio interface, and this where the protein corona forms. There are thousands of proteins in blood; about 3 700 [33] to 10 000 [36]. Yet some researchers have shown that of the thousands of proteins constituting the blood proteome only about 10 – 50 plasma proteins form the protein corona [33, 37]. On the other hand, Tenzer and co-workers detected hundreds of plasma proteins in protein coronas which formed around silica nanoparticles [3]. Despite the discrepancies and lack of consensus in literature, what is apparent is that the proteins that constitute the corona at the nano-bio interface are only a very small fraction of the total proteome in blood.

Literature agrees that the corona which forms at the nano-bio interface actually constitutes other biomolecules besides proteins. However, since proteins constitute the bulk of the corona, it is loosely referred to as the protein corona [9, 38, 39]. The corona formation process is competitive and dynamic in nature [37, 40]. Biomolecules present in the biological milieu constantly compete for the surface of nanoparticles.

2.2.1.1 The architecture of protein coronas: Hard corona *versus* Soft corona

The inner layer of proteins which strongly bind to the nanoparticle surface with a lifetime of several hours is referred to as the hard corona. It has been shown to be in slow exchange with the surrounding medium environment. Just after this layer is a pristine outer layer which is composed of a weak association of proteins that are in constant fast exchange with the surrounding medium environment [37]. This is referred to as the soft corona, illustrated in **Figure 2.3**. The significance of the soft corona has been disregarded and it is now believed that it is the hard corona that actually interacts with MPS cells as the stronger interactions result in an exposure of epitomes which bind to cell receptors [41]. More meaning of nano-bio interactions can be derived from isolating proteins that form the hard corona.

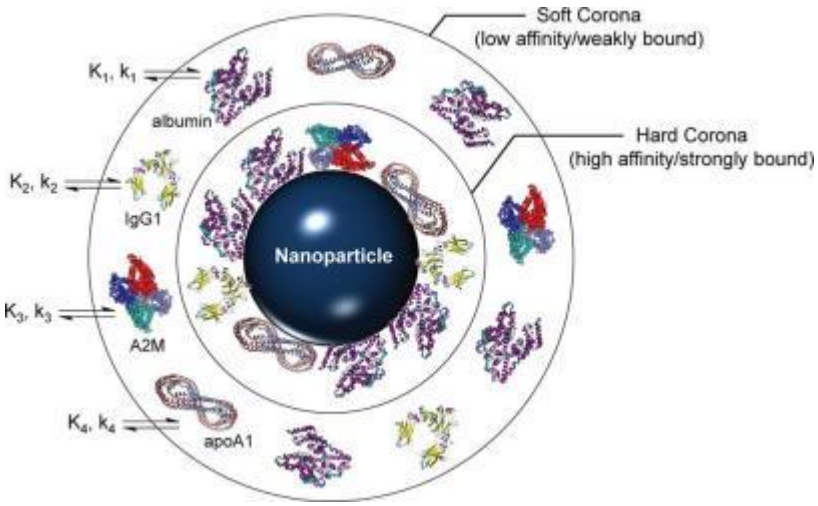

Figure 2.3 *Diagram of a nanoparticle surrounded by a protein corona, indicating the two layers that constitute the protein corona. There is a constant exchange of proteins between the corona and the surrounding medium until equilibrium is reached [42].*

2.2.1.2 The kinetics and dynamics of the nanoparticle-protein corona

The entropic nature of the nano-bio interface and the environment surrounding it calls for a need to understand the thermodynamics and kinetics involved in the formation of the nanoparticle-protein corona, as these factors determine its composition. Isothermal titration calorimetry is one of the techniques that is recommended for its ability to determine the stoichiometry, affinity and enthalpy of nano-bio interactions [43]. Understanding the kinetics of protein adsorption at the nano-bio interface helps in predicting the fate of nanoparticles in physiological environments. Since there is an interplay of quite a number of phenomena in nanoparticle-protein corona formation a complete understanding of this rather complex process is difficult. Stern and Vroman contributed in narrowing the knowledge gap by proving that at the nano-bio interface proteins that bind to the nanoparticle surface in the initial stages of corona formation are later replaced by other proteins with a higher affinity for the surface [33]. This phenomenon is known as the Vroman effect and it depends on the protein concentration, available surface area and diffusion coefficients in the biological medium [33]. The Vroman effect makes the corona constantly evolve. This reality has always made it difficult for the currently available techniques used in studying nano-bio interactions to reliably give in-depth real time details of the corona composition.

2.2.1.3 Factors that affect nano-bio interactions

Physicochemical properties of nanoparticles can influence nanoparticle protein adsorption [8] and in turn determine the composition of the protein corona [42, 44]. Yoo and co-workers reviewed literature showing that changes in physicochemical properties of nanoparticles also influence the circulation time of nanoparticles in blood [45]. Guided by these facts, a lot of work is currently underway aimed at making the *in vivo* behaviour of NDDS more predictable by controlling nanoparticle physico-chemical properties like hardness, size and surface chemistry [46].

Nanoparticle size determines curvature of the surface to which proteins bind. When a protein binds to either a flat or curved surface of the same material, the extent of conformational change from its native structure will be different. In turn, the extent to which proteins change their native conformational structure determines the quantity of proteins that bind to the surface [33]. Lacerda and co-workers in 2009 investigated the effect of particle size on adsorption of common plasma proteins onto gold nanoparticles with diameters ranging from 5 nm – 100 nm [47]. As particle size increased, a gradual increase in protein corona thickness was observed. It was also concluded that the binding constant was dependent on particle size and native protein structure. However, since these are metallic nanoparticles their conclusion cannot be broadly applied to all nanoparticles. Based on the work of Fang and co-workers [48], it appears that polymeric nanoparticles show inconsistent trends in the relationship between particle size and thickness of protein corona. In their study, Fang and co-workers did not observe any significant change in the amount of serum protein adsorbed on poly cyanoacrylate-co-*n*-hexadecyl cyanoacrylate (PHDCA) nanoparticles of three different sizes, whereas their PEGylated counterparts exhibited a change from 34% to 6% protein adsorbed, from the largest size to the smallest [48].

The influence of nanoparticle hardness on nano-bio interactions was demonstrated recently by Anselmo and co-workers [49]. They demonstrated that soft nanoparticles have persistent circulation, less opsonization and lower phagocytic uptake, compared to their hard counterparts. Though the amount of adsorbed proteins was not measured, it is logical to assume that the differences observed in their study might

have also been a result of differences in nanoparticle-protein interactions, in addition to the several other reasons they stated [49].

Regarding nanoparticle morphology and shape as factors affecting nano-bio interactions, spherical particles are more likely to be opsonized due to their high surface curvature [50, 51]. Anselmo and co-workers agree with this notion [49]. They suggested that the elongated particle shape assumed by elastic hydrogel nanoparticles could be a probable reason for their decreased uptake by phagocytic cells.

The binding, or lack thereof, observed in nano-bio interaction studies can also be a result of the nanoparticle core material binding properties. Nanoparticles made of materials with a high protein-binding affinity reach maximal protein coating within seconds to minutes [52]. Previously, Gref and co-workers had formulated nanoparticles from three polymers and demonstrated that the binding activity differed based on the type of nanoparticle core material [8]. PLGA is hydrophobic and therefore likely to exhibit high protein binding, since hydrophobic interactions are thought to be the dominant force involved in nano-bio interactions, despite the contributions made by electrostatic interactions [43]. The more hydrophobic the polymer the greater the protein affinity. Due to the high affinity for hydrophobic surfaces, when bound to hydrophobic nanoparticles, proteins have a less native structure and are more likely to denature and expose new epitopes which might change the way they interact with cells *in vivo* [53], unlike when adsorbed to hydrophilic nanoparticles. Buijis and co-workers also found a clear correlation between affinities of biomolecules for nanoparticle surfaces and extent of biomolecule conformational change, in a study were insulin was used as a model protein [54]. The greater the affinity the larger the extent of protein conformational change on binding and the greater the amounts of protein that form the corona.

To overcome the influence of nanoparticle core material in nano-bio interactions altering of surface chemistry seems to be the most favoured strategy. Molecules can be attached onto surfaces so as to reduce the binding affinity of the surface as well as alter the surface charge. The grafting of safe, approved molecule like polyethylene glycol (PEG) on to nanoparticle surfaces has yielded great results [28]. Currently, new

molecules are being tried, such as poly(amino acids), poly(glycerol) and poly(N-(2-hydroxypropyl) methacrylamide), just to mention a few [55, 56].

The extent to which each of the above-mentioned factors affect nano-bio interactions is not yet known. However, Tenzer and co-workers reported that silica nanoparticle size is dominant over surface functionalization in influencing protein corona formation [3]. They however concluded that none of the nanoparticles' physicochemical properties alone can exclusively control the formation, composition and evolution of the protein corona.

In this study, control of nano-bio interactions was achieved by altering the surface chemistry of nanoparticles. This was achieved by having the hydrophilic polymer, PEG on the surface of PLGA nanoparticles which are inherently hydrophobic. This is a process referred to as PEGylation. The presence of PEG imparts some hydrophilicity to the nanoparticle, hence lowering their protein binding affinities.

2.3 PEGylation

The modification of nanoparticle properties discussed in the previous section (Section **2.2.1.3**) has been amongst the strategies used by scientists to control protein corona formation, with the aim of prolonging nanoparticle circulation time. That is, modification of particle surface chemistry, morphology and elasticity. Other interesting innovative strategies for improving circulation time have emerged; for example, nanoparticle hitchhiking on erythrocytes. However, of all these available strategies, the modification of nanoparticle surfaces with PEG (**Figure 2.4**) was the first strategy developed for this purpose [45]. PEGylation is an over-forty year old technique, which was initially developed to 'stealth' systemically administered recombinant proteins with the aim of reducing immunological reactions against them [18, 57, 58].

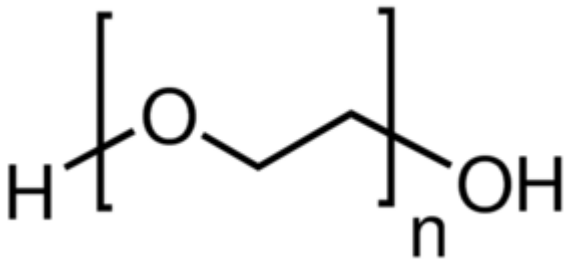

Figure 2.4 *Chemical structure of PEG [59].*

2.3.1 How are nanoparticles PEGylated?

Surface modification of NDDS with PEG has proven to be one of the most successful approaches used in sustaining nanoparticle circulation *in vivo*. Several techniques can be used to modify nanoparticle surfaces using PEG. These techniques include physical adsorption, or covalent attachment to reactive surface groups (grafting) as well as PEG incorporation during the production of the NDDS [60]. The techniques used in PEGylating polymeric nanoparticles are discussed in this section. Of the various PEGylation techniques currently available, those used in the PEGylation of polymeric nanoparticles can be broadly classified into two categories based on the stage at which PEGylation is performed. Unlike with metallic nanoparticles which are PEGylated only after nanoparticle synthesis, polymeric nanoparticles can also be PEGylated during the nanoparticle synthesis process.

2.3.1.1 PEGylation by attachment of PEG to a nanoparticle surface

PEGylation can be achieved by physio-adsorption or chemical conjugation of PEG molecules or PEG-containing molecules, onto pre-formed nanoparticles [31]. Physio-adsorption relies on electrostatic and hydrophobic interactions between the material forming the nanoparticle and PEG or PEG-containing molecules. Pluronics are an example of PEG-containing molecules that attach to nanoparticles via hydrophobic interactions [61]. Pluronics are co-polymers in which PEG is bonded to a hydrophobic chain of poly(propylene oxide). PEG-containing phospholipids have also been used to PEGylate PLGA nanoparticles [62]. Other researchers have relied on electrostatic interactions between charged nanoparticle surfaces and charged PEG-containing molecules. A cationic PEG-containing molecule can easily bind to nanoparticles with

negative zeta potentials [63]. There are cases where PEG is not necessarily incorporated onto nanoparticles after the completion of nanoparticle synthesis. For example, Booysen and co-workers incorporated PEG during the final stage of nanoparticle synthesis by using an aqueous solution containing 1% (w/v) PEG in the second emulsification step of nanoparticle synthesis, to PEGylate PLGA nanoparticles [64].

The attachment of PEG or PEG-containing molecules on pre-formed nanoparticles guarantees better drug loading, since all the PEG will be on the surface and not part of the nanoparticle core, where it could interfere with the particle's drug loading capacity [31, 61]. Unchanged nanoparticle synthesis parameters also make it an easy and attractive technique compared to other PEGylation techniques [61]. Therefore, this approach allows researchers to have better control over particle size and drug loading. However, the fact that PEG attachment in this technique is dependent on weak forces of attraction, PEG desorption might occur.

Attachment of PEG onto pre-formed nanoparticles can also be achieved by the chemical conjugation of PEG with molecules on the nanoparticle surface. This technique is commonly referred to as grafting [31]. The technique relies on the presence of tethering sites on the nanoparticle surface, which are reactive to the extent of forming covalent bonds with other reactive moieties. Walkey and co-workers grafted gold nanoparticles using thiolated, methoxy-terminated PEG [65]. The thiol group is oxidized by gold and in the process there is formation of a strong covalent bond, as illustrated in **Figure 2.5**.

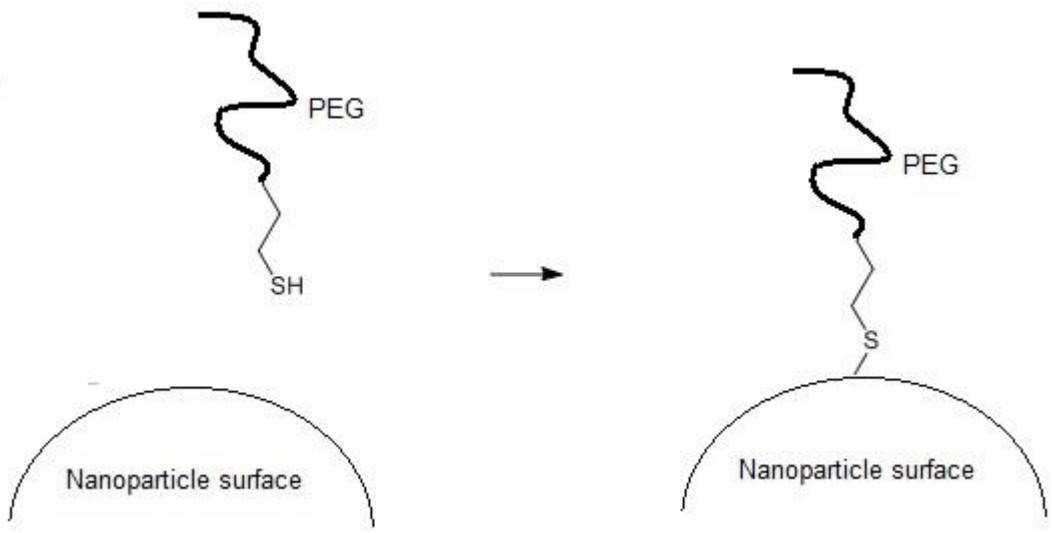

Figure 2.5 *PEGylation of a nanoparticle by grafting. A PEG molecule containing the reactive thiol group reacting with the nanoparticle surface to form a covalent bond.*

For such strong bonds to be formed, strong (high energy level) chemical reactions have to take place. This gives rise to the question of whether such reactions will not affect the structural integrity of the reacting molecules and result in the formation of new drug entities, especially when applied to polymeric nanoparticles. Indeed, there are some changes which might take place. Walker and co-workers stated that at the relatively high temperatures used in PEGylating gold nanoparticles (60 ºC) partial dehydration of PEG molecules takes place and results in conformational changes [65].

Carboxyl-modified polystyrene particles have been PEGylated by grafting with diamine-PEG [66]. A carboxyl-amine reaction results in PEG being covalently bound on the nanoparticle surface. These methods require incubation of nanoparticles in reaction solutions containing PEG molecules. In some instances, the incubation is done more than once resulting in a total incubation time of 2.5 h [66] or overnight [67]; surely drug leakage from polymeric nanoparticles is likely to take place under such circumstances.

2.3.1.2 PEGylation by synthesizing nanoparticles using PEG copolymers

This PEGylation technique relies on the use of amphiphilic PEG copolymers in the nanoparticle synthesis stage. PEG is hydrophilic and in the co-polymer it will be covalently bonded to a hydrophobic polymer. When nanoparticles are synthesized

either by an emulsification-evaporation technique or nanoprecipitation, there is spontaneous arrangement of co-polymer strands to form polymeric assemblies whose core is made up of the hydrophobic portion whilst PEG partitions to surface [68, 69]. These assemblages are later solidified to form PEGylated nanoparticles. Co-polymers of PEG with poly (lactic-co-glycolic acid) (PEG-PLGA) have been extensively used in this regard to synthesize PEGylated PLGA nanoparticles [8, 70-72]. **Figure 2.6** illustrates the chemical structure of a PEG-PLGA co-polymer.

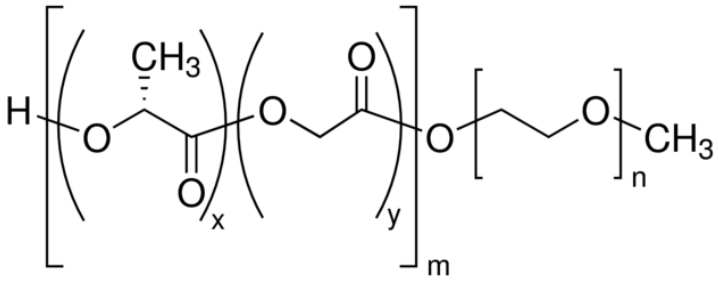

Figure 2.6 *The chemical structure of poly(ethylene glycol) methyl ether-block-poly(lactic-co-glycolic acid) [73].*

Self-assemblage of amphiphilic PEG co-polymers results in the immediate formation of polymeric nanoparticles with a stable PEG coating, since PEG remains chemically linked to the hydrophobic polymer which makes up the nanoparticle core [6], as illustrated in **Figure 2.7**. This fact makes the approach more appealing to researchers as it saves time.

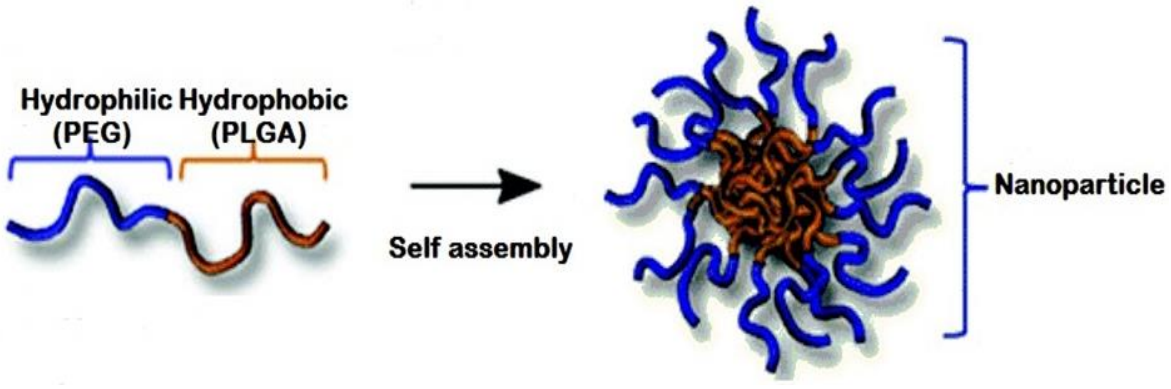

Figure 2.7 *The spontaneous arrangement of PEG copolymer strands to form PEGylated polymeric nanoparticles.*

This PEGylation technique guarantees slower PEG loss when the polymeric structure erodes and degrades [4, 70], a trait which might translate to longer circulation time *in vivo*. The technique also allows for better control of nanoparticle PEG content and density, by blending polymers and varying the composition of the total polymer mass used during nanoparticle synthesis [31]. Xu and co-workers in 2015 controlled nanoparticle PEG content by blending PLGA and PEG-PLGA co-polymers to make PEGylated nanoparticles for vaginal administration [71]. Beletsi and co-workers also blended PLGA and PEG-PLGA as a method for synthesizing PEGylated nanoparticles of predetermined PEG content [70]. An in-depth review on nanoparticle PEG content is covered in Section **2.3.3.2.2**.

On the other hand, PEGylating by self-assembly of PEG co-polymers results in low drug loading which might be due to entrapment of PEG molecules in the nanoparticle core. Spek and co-workers studied the core of PEGylated PLGA nanoparticles and found significant amounts of PEG in the nanoparticle core [74]. Their research demonstrated that not all PEG migrates to the surface of the nanoparticle during spontaneous arrangement of polymer strands in the nanoparticle synthesis process. Interestingly they also found a positive correlation between nanoparticle PEG content and the amount of polyvinyl alcohol (surfactant used in nanoparticle synthesis) entrapped in the nanoparticle core, a factor which might seriously affect drug loading in highly PEGylated nanoparticles.

The other disadvantage of using PEG-copolymers is that the covalent conjugation of PEG to another polymer results in a new chemical entity, which may be subject to a lengthy and expensive regulatory approval process for the nanomedicine [61].

2.3.2 Mechanism of “stealth” of PEGylated surfaces

As agreed in literature, PEGylated surfaces do not bind as much protein as non-PEGylated surfaces. The question which would naturally come to mind is: How do PEGylated surfaces resist protein adsorption?

The widely accepted mechanism suggests that the adsorption of proteins onto surfaces is driven by the displacement of water molecules from the surface in an

entropic manner [75, 76]. However, water tightly binds to PEG chains, with some researchers suggesting that approximately 2 to 3 water molecules bind to each ether group on a PEG chain [77], but Neil Graham claimed that it is exactly 3 molecules per ether group [78]. This property of PEG results in the entrapment of water molecules on the surface on which the PEG chains are attached, thus preventing the adsorption of proteins onto the surface [58]. The overall result is the denial of protein adsorption by steric hindrance due to the presence of a hydrated layer on the PEGylated surface [79, 80], as illustrated in **Figure 2.8**.

Other proposed mechanisms suggest that stealth is a result of the high mobility of PEG strands or a result of the lack of ionic and hydrophobic protein binding sites; as well as the possibility of having repulsive forces due to configurational entropy when a protein approaches PEG strands [75].

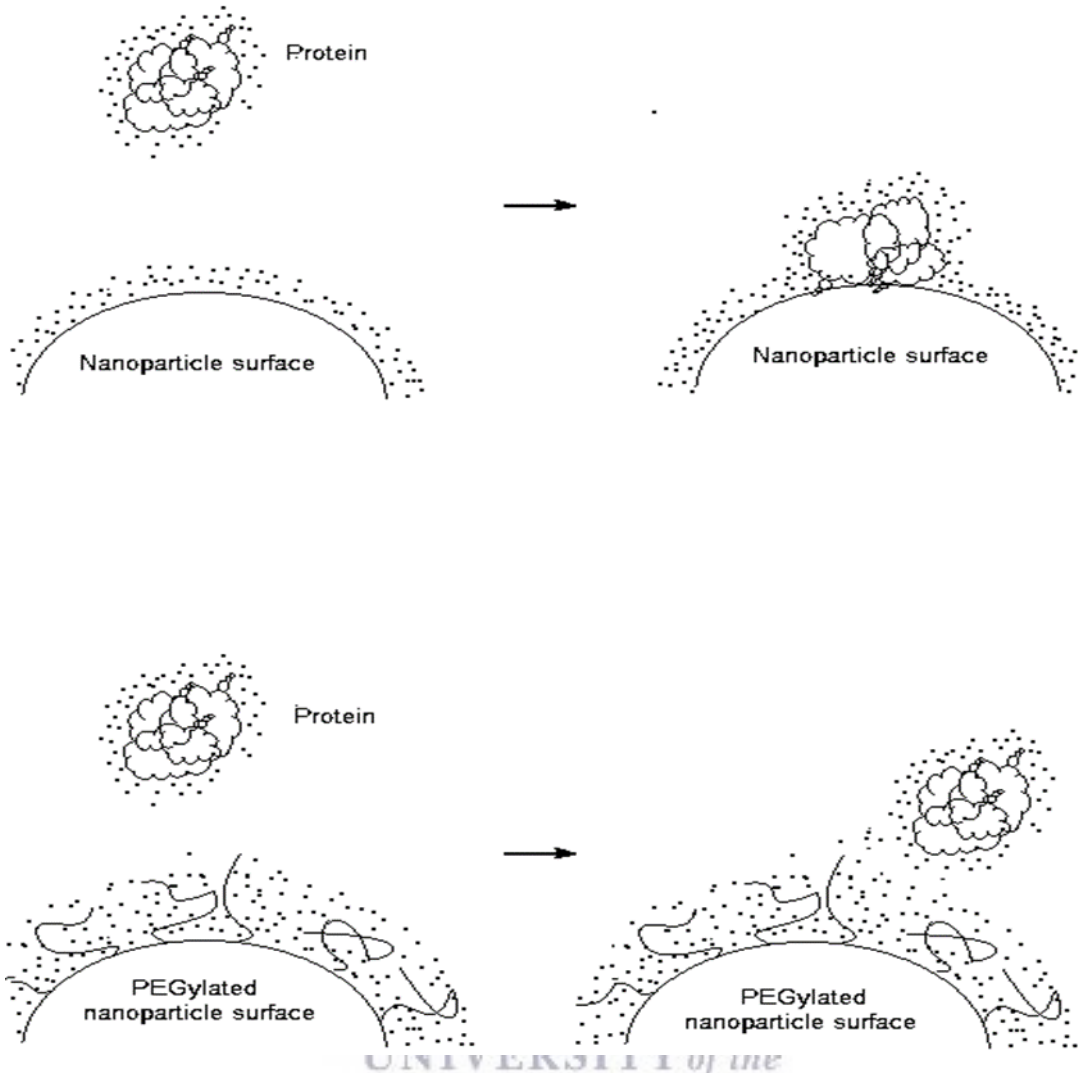

Figure 2.8 *Mechanism of stealth in PEGylated nanoparticles. Illustration of the displacement of water molecules on non-PEGylated nanoparticles and steric hindrance to protein adsorption due to the presence of PEG strands that trap water molecules and for a hydrated cloud around PEGylated nanoparticles.*

2.3.3 PEGylation and nanoparticle drug delivery

2.3.3.1 Benefits of PEGylation in nanoparticulate drug delivery

2.3.3.1.1 Prolonged circulation time and pharmacokinetics

The general consensus in literature is that the mechanism of stealth previously described in Section **2.3.2** yields increased blood circulation time of PEGylated NDDS. In liposomal NDDS similar results have been observed. PEGylation increased the blood circulation time of liposomes from 30 minutes to 5 h in a study by Klibanov and co-workers [5]. As evidenced in the case of Doxil®, which is a PEGylated liposomal

delivery system of doxorubicin. Free doxorubicin has an elimination half-life of 36 h which is increased to 72 h if it is administered as Doxil®. In his 2013 perspective on the inconvenient truths of nanotechnology in drug delivery, Park argues that though Doxil® is the commonly given example of a successfully registered NDDS, its development was not inspired by modern day nanotechnology [18].

When a comparison of the circulation times of radioactively-labelled PEGylated and non-PEGylated polymeric nanoparticles was done by Peracchia and co-workers, non-PEGylated particles were cleared from blood circulation within a few minutes, whereas PEGylated particles exhibited longer circulation with 30% of radioactivity being detected in blood 6 h after administration of labelled PEGylated nanoparticles [6]. It is also interesting to note that PEGylated particles exhibited similar circulation times regardless of PEG content and the authors suggested that studies on optimal nanoparticle PEG content be done, an issue we sought to address in our study.

2.3.3.1.2 Reduced immunogenicity

The reason why PEG is so popular in the drug delivery field is its chemical and biological inertness. On its debut, it was claimed that it lacked the ability to trigger immunological reactions and for that reason molecules and structures administered for therapeutic purposes could be “hidden” from the immune system by attaching PEG molecules [58].

A theory of accelerated blood clearance of PEGylated NDDS when administered multiple times, has been propagated and substantiated. Rapid clearance from blood circulation has been observed for PEGylated liposomes on repeated dosing in mice [81, 82]. The reduced circulation time has been attributed to the production of PEG-specific Immunoglobin M (IgM) antibodies after the first dose [83]. However, in spite of the evidence in support of this theory, PEG is still being referred to as a “bio-inert” molecule [83].

It is also interesting to note that PEG-specific IgM antibodies (anti-PEG IgMs) affect the pharmacokinetics or blood circulation half-life of PEGylated liposomes more than PEGylated polymeric micelles made of PEG-b-poly(β-benzyl L-aspartate) block

copolymer (PEG-PBLA) [84]. Accelerated blood clearance due to the presence of anti-PEG IgMs has also been observed in repeated administration of prostaglandin-E1-loaded PEG-poly(lactic acid) (PEG-PLA) nanoparticles in 5 – 7 weeks old wistar rats.

Based upon the afore-mentioned studies Shiraishi and co-workers strongly criticize the use of PEGylated NDDS as shown in the sentiment below:

"…*results show that immune-response induction against PEG strongly restricts the use of PEGylated drug carriers, owing not only to rapid elimination of PEG nanoparticles from the bloodstream, but also to PEG nanoparticles' serious side effects resulting from undesired bio-distribution* " [83].

However, there are PEGylated NDDS doing well on the market [2], and these have been shown to actually have less side effects and better bio-distribution. An example is Doxil® (PEGylated liposomal formulation of doxorubicin) which has been found to reduce cardiotoxicity and it generally significantly improves the therapeutic index of doxorubicin [7]. Shiraishi and co-workers failed to provided supporting evidence suggesting that PEGylated NDDS have "serious side-effects". Therefore, the effects of immunological reactions to PEGylated NDDS should not be generalized but rather dealt with on a case-by-case basis, especially considering that the overall interaction of NDDS and physiological systems relies much on the physico-chemical properties of the NDDS.

2.3.3.1.3 Control of bio-distribution

Peracchia and co-workers found that PEGylated PHDCA nanoparticles accumulated less in the liver compared to non-PEGylated counterparts [6]. Only 40% of PEGylated particles were detected in the liver, whereas within 180 seconds 90% of non-PEGylated nanoparticles had already accumulated in the liver of female OF1 mice. The effect of PEGylation on bio-distribution is most likely to be a result of the evasion of the MPS cells of which form a significant constituency of organs like the lung, spleen and liver. Which means that the change in bio-distribution is more of a passive process rather than an active re-distribution process to particular organs. Active re-distribution

is only achievable when other ligands meant to target specific receptors are included in the PEGylated nanoparticle architecture.

Gref and co-workers [8], are said to have been the first to work with PEGylated PLGA nanoparticles [31]. In their study they discovered that PEGylation significantly increased the circulation time of nanoparticles while reducing liver uptake compared to otherwise identical non-PEGylated PLGA nanoparticles, similar to what Peracchia and co-workers found [6].

2.3.3.1.4 Reduced toxicity

The interaction of nanoparticles with physiological systems is likely to interfere with the integrity of cells, organs and normal physiological processes. This concern has evoked a lot of enthusiasm over the toxicological consequences of nanoparticles and has led to vast amounts of research focusing on the possibility of cytotoxicity, genotoxicity, haemolysis and organ histological alterations, due to nanoparticle exposure. The toxicity of nanoparticles is as a result of the high surface charge and interactions they have with cell components [85]. The role of PEG is to minimize hydrophobic and electrostatic interactions between nanoparticles and cells of body tissues [86]. Recently, PLGA nanoparticles have been studied for their cytotoxicity against porcine brain capillary endothelial cells and no significant cell death was observed [87]. This is expected and it would have been unusual to observe dire cytotoxicity from nanoparticles made of 'Generally Regarded as Safe' (GRAS) materials like PLGA, which have been applauded for being biocompatible [31]. However, the fact that PLGA is hydrophobic might be a cause of concern, as Prabhu and co-workers state that hydrophobic interactions might result in nanoparticle agglomeration which leads to large clusters which might be potentially toxic [85].

In vitro cytotoxicity studies of nanoparticles revealed that the PEGylation of a cyanoacrylate polymer (PHDCA) reduced cytotoxicity [6]. That is, PEGylated and non-PEGylated PHDCA nanoparticles were tested for cytotoxicity in mouse macrophage cell line J774. After 1 h of incubation the cell viability of cultures exposed to non-PEGylated nanoparticles was only 20% compared to 50% in those exposed to PEGylated nanoparticles [6]. Tenzer and coworkers demonstrated that pristine silica

nanoparticles caused haemolysis when they were in contact with red blood cells [3]. PEGylated superparamagnetic iron oxide nanoparticles (SPIONs) were found to have no significant systemic toxicity, compared to their pristine counterparts [85].

2.3.3.1.5 Improved targeting

PEGylation of NDDS is thought to improve active targeting [32]. In such NDDS, a targeting moiety that is recognised and interacts with over-expressed receptors of diseased cells is attached to the surface of the NDDS. To prove that this is not just a mere concept, currently there is quite a number of nanomedicines for targeted delivery in clinical trials [88-90]. Work by Salvati and co-workers suggests that PEGylated transferrin-functionalized silica nanoparticles did not adsorb serum proteins as much as the non-PEGylated counterparts [91]. As Vllasaliu and co-workers put it, such results might be indicative of the ability of PEGylation to improve NDDS active targeting [32]. However, it is pre-mature to confidently claim that PEGylation definitely improves targeting as extensive *in vivo* research on this hypothesis is yet to be done. Some have suggested that when NDDS blood circulation time is increased, this increases the likelihood of it encountering available target receptors [31].

2.3.3.2 Factors to consider in PEGylated nanoparticulate drug delivery

2.3.3.2.1 PEG molecular weight

The molecular weight (Mw) of PEG influences the extent of protein binding [8, 58]. There is a negative correlation between PEG Mw and amount of protein bound to the nanoparticle. The logic behind this trend is that as PEG Mw increases the length of the polymer strand increases. In line with the proposed mechanism of stealth previously discussed, longer PEG strands could provide a thicker steric barrier to proteins, by entrapping more water molecules as illustrated in **Figure 2.9**. However, there is no unison in literature on the exact minimal PEG Mw sufficient to achieve maximal stealth.

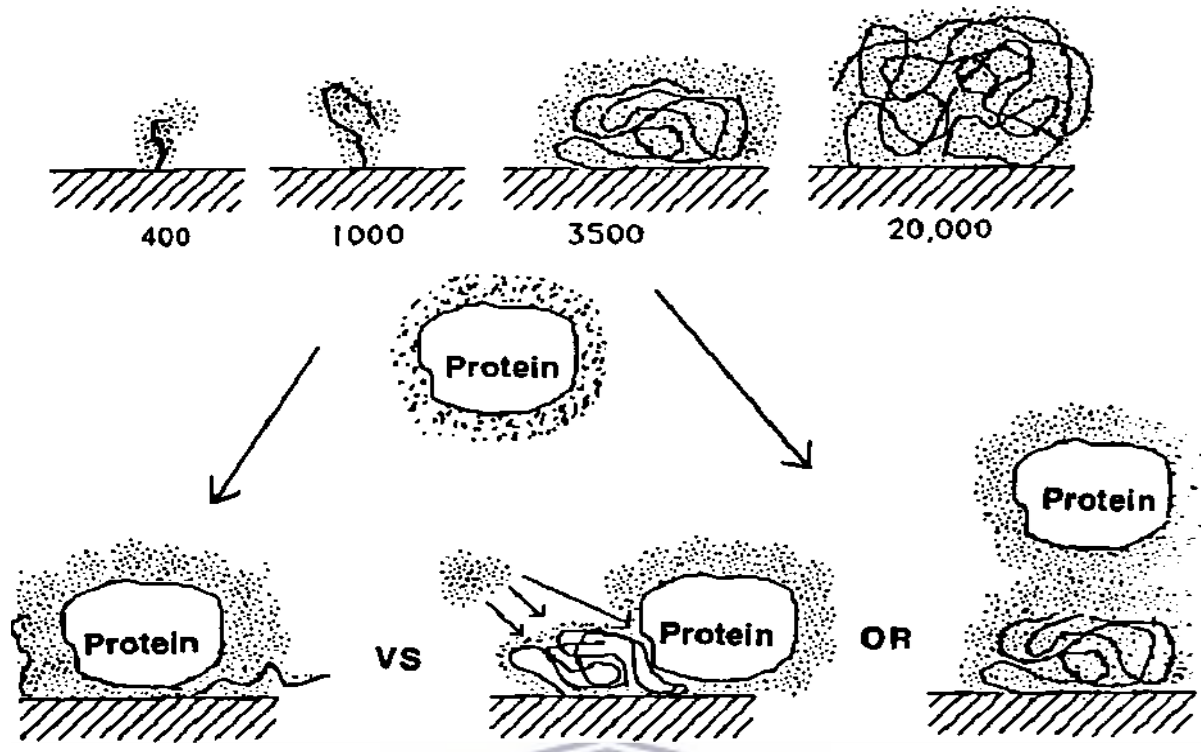

Figure 2.9 *The effect of PEG molecular weight on protein binding. Diagram shows that when the PEG molecular weight increases to an extent where the polymer strand forms a random coil that tightly entraps water molecules, it can repel protein molecules [58].*

Gref and co-workers studied amongst other parameters the effect of PEG Mw on nanoparticle protein binding [8]. They observed that for poly(lactic acid) (PLA) nanoparticles maximal stealth was attained by PEG with Mw of 5 kDa. PLA nanoparticles with PEG Mw of 2, 5, 10, 15 and 20 kDa were investigated. Between 2 kDa and 5 kDa a steep decrease in the amount of plasma protein adsorbed was observed. Beyond 5 kDa PEG there was no significant change in protein adsorption, implying that PEG Mw of 5 kDa was sufficient to provide maximal stealth under the circumstances of the investigation. But there is need to be cautious of such a conclusion, as it is possible that a molecular weight between 2 and 5 kDa could actually exhibit maximal stealth, as has been observed elsewhere [92].

Gombotz and co-workers grafted PEG of different molecular weights on to poly(ethylene terephthalate) (PET) films and traced their adsorption of ^{125}I-labelled baboon fibrinogen and bovine serum albumin [92]. Results revealed that adsorption of both albumin and fibrinogen to the PEGylated surfaces decreased with increasing

PEG Mw up to 3.5 kDa and further increases in molecular weight led to only slight decreases in protein adsorption [92]. However, it might not be safe to conclude that 3.5 kDa was the optimal PEG molecular weight to prevent protein adsorption because their gravimetric analysis results revealed that the PEG density on the films was dependent on the molecular weight of PEG. Therefore, lower molecular weight PEG strands had higher surface densities whilst high molecular weight PEG had fewer strands attached to the film surface. As a result of the differences in PEG surface density, low and high Mw PEG might have equally hindered protein binding and this can easily be misconstrued as the effect of PEG Mw.

Another study investigated the effect of PEG Mw on fibrinogen adsorption to polystyrene solid surfaces and result showed that for linear PEG molecules a Mw of 1.5 kDa was the maximum threshold for maximal reduction of protein adsorption, under the study circumstances [93].

The above cited studies reveal that the optimal PEG Mw depends on the nanoparticle core material, curvature of surfaces to which PEG is attached as well as the biological medium and it would be prudent for researchers to first carry out similar studies for each different kind of material they intend to use to engineer PEGylated NDDS. Despite all these considerations, in studies on the potential use of PEGylated PLGA nanoparticles in drug delivery, most researchers have settled for a PEG Mw of 5 kDa [70, 71, 94]

2.3.3.2.2 PEG content and density

The easiest way to control nanoparticle PEG content is through blending of polymers with PEG-copolymers at varying mass ratios. The general assumption is that an increase in PEG content will lead to a high PEG surface density which will lead to a brush conformational arrangement of PEG strands on the nanoparticle surface, hence better stealth [95, 96]. Dense PEG surface coatings help shield nanoparticles from serum protein adsorption and subsequent MPS uptake, a concept previously discussed and referred to as “stealth effect” [8, 65]. **Figure 2.10** illustrates the difference between nanoparticles with low and high PEG surface densities.

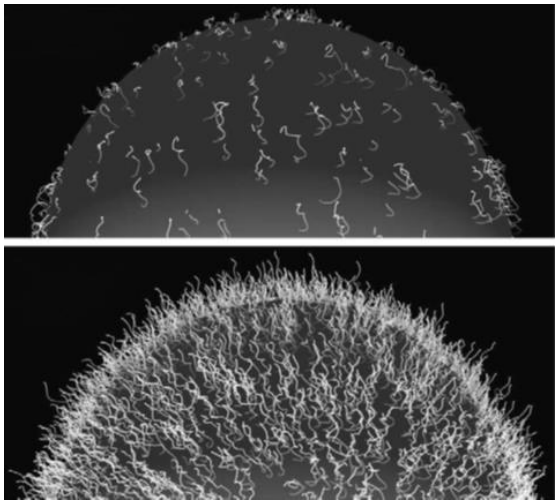

Figure 2.10 *A 3D schematic showing a nanoparticle with a low PEG surface density where the PEG strands assume a mushroom conformation (upper image) and a nanoparticle with a high PEG surface density where the PEG strands assume a brush conformation (lower image) [4].*

Gref and co-workers reported that the PEG content required to imparting maximal “stealth effect” on PLA nanoparticles is 5% (w/w) [8]. However, Xu and co-workers argue that the exact PEG content or PEG surface density necessary to impart ”stealth” on nanoparticles varies depending on the core material, nanoparticle size, PEG molecular weight and type of protein; hence Gref and co-workers’ findings cannot be applied to all NDDS [71]. Based on this premise the PEG content required to impart “stealth” on rifampicin loaded PLGA nanoparticles, is still unknown, an issue which was investigated in our study. As for liposomes the optimal plasma circulation half-life has been reported to be achieved at 2 molar % PEG content for 1,2-distearoyl-sn-glycero-3-phosphatidylethanolamine (DSPE) liposomes modified with PEG Mw = 2 kDa [97].

So much effort has been put in trying to calculate surface densities of PEG on nanoparticle surfaces yet some studies have shown that even at low PEG content nanoparticles exhibit an effective “stealth effect” against plasma proteins [8]. At such low PEG content, PEG strands will not have assumed a brush confirmation. This has triggered a debate on whether to define PEGylated NDDS by their PEG content or by their PEG surface density. Suk and co-workers argue that it is essential to accurately quantify nanoparticle surface PEG density [31]. On the other hand, research by Spek and co-worker has shown that a significant amount of PEG is found in the polymer matrix forming the nanoparticle core of polymeric NDDS and not on the surface [74].

These findings by Spek and co-workers, imply that as for polymeric nanoparticles calculating PEG surface density might be inaccurate as not all PEG strands are found on the nanoparticle surface and therefore it is rather more accurate to identify PEGylated polymeric nanoparticles with their PEG content.

Proton (^{1}H) NMR methods can be used to provide qualitative and quantitative information about the amount of PEG incorporated in nanoparticles [98, 99]. Protons in the ethylene unit of PEG produce a peak around 3.65 ppm on the ^{1}H NMR spectrum, which can be used for qualitative and quantitative analyses of nanoparticle PEG [71, 74]. The integral of the peak, that is the area under the curve (AUC) increases as PEG content increases [99]. Therefore, the AUC of the peak at 3.65 ppm can be used to confirm if PEGylated nanoparticle samples have different PEG content. Recently, Xu and co-workers went a step further and plotted a proton NMR calibration curve of PEG and used it to calculate the exact PEG content on PEGylated PLGA nanoparticles [71]. They reported that the PEG content determined by NMR was similar to the target PEG content they had aimed for when they varied the mass ratio of polymers, in the synthesis process. Xu and co-workers then determined PEG surface density by dividing the obtained PEG content with the total nanoparticle surface area of nanoparticles present in a sample. The surface PEG density was expressed as the number of PEG molecules per 100 nm^2 surface area on nanoparticles, and they assumed that all PEG strands were present on the nanoparticle surface and fully stretched to form a brush.

2.4 PEGylation and drug release – Current position

The pertinence of understanding the effect of PEGylation on drug release from NDDS lies in the fact that drug release testing is one of the quality control tools currently used in pharmaceutical formulation development [100, 101]. In addition, nanoparticle drug release is considered to be an important indicator of therapeutic efficiency [102]. Therefore, beyond understanding the effect of PEGylation on nano-bio interactions, a clear understanding of its effect on release of loaded drugs is an issue that needs further research.

There is a unavailability of a universally accepted approach in assessing NDDS drug release [102]. Several factors affect the drug release process in these drug carriers, hence making it complex to understand the extent to which each of these factors affect drug release [101]. Besides the intrinsic nanoparticle factors affecting drug release, some researchers have questioned the procedures undergone in drug release studies.

What is apparent from the review of literature on PEGylation of NDDS is that researchers are more concerned about seeking to understand nanoparticle-biological interactions so as to be able to predict the *in vivo* fate of NDDS. This is as a result of the notion that PEGylation will enable better control of the nano-bio interface and allow for better delivery of the drug cargo with the hope of realising the benefits previously stated in Section **2.3**. It is interesting to note that the role of PEGylation on the release kinetics of the PEGylated NDDS cargo is often overlooked. To the best of the author's knowledge no detailed review on such an issue is currently available. It is reasonable to ask about the effect of PEGylation on the release kinetics of encapsulated drugs from especially polymeric nanoparticles. Often-times researchers make conclusions based on empty nanoparticles yet the presence of a drug on the surface and within the core of the NDDS could alter the overall physicochemical outlook of the NDDS, thus also affecting nano-bio interactions.

Recently, Luo and co-workers reported on a first-of-its-kind study on doxorubicin-loaded PEGylated nanoparticles that are capable of light-triggered drug release. To impart an optimal near infrared (NIR) light-triggered response, 2 molar % porphyrin-phospholipid was incorporated into PEGylated liposomes' architecture [11]. Upon administration in mice the liposomes had a long blood circulation time of 21.9 h. Interestingly, PEGylation aided with drug loading but undesirably slowed the light triggered release of doxorubicin. The mechanisms behind this effect brought about by PEGylation are yet to be understood. It is probable that the hydrated cloud formed around the liposomes due to the presence of PEG might have retarded the release of doxorubicin, a hydrophobic drug. In an earlier study on PEGylated PLGA nanoparticles Avgoustakis and co-workers concluded that an increase in PEG content increases cisplatin release [10].

Once administered and prolonged circulation or targeting is achieved, PEGylated NDDS should be able to release the drug payload at an appropriate rate that ensures that the therapeutic goal is achieved [11]. It is the hypothesis of this study that the release of the drug payload can be controlled by PEGylation.

2.5 *In vitro* performance evaluation of PEGylated nanoparticles

After formulating PEGylated nanoparticles for drug delivery, the performance has to be assessed similar to conventional drug formulations. The assessment of PEGylated NDDS usually focuses on protein binding studies and nanoparticle cell interaction studies. The often forgotten assessment is that of drug release and how it is affected by PEGylation, as proven by the lack of literature addressing this issue. This study assessed the performance of PEGylated PLGA nanoparticles in terms of protein binding, nanoparticle stability in biological milieu and drug release.

2.5.1 Assessment of nanoparticle-protein interactions

As previously described, the protein corona which forms around nanoparticles in biological milieu, is complex and dynamic in nature [37, 40]. This property of protein coronas makes it difficult to study nanoparticle-protein interactions. As a result, a range of simple to complex methods for characterizing the protein corona have been developed. Approaches to assessing protein coronas include monitoring of particle size and/or charge after incubation in biological milieu. In this approach transmission electron microscopy (TEM) or dynamic light scattering (DLS) techniques can be employed [103]. Other approaches provide qualitative and quantitative proteomic data in which a range of analytical techniques are employed, for example fluorescence and ultraviolet-visible spectroscopies, isothermal titration calorimetry, size-exclusion chromatography, circular dichroism spectroscopy, quartz crystal micro balance, surface plasmon resonance, infrared and Raman spectroscopies, mass spectrometry and atomic force microscopy, are amongst the techniques [33, 37, 40, 43]. Quantitative data obtained from some of these techniques can be used for kinetic modelling of nanoparticle-protein interactions [3].

Considering the rising need for knowledge of the *in vivo* identity of NDDS, a technique has to be robust, easily accessible and high throughput, where possible [40]. Fluorescence techniques and circular dichroism spectroscopy are easily accessible, whilst techniques like mass spectrometry and surface plasmon resonance highly specialized techniques [40].

There seems to be a general protocol used to assess nano-bio interactions. The technique used then depends on the stage and objectives of assessment. The first stage is the incubation of NDDS in a biological medium like serum, immediately after which particle size growth can be monitored with DLS or TEM [71]. Fluorescence spectroscopy can also be used at this stage to determine the reduction of the intrinsic protein fluorescence or an attached fluorophore, upon binding to nanoparticle surfaces. The change in the maximum of the fluorescence emission spectrum intensity arises from conformational changes of proteins upon binding to nanoparticles [33]. This change in fluorescence can be referred to as fluorescence quenching and can be used to quantify protein binding efficiency. UV-VIS spectrophotometry and circular dichroism can also be used at this stage. Though most of the techniques used at this stage suffer the limitation of spectral interference from some nanomaterials, they are accredited for their ability to directly measure the adsorption process in the presence of the free unbound proteins [104].

Researchers go beyond the first stage when a qualitative and quantitative elucidation of the hard corona proteins is required, hence the second stage aims at removing unbound proteins, if need be. Centrifugation is employed at this stage, after which some researchers analyse particle size with DLS [105]. In the third stage, bound proteins forming the hard corona are harvested through forced elution with denaturing agents [38, 106]. This leads to the fourth stage, in which the eluted proteins are separated using chromatographic [43] or electrophoretic techniques [104]. If need be, the final stage involves protein identification using mass spectrometry [107].

2.5.2 Assessment of *in vitro* drug release from nanoparticles

Several *in vitro* techniques have been developed for the assessment of NDDS drug release studies. These can be categorized as: sample and separate techniques,

membrane-based techniques, continuous flow techniques and in situ techniques [101, 102]. The universal limitation of having numerous techniques for assessing drug release is the lack of a universally acceptable technique. This is a reality which has made it difficult to standardize *in vitro* drug release assessments of NDDS.

Membrane based techniques seem to be the most popular because of guaranteed separation of nanoparticles and the sampled release medium [100, 108]. Nanoparticles are entrapped in a dialysis membrane and immersed in release medium. Membrane pores do not allow passage of nanoparticles. At set time points the amount of drug in the release medium is analysed. In addition, the technique is said to be cost effective. On the other hand, membrane-based techniques are criticized for the membrane acting as a drug release rate modulator, which might lead to incorrect conclusions of controlled release even in cases where there is none [109, 110]. As a result, there might be need for mathematical corrections to cancel out the effect of the membrane.

In sample and separate techniques, a sample of release medium in which nanoparticles are suspended is collected and the particles separated from the medium using either centrifugation or filtration methods, after which the medium is analysed for drug. This approach allows for the direct investigation of drug release without membrane interference. However, some researchers say that it is too aggressive an approach, and might result in the forced release of drug during centrifugation [102, 111].

In situ and continuous flow techniques are uncommon techniques as they require special detection methods which might be costly [109, 112].

2.5.2.1 Analysis of drug release data

After collecting relevant data at pre-set time points of drug release studies, the data is collated and concentration against time graphs are plotted. The plotting of drug release profiles is considered to be the simplest approach to understanding the release behaviour of a drug delivery system [113]. Statistical analysis, mathematical models and model-independent methods can also be used to determine the release kinetics

and/or mechanisms of release. Each of these approaches has limitations, and some approaches have even been deemed pharmaceutically irrelevant and are not recommended by pharmaceutical regulatory authorities like the FDA. For example, the use of analysis of variance (ANOVA) in statistical analysis of drug release data has been criticized by Zhang and co-workers [113]. Zhang and co-workers argue that in cases were drug release profiles are compared, ANOVA analysis sometimes addresses statistical sameness and not pharmaceutical sameness. They say that there are cases where compared profiles are clearly different but an ANOVA statistical analysis will indicate similarity [113]. This might be fatal in cases were the drug has a narrow therapeutic window.

Mathematical modelling of drug release data has been used to explore the effect of NDDS parameters on drug release, as well as elucidate the mechanism of release. The unfortunate outcome of the application of modelling in drug release assessment is that numerous mathematical models have been produced [102]. Some of these models' relevance and sufficiency in meaningfully interpreting drug release data has been questioned [114, 115]. The other limitation is the fact that mathematical models rely on experimental data and it implies that as long as there is no standardization of procedures for drug release studies different release kinetics and mechanisms might be inferred from release data of the same NDDS obtained in different experimental settings.

When modelling, different models are tried on the collected drug release data and based on the selection criteria the model which fits well with the data can be established. The model which better suits the selection criteria is referred to as the model of best fit. On one hand, there are models that can only describe the overall shape of the drug release profile without any kinetic basis, these are referred to as empirical models [116]. On the other hand, there are those models that go beyond describing the shape of the curve but also elucidate on the mechanism of release, these are called semi-empirical models [116]. Some of the semi-empirical models that have been used to describe drug release from polymeric nanoparticles are: Peppas-Sahlin (**Equation 2.1**), Korsmeyer-Peppas models (**Equation 2.2**) and Weibull (**Equation 2.3**).

$$Q_t = k_1 t^m + k_2 t^{2m}$$ **Equation 2.1**

Where k_1 and k_2 are constants of diffusion and polymer relaxation, respectively; and m is the diffusional exponent for a device of any geometric shape which inhibits controlled release [113, 117].

$$Q_t = kt^n$$ **Equation 2.2**

Where k is the release constant incorporating structural and geometric characteristics of the drug-dosage form. n is the diffusional exponent indicating the drug-release mechanism [113]. In this model the magnitude of the exponent, n is used to describe the mechanism of release. When $n < 0.43$ release is said to be via Fickian diffusion of the drug molecules from the polymeric matrix. A value within the range of $0.43 < n < 0.85$ is indicative of an anomalous release fashion which is characterised by diffusion and polymer relaxation and swelling. When $n > 0.85$ this is referred to as a super case II scenario which is pre-dominantly polymer matrix erosion and relaxation [113, 117].

$$Q_t = 100\left(1 - e^{-tb/a}\right)$$ **Equation 2.3**

Where α is the scale parameter which defines the time scale of the process; b is the shape parameter which characterizes the curve [113]. Interpretation of this model is based on the value of b. When b is ≤ 0.75 the mechanism is Fickian diffusion; for $0.75 < b < 1$ it is a combined mechanism, and for $b > 1$ the drug is released through a complex mechanism [113, 117].

In all models, Q_t is the fraction (%) of drug released in time t [113].

Recently in 2016, Khan and co-workers modelled the release profile of bendamustine from PEGylated PLGA nanoparticles and Korsmeyer-Peppas model was the model of best fit [72], while Silveira and co-workers modelled the release profile of lapazine from PLGA nanoparticles and the model of best fit was the Higuchi model [94].

Factors that affect drug release from polymeric nanoparticles include length of the diffusional path of drug molecules, matrix erosion due to polymer degradation, solubility of drug, as well as drug localization [100]. In spite of the numerous models proposed in literature, none of the models take into consideration the effect of PEGylation on nanoparticles, a parameter that can affect drug release. In other words,

semi empirical models fail to take into account the effect of different physicochemical properties of nanoparticles. For example, the fact that polymers degrade at different rates in specific drug release media has been overlooked. With semi-empirical models, drug release from biodegradable polymeric NDDS made of poly(lactic-co-glycolic acid) is said to be controlled by matrix erosion rather than diffusion of the drug within the matrix equation [100]. On the other hand, Corrigan and co-workers argue that the duration of most drug release studies are not sufficient for erosion to become the dominant release mechanism especially when the relatively short duration of most drug release studies is considered [118]. They went on to propose a mathematical model specifically for PLGA microparticles and nanoparticles drug release.

A consideration of the different physicochemical properties would mean that for every material used to design NDDS there has to be a unique mathematical model to more accurately evaluate and predict the release behaviour of that particular NDDS. However, such an approach is tedious and has made researchers rely mostly on semi-empirical models that can be applied generally. In light of these limitations, all models cannot be regarded as precisely accurate, but they are still useful [119, 120]. They are a useful tools in predicting drug release mechanisms and kinetics, but are not yet heavily relied on.

2.6 Nanoparticle drug delivery and tuberculosis

Tuberculosis (TB) is one of the world's deadliest communicable diseases, and as of 2015 it had an estimated worldwide incidence of 10.4 million people and a death toll of 1.4 million [114]. Though experts say TB incidence is slowly declining, the death toll from the disease is still unacceptably high, especially considering the fact that most deaths from TB are preventable [121]. Several interventions have been proposed, with the overall aim of making TB therapy patient-friendly and more efficient. Amongst such interventions is the delivery of anti-TB drugs in biodegradable nanoparticles that can circulate longer in blood and release drugs at a controlled rate [122-125].

2.6.1 State of the art: Nanomedicines for tuberculosis

Currently, there are no registered nanomedicines for the treatment of tuberculosis. Most of the work is still lab based and only proof of concept data has been provided. Upon infecting a host organism, *Mycobacterium tuberculosis* resides within macrophages. Unfortunately, current conventional therapy reaches these infected cells in low concentrations due to rapid clearance. This challenge has prompted researchers to develop anti-TB NDDS for the delivery of conventional drugs with the hope of increasing drug concentrations in infected macrophages. Some researchers have opted for the intracellular targeting of these macrophages, a task which is proving to be daunting [23, 125]. Others have opted for the development of long circulating NDDS [64, 126] as it has been proven that a sustained high extracellular concentration of anti-TB drugs will result in an increase in macrophages' intracellular drug concentration [127].

Liposomal NDDS for anti-TB drug delivery have been investigated in a number of studies. However, their instability and low drug loading efficiency due to leakage limits their use [125]. On the other hand, solid lipid nanoparticles (SLN) have also been investigated [128], but researchers are not keen on solid lipid NDDS in anti-TB drug delivery because of high pressure-induced drug degradation, the coexistence of different lipid modifications and different colloidal species in a sample and the low drug-loading capacity associated with SLN [129].

Polymeric NDDS are favoured for anti-TB drug delivery because polymers can be readily engineered for improved drug loading, release rate, pharmacokinetics and targeting [64, 130]. That being said, it has to be noted that PLGA is still the favoured polymer in anti-tuberculosis polymeric nanoparticulate drug delivery [64, 131-133].

2.7 Conclusion

From this review of literature, knowledge gaps can be identified. For example, it is clear that the optimal PEG content required for PLGA nanoparticles to have maximal resistance to blood protein binding is still not clear. Those that attempted to address this concern used empty nanoparticles, yet the presence of drug can change the

physicochemical properties as well as the biological interactions of NDDS. More meaning can be derived from studies on PEGylation of NDDS if a holistic approach is taken. That is, in addition to evaluating the nano-bio interactions of empty PEGylated NDDS similar evaluations on the drug loaded counterparts have to be done, as well as drug release studies. Understanding this effect can help tailor NDDS whose drug release can be controlled by PEGylation.

CHAPTER 3
WORK PLAN

3.1 Problem statement

The rapid clearance of NDDS is a challenge that can be solved by PEGylation of the delivery devices. Extensive studies have been done to understand nano-bio interactions and the effect of PEGylation on these interactions. However, the optimal PEG content for maximum resistance to protein adsorption is still not known. It is unlikely that a universal PEG content for NDDS exists, due to the differences in physicochemical properties. The presence of a drug in the NDDS is expected to alter the physicochemical properties of the NDDS. Similarly, PEGylation is likely to affect drug release from PEGylated NDDS. A thorough *in vitro* evaluation of NDDS-protein interactions and drug release kinetics from PEGylated NDDS is needed.

3.2 Hypothesis

It was hypothesized that:
The content of PEG on PLGA nanoparticles modulates protein binding and drug release.

3.3 Objectives

The overall aim was to synthesize and characterize empty and rifampicin-loaded PLGA nanoparticles with varying PEG content:

1. To evaluate nanoparticle colloidal stability in human serum.
2. To evaluate the binding of serum proteins to nanoparticles of different PEG content.
3. To characterize the *in vitro* release of rifampicin from the PLGA nanoparticles of different PEG content.

3.4 Why poly(lactic-co-glycolic acid) (PLGA) nanoparticles?

Polymeric nanoparticles are preferred to liposomes as NDDS, since liposomes have limitations of formulation instability and drug leakage [125]. PLGA was the polymer of

choice since it is FDA approved and is unique for its bio-degradation to lactic acid and glycolic acid, which are endogenous compounds found in the body. In addition to PLGA nanoparticles being the most studied NDDS, they generally have a high drug loading capacity, are biocompatible as they have low toxicity and also have a versatile structure that allows surface functionalization [87].

3.5 Why PEG and why vary nanoparticle PEG content?

Though concerns have been raised over PEG not being as inert as its pioneers suggested, it is still the stealth polymer of choice and is safer to use compared to the recently proposed PEG alternatives like poly(amino acids) and poly(gylcerol) [55, 56], which are not extensively studied. Therefore, PEG was selected since it has been extensively studied and PEGylated NDDS are currently in clinical use without any serious concerns being raised over the production of anti-PEG antibodies.

Distinct nanoparticle-specific protein-binding profiles have been observed in other studies [3]. Therefore, this is the rationale upon which this study was based. The logic is that by varying PEG content different protein binding behaviour would be observed, as well as different drug release kinetics. Knowledge of such differences, if any, could be used to tailor NDDS specific-for-purpose. Knowledge of the effect of physico-chemical properties on nanoparticle-protein interactions and drug release can be used to create NDDS libraries that can be referred to in future. This will save time when redesigning or reformulating NDDS.

3.6 Why human serum?

Human serum is a biologically relevant medium. Concerns have been raised over the use of biologically irrelevant milieu in some *in vitro* studies on nanoparticle biological behaviour [102]. The use of single-protein milieu or animal sera might not give a true indication of nanoparticle *in vivo* behaviour in humans. Ideally, the best biological medium would have been human blood. Unfortunately, blood is too opaque for analysis on DLS and contains too many particles that violate all assumptions of the DLS technique. Blood can only be analysed on DLS after it has been diluted and lysed with chemicals like Triton-X, which might interfere with nanoparticle-protein

interactions [134]. Some researchers have opted for human plasma [3] but the possibility of coagulation and use of anti-coagulants like heparin [135] is also a limitation in such studies. In this study, human serum purchased from Sigma Aldrich was used and no ethical approval was required.

3.7 Limitations and significance of the study

This study was performed in a static biological system that does not address the highly dynamic and reactive nature of real physiological systems. For example, NDDS might flow at relatively high speeds of 60 cm per second in the aorta, in a lateral and turbulent manner [3]. Mimicking these conditions *in vitro* can be challenging. Therefore, this study may not be totally representative of the *in viv*o situation.

There are other factors that affect drug release such as: drug solubility, nanoparticle size, drug loading, and diffusivity [118]. The challenge is on quantifying the extent to which each of these factors influence the rate of release. Considering the nature of this study where the effect of a change in PEG content on nanoparticle drug release was the aim, it is difficult to factor out the effects of other factors which might influence drug release as well as nanoparticle-protein interactions. This challenge of confounding factors is brought about by the spontaneous nature in which nanoparticles are formed, which leads to heterogeneity even within the same batch [60]. The greatest challenge is in keeping all the possible confounding factors equal and yet only vary the PEG content of nanoparticles.

On the other hand, such studies help in establishing NDDS-specific optimal PEG contents for resistance to protein binding. Varying nanoparticle PEG content could gradually change the chemical composition of the nanoparticle surface. This in turn could influence nanoparticle-protein interactions up to a PEG content at which maximal resistance to protein binding is achieved.

The study also gives insight on the effect of PEGylation on drug release of a hydrophobic drug from a hydrophobic nanoparticle core, thereby provoking the idea of the possibility of controlling drug release from NDDS via PEGylation. Such an idea can also be applied in liposomal drug delivery systems, which are known to be leaky.

It is studies like these, from which NDDS libraries can be built and used for future reference.

CHAPTER 4
NANOPARTICLE SYNTHESIS, CHARACTERIZATION AND PROTEIN INTERACTIONS

This chapter describes the synthesis and characterization of empty and rifampicin-loaded PLGA nanoparticles with a PEG content of 0% - 17% (w/w). Further, their behaviour in human serum is also evaluated and results are discussed.

4.1 Hypothesis and aims

In this part of the study, it was hypothesized that varying the content of PEG on nanoparticles would affect their physicochemical properties as well as the extent to which they interact with proteins in human serum. The end-goal was to determine the minimal PEG content required for maximal resistance to protein binding. Therefore, the aims of this part of the study were to:

i) Synthesize empty and rifampicin-loaded PLGA nanoparticles with PEG content ranging from 0% - 17% (w/w).

ii) Determine the effect of PEG content on nanoparticle size, polydispersity index (PDI), zeta potential, morphology and drug loading.

iii) Determine the effect of PEG content on colloidal stability of nanoparticle-human serum dispersions.

iv) Quantify the extent (fluorescence quenching efficiency) to which nanoparticles bind to human serum albumin, and evaluate how it is affected by nanoparticle PEG content.

4.2 Materials

4.2.1 Consumables

Solvents and reagents: Acetone (Sigma Aldrich, USA); Ascorbic acid (99%) (Sigma Aldrich, USA); Carbon dioxide (Afrox, South Africa); Chloroform 99% (B&M Scientific, South Africa); Distilled water (Millipore, Milford, MA, USA); Deuterochloroform (99.8 atom % D, with 1% TMS) (Sigma Aldrich, USA); Ethyl acetate (≥ 99.5%) (Sigma Aldrich, Germany); Human serum concentrate (Sigma Aldrich, USA); Phosphate buffer powder (Sigma Aldrich, USA); Poly(D,L-lactide-co-glycolide) (M_w = 30 000 – 60

000, Lactide:Glycolide = 50:50) (Sigma Aldrich, USA); Poly(ethylene glycol) methyl ether-block-poly(L-lactide-co-glycolide) (PEG average M_n = 5 000, PLGA average M_n 25 000) (Sigma Aldrich, USA); Poly(ethylene glycol) methyl ether-block-poly(lactide-co-glycolide) (PEG average M_n = 5 000, PLGA M_n = 55 000) (Sigma Aldrich, USA); Polyvinyl alcohol (PVA) Mw 31,000 Da,86.7-88.7 mol % hydrolysis, 10.0 - 11.6% residual content of acetyl ((Mowiol® 4–88), Sigma Aldrich, South Africa); Rifampicin powder (HPLC grade, ≥ 97%) (Sigma Aldrich, China).

Other consumables: Centrifuge tubes (Biologix, USA); Cuvette Micro PS (Lasec, South Africa); Disposable 12 mm square polystyrene cuvettes (Malvern, UK); Disposable polystyrene low volume cuvette (minimum volume 50 µL, compatible with Zetasizer Nano ZS90) (Malvern, UK); Disposable folded capillary cell (Malvern, UK); Graduated micro-tubes (SSI, USA); Hypodermic needles (Lasec, South Africa); Nylon 0.45 µm syringe filters (25 mm, StarLab Scientific); Nylon 0.22 µm syringe filters (KimLab, South Africa); Microplate (96 well, flat-bottom) (Greiner Bio-One, Germany); Pipettes – 20, 200 & 1000 µl (Lasec, South Africa); Pipette tips - 200 and 1000 µl (Bio-smart Scientific,UK); Protein Lo Bind tubes (Eppendorf, Germany); UV quartz cuvettes 10 mm pathlength (Z276669, Sigma Aldrich, South Africa)

4.2.2 Equipment

The following equipment were used:

Upright ultralow -86°C freezer (NU-9668E, NuAire, USA); Analytical balance (Mettler®, model PE 6000); Centrifuge (Digicen 21, Orto Alresa, United Scientific); Fluorescence micro-plate reader (Synergy Mx, BioTek Instruments, USA); Freeze-dryer (Virtis, Freeze mobile model 125L); Malvern Zetasizer NanoZS90 (Malvern instruments, Ltd., UK); NMR spectrometer (Bruker Avance IIID Nanobay, Bruker BioSpin GmbH, Rheinstetten, Germany); Probe sonicator (Sonoplus GM 2070, Bandelin, Germany); pH meter (Basic 20, Lasec, South Africa); Rotary evaporator (Büchi, Labotec, South Africa); Sputter coater (Emitech K550X, England); Scanning electron microscope (Auriga HR-SEM F50, Zeiss, South Africa); Scientific balance (Ohaus®, model GA 110); Thermomixer (Comfort, Eppendorf, Germany); UV-Visible spectrophotometer (Cintra 202, GBC Scientific Equipment, Australia); Vacuum pump

(Rocker, Singhla Scientific, Haryana, India); Vortex mixer (VM-400, Gemmy Industrial Corp., Taiwan); Water bath (Labcon®, model CDH 110 Maraisburg, South Africa).

4.3 Methods

4.3.1 Preparation of PLGA nanoparticles with varying PEG content

Six nanoparticle formulations were prepared by blending PLGA and PEG-PLGA co-polymers to achieve nanoparticle PEG contents ranging from 0 – 17% (w/w), as 17% was the maximum PEG content which could be obtained from the polymers used (**Table 4.1**).

Table 4.1 *Illustration of how nanoparticle PEG content was varied. Desired PEG contents were achieved by blending various ratios of a di-block copolymer of PLGA and polyethylene glycol of Mw = 5 kDa (PEG_{5k}-PLGA) with PLGA or another di-block copolymer of PEG_{5k}-PLGA containing PLGA of a different molecular weight. Total mass of polymer(s) used in nanoparticle synthesis was maintained at 50 mg*.

Target PEG content %(w/w)	**Composition of total mass of polymer(s) used in nanoparticle synthesis**		**Mass ratio of P1 : P2**	
	Polymer 1 (P1)	**Polymer 2 (P2)**	**P1 (mg)**	**P2 (mg)**
0	PLGA	-	50	-
2	PLGA	PEG_{5k}-$PLGA_{55k}$	40	10
5	PLGA	PEG_{5k}-$PLGA_{25k}$	35	15
8	PEG_{5k}-$PLGA_{55k}$	-	50	-
13	PEG_{5k}-$PLGA_{25k}$	PEG_{5k}-$PLGA_{55k}$	25	25
17	PEG_{5k}-$PLGA_{25k}$	-	50	-

PEG content was calculated using **Equation 4.1**.

$$\%\ PEG\ content = \frac{(PEG\ Mw\ ratio\ in\ P1 \times P1\ \text{mass}\ in\ blend) + (PEG\ Mw\ ratio\ in\ P2 \times P2\ \text{mass}\ in\ blend)}{Mass\ of\ polymer\ blend} \times 100$$

Equation 4.1

Where, ***PEG Mw ratio*** is the quotient of the molecular weight of PEG compared to the overall molecular weight of a PEG copolymer. ***P1*** *and* ***P2*** are polymers that constitute a polymer blend used for nanoparticle synthesis.

Illustrated in **Table 4.1** are polymer masses used to achieve the desired PEG content. The emulsification-evaporation technique reported previously by Dube and co-workers [132] as well as Xu and co-workers [71] (adjusted accordingly) were used to synthesize the nanoparticles. PLGA and PEG-PLGA co-polymer at determined ratios (total weight = 50 mg) were dissolved in 2 ml of chloroform and probe sonicated where necessary to allow complete dissolution, then poured into 20 mL of 1% (w/v) PVA aqueous solution under probe sonication (80% amplitude) for 2 min over an ice bath. The resultant emulsion was transferred into a round bottomed flask and chloroform was removed by evaporation under reduced pressure at 40 ˚C for 1 h. Nanoparticles were collected by centrifugation at 4 109 x *g* (5 000 rpm) for 1 h at 25 ˚C and thereafter washed thrice with distilled water and freeze dried. To synthesize rifampicin-loaded nanoparticles the same procedure described above was used. However, 5 mg of rifampicin was dissolved together with the polymer blend in 2 ml of chloroform. All nanoparticles were synthesized in triplicates.

4.3.2 Characterization of nanoparticles

After washing, nanoparticles were suspended in distilled water and 1.5 ml of the nanoparticle suspension was transferred to a disposable 12 mm square polystyrene cuvette for analysis on a Malvern Zetasizer Nano ZS90. This instrument measures particle size and PDI at a 90˚ scattering angle using dynamic light scattering (DLS) principles and it also measures zeta potential using laser doppler micro-electrophoresis. For zeta potential measurements, the nanoparticle suspension was injected into a disposable folded capillary cell until both electrodes were covered by

the suspension medium and then analysed. All measurements were done at 37 ˚C and in triplicates.

The morphology of nanoparticles was characterized by scanning electron microscopy (SEM). The nanoparticle pellet obtained after the third washing step was smeared on an aluminium stub with a carbon adhesive, left to dry overnight in a fume cupboard at room temperature, coated with a thin film of gold palladium at 40 mA for 1 min using a sputter coater (Emitech K550X, England) and then observed under the microscope.

4.3.3 Confirmation of nanoparticle PEG content variation

Proton (^{1}H) NMR was used to confirm the presence of PEG in the nanoparticle formulations as well as to confirm the difference in PEG content, as previously described by Xu and co-workers [71]. Briefly, 5 mg of lyophilized nanoparticles were dissolved in deuterated chloroform ($CDCl_3$) containing 1% (w/w) hexadeuterodimethyl sulfoxide as an internal standard. ^{1}H NMR analysis was done using a Bruker 400 REM instrument running at 400 MHz with relaxation time set at 10 seconds and ZG at 90˚. Data was analysed using Bruker TopSpin 3.2 software.

4.3.4 Quantification of rifampicin in nanoparticles

To determine the amount of rifampicin loaded into the nanoparticles, 1 mg of nanoparticles was probe sonicated in 2 mL chloroform for 30 seconds to allow for complete disintegration of nanoparticles. This was followed by centrifugation at 13 000 rpm for 5 min and filtration of supernatant, before 1 ml of the supernatant was diluted with an equal volume of chloroform and analysed on a UV-VIS spectrophotometer at 475 nm, for quantitation of rifampicin. Triplicate samples were analysed. The concentration of the rifampicin was obtained from a calibration curve (obtained as described in Section **4.3.4.1**). Rifampicin loading (DL) and encapsulation efficiency (EE) were calculated using the following equations:

$$DL\ (\%) = \frac{Rifampicin\ weight\ in\ nanoparticles}{Nanoparticle\ weight} \times 100$$

Equation 4.2

$$EE\ (\%) = \frac{Actual\ weight\ of\ rifampicin\ in\ nanoparticle}{Theoretical\ weight\ of\ rifampicin} \times 100$$

Equation 4.3

4.3.4.1 Validation of UV-VIS assay method for rifampicin in chloroform

4.3.4.1.1 Preparation of calibration standards

A stock solution of rifampicin (100 µg/ml) was prepared by dissolving a known weight of rifampicin standard in chloroform. Standard solutions were prepared on the day of use, by diluting the stock solution with chloroform to make concentrations of 1, 2, 5, 10, 20, 40, 60 and 80 µg/ml.

4.3.4.1.2 Determination of linearity and range

2 ml volumes of the rifampicin concentrations (1-80 µg/ml) were placed in a quartz cuvette and analysed on a UV spectrophotometer at a wavelength of 475 nm. Absorbance was plotted against concentration to obtain a calibration curve. The linearity of the curve over the concentrations studied was treated by linear regression analysis.

4.3.4.1.3 Determination of accuracy and precision

Repeatability (intra-day) and intermediate precision (inter-day) were determined. For this, three replicates of three concentrations of rifampicin (within the calibration curve concentration range) were assayed each day on three consecutive days and on each occasion the average, standard deviation (SD) and % relative standard deviation (RSD) calculated and compared to determine the intra-day and inter-day precision. The accuracy of the method was determined by the mean concentrations obtained from the replicates and the percentage difference.

4.3.5 Assessment of nanoparticle stability in human serum

Changes in nanoparticle size and size distribution (PDI) were determined after incubation in human serum (Sigma Aldrich, USA) and were used as indicators of colloidal stability.

Stability assessment was performed according to a technique previously described by Mirshafiee and co-workers [105] and modified accordingly. A concentrate of human serum (Sigma Aldrich, USA) was diluted with a pH 7.4 phosphate buffered saline (PBS) to mimic the *in vivo* concentration of serum proteins; that is 55% (v/v) human serum was prepared. Nanoparticles were incubated with 55% (v/v) human serum in Protein Lo Bind Eppendorf® tubes at a concentration of 1 mg/ml, at 37 ˚C on a thermomixer set at a gentle stirring speed of 150 rpm. Particle size and PDI were measured at set time points (5 min, 60 min and 24 h) using a Malvern Zetasizer Nano ZS90. For each sample, nanoparticles suspended in PBS pH 7.4 were used as the control and for the reference reading of particle size and PDI (that is, the size and PDI before incubation or 0 min reading). Triplicate samples were analysed.

4.3.6 Nanoparticle quenching of human serum albumin fluorescence

To evaluate the influence of PEG content on nanoparticle interaction with human serum albumin a fluorescence quenching technique was used. As previously mentioned in Chapter 2, human serum albumin fluoresces, when excited at 280 nm and this property can be used as an indicator of nanoparticle-protein binding by measuring changes in the fluorescence intensity.

Nanoparticles were incubated in 55% (v/v) human serum medium prepared as described in Section **4.3.5,** and at set time points (5 min, 20 min and 60 min) 100 µL were transferred to microplate wells and analysed in a fluorescence microplate reader. Fluorescence spectra were acquired in the range of 300−500 nm after excitation at 280 nm (excitation wavelength of human serum albumin (HSA)). Triplicate samples were analysed at 37 ˚C.

Fluorescence data was used to calculate HSA quenching efficiency of nanoparticles using the Stern-Volmer equation (**Equation 4.4**) [36]. In these calculations an

assumption was made that a linear relationship exists between nanoparticle concentration and quenching of fluorescence as was reported previously [36]. The calculations were used to provide an indication of how the quenching efficiency varied with PEG content at a constant nanoparticle concentration (≈ 1 mg/ml).

$$\frac{F_0}{F} = 1 + K_{SV}[C] \qquad \textbf{Equation 4.4}$$

Where F_0 and F are fluorescence intensities in the absence and presence of the nanoparticles; **[*C*]** represents the concentration of nanoparticles. The quenching constant (K_{sv}) is conventionally taken as a representative of the quenching efficiency [36].

4.3.7 Data analysis

Data was analysed using GraphPad® Prism 6.0 and expressed as mean ± standard deviation or relative standard deviation. One-way analysis of variance (ANOVA)was done to establish the significance of any differences between means. Values were considered significant if the p-value was less than 0.05. Since ANOVA tests indicate whether there is an overall difference amongst formulations, but do not indicate which specific formulations differ, post hoc tests were performed to overcome this limitation. Post hoc tests confirm where the differences occur between formulations [136]. However, they were only run after a one-way ANOVA analysis showed an overall statistically significant difference amongst formulation means.

4.4 Results and discussion

4.4.1 Nanoparticle preparation and characterization

PLGA nanoparticles with different PEG content (0%, 2%, 5%, 8%, 13% and 17% (w/w)) were successfully synthesized using an emulsification-solvent evaporation technique. PEGylation was achieved by use of PLGA and PEG-PLGA copolymer blends in the nanoparticle synthesis process. All copolymers had a PEG Mw of 5 kDa as it was the molecular weight of choice in previous studies on PEGylated PLGA nanoparticles [70, 71]. Nanoparticle PEG content was controlled by varying the mass ratios of polymers used in nanoparticle synthesis. For each desired nanoparticle PEG

content, empty and rifampicin-loaded nanoparticles were synthesized, with the only difference in the synthesis process being the addition of rifampicin in the organic phase before the emulsification step.

4.4.1.1 Characterization of empty nanoparticles

Nanoparticle hydrodynamic diameters (D_H), PDI and zeta potentials were determined after nanoparticle synthesis and washing (**Table 4.2**). The range of nanoparticle mean D_H was 281 ± 6 nm to 388 ± 47 nm and nanoparticle formulations were monodispersed with PDI ranging from 0.17 ± 0.12 to 0.23 ± 0.04. There were no statistically significant differences amongst D_H means as well as amongst PDI means, as determined by one-way ANOVA ($p > 0.05$).

All nanoparticle formulations had negative zeta potentials ranging from -18.0 ± 0.2 to -32.8 ± 1.0 mV. There was a statistically significant difference in nanoparticle zeta potential means as determined by one-way ANOVA ($p < 0.05$). A Tukey post hoc test (comparison of the mean of one formulation to the mean of each of the other formulations) revealed that there were no statistically significant differences amongst nanoparticle formulations with 5% PEG, 8% PEG and 17% (w/w) PEG ($p > 0.05$), whilst 0% and 2% were significantly different from each other and the rest of the formulations.

Table 4.2 *The physicochemical characteristics of empty nanoparticles. Samples were analysed in a Malvern Zetasizer NanoZS90 (Malvern instruments, Ltd., UK) at 37 ºC. Data was obtained in triplicates and presented as mean ± standard deviation. Asterisks represent samples that were statistically significantly different from the rest.*

PEG content % (w/w)	EMPTY NANOPARTICLES		
	Hydrodynamic diameter (nm)	PDI	Zeta potential (mV)
0	331 ± 13	0.17 ± 0.02	-18.0 ± 0.2*
2	353 ± 89	0.19 ± 0.07	-25.0 ± 0.3*
5	388 ± 47	0.17 ± 0.12	-32.8 ± 1.0
8	281 ± 6	0.22 ± 0.01	-32.5 ± 0.4
13	363 ± 33	0.18 ± 0.05	-31.0 ± 0.4
17	353 ± 3	0.23 ± 0.04	-32.5 ± 0.4

The coefficients of determination obtained from the ANOVA analyses indicated that there was a weak association between nanoparticle PEG content and nanoparticle hydrodynamic diameter (R^2 = 0.467) or PDI (R^2 = 0.251). Therefore, PEGylation had no clear effect on both particle size and PDI. PDI. There seemed to be a strong association between nanoparticle PEG content and zeta potential (R^2 = 0.994). As illustrated in **Table 4.2**, when nanoparticle PEG content increased from 0% to 5% the zeta potential became more negative. However, with a threefold increase in PEG content from 5% to 17% the zeta potential remained at -32 mV.

4.4.1.2 Characterization of rifampicin-loaded nanoparticles

Nanoparticle hydrodynamic diameters of rifampicin-loaded nanoparticles were found to range from 241 ± 42 nm to 329 ± 33 nm (**Table 4.3**). There was a statistically significant difference in nanoparticle D_H means as determined by one-way ANOVA ($p < 0.05$). A Tukey post hoc test revealed that the nanoparticles with 2% PEG had a mean D_H which was statistically significantly smaller (241 ± 42 nm, $p < 0.05$) compared to each of the other nanoparticle formulations. There were no statistically significant differences amongst the other nanoparticle formulations ($p > 0.05$).

Formulations were monodispersed as PDI ranged from 0.18 ± 0.01 to 0.29 ± 0.08 and there were no statistically significant differences amongst PDI means, as determined by one-way ANOVA ($p > 0.05$).

All nanoparticle formulations had negative zeta potentials ranging from -19.8 ± 0.4 mV to -32.1 ± 0.9 mV. There was a statistically significant difference in nanoparticle zeta potential means as determined by one-way ANOVA ($p < 0.05$). A Tukey post hoc test revealed that there were no statistically significant differences amongst zeta potential means of nanoparticle formulations with 5% PEG, 8% PEG, 13% PEG and 17% (w/w) PEG ($p > 0.05$).

Table 4.3 *The physicochemical characteristics of rifampicin-loaded nanoparticles. Samples were analysed in a Malvern Zetasizer NanoZS90 (Malvern instruments, Ltd., UK) at 37 ºC. Data was obtained in triplicates and presented as mean ± standard deviation. Asterisks represent samples that were statistically significantly different from the rest.*

PEG content % (w/w)	**RIFAMPICIN-LOADED NANOPARTICLES**		
	Hydrodynamic diameter (nm)	PDI	Zeta potential (mV)
0	322 ± 7	0.18 ± 0.01	-19.8 ± 0.4*
2	241 ± 42*	0.26 ± 0.10	-23.2 ± 1.1*
5	329 ± 33	0.24 ± 0.09	-30.7 ± 1.2
8	318 ± 5	0.22 ± 0.01	-30.1 ± 1.0
13	343 ± 9	0.18 ± 0.10	-32.1 ± 0.9
17	318 ± 5	0.29 ± 0.08	-30.1 ± 1.0

The coefficients of determination obtained from the ANOVA analyses indicated that there was a weak association between nanoparticle PEG content and nanoparticle hydrodynamic diameter ($R^2 = 0.764$) or PDI ($R^2 = 0.305$). Therefore, PEGylation had no clear effect on both particle size and PDI. However, there was a strong association between nanoparticle PEG content and zeta potential ($R^2 = 0.970$). **Table 4.3** shows that as nanoparticle PEG content increased the zeta potential became more negative.

4.4.1.3 Comparison of empty and rifampicin-loaded nanoparticles

The nanoparticle hydrodynamic diameter ranges observed in the study are in agreement with published literature on PLGA nanoparticles [64, 131, 132, 137]. For both empty and loaded particles there was absence of any particular trend regarding the effect of PEG content on nanoparticle hydrodynamic size.

There seems to be contradicting evidence in literature, regarding the effect of PEGylation on PLGA nanoparticle size. Recently, Spek and co-workers demonstrated that as the PEG content in PLGA nanoparticles increases a significant particle size increase is observed [74]. The size increase was attributed to changes in viscosity of polymer solutions used in nanoparticle synthesis, as PEG content increases. An increase in viscosity leads to reduced spontaneity of polymer self-assemblage during the emulsification stage of nanoparticle synthesis [74]. This results in the formation of larger particles, if similar preparation conditions are maintained for all nanoparticle formulations. On the other hand, Beletsi and co-workers observed a decrease in particle size as PEG content increased [70].

A colloidal formulation is considered monodispersed when the PDI is within the range 0.1 to 0.25. PDIs below 0.4 are generally acceptable, whereas values ranging from 0.4 – 1.0 indicate a polydispersed colloidal system [138, 139]. All nanoparticle formulations (empty and loaded) regardless of PEG content had PDI values below 0.4, suggesting high to moderate monodispersity of the formulations. The was a weak association between PDI and nanoparticle PEGylation, which is concurrent with findings from studies by Beletsi and co-workers [70] as well as Xu and co-workers [71].

An association between PEG content and zeta potential was observed for empty nanoparticles formulations as well as loaded formulations. The effect of PEG on zeta potential is still not clear because of contradictions in literature. Spek and co-workers demonstrated that zeta potential was independent of PEGylation extent, with all PLGA nanoparticle formulations of PEG content ranging from 0 – 15% (w/w) exhibiting a zeta potential between -36 to -38 mV [74]. On the other hand, Beletsi and coworkers reported that the presence of PEG molecules on the nanoparticle surface shielded the

surface charge and resulted in lower magnitudes of zeta potential as PEG content increased [70].

Findings from this study add on to the current discrepancies in literature. This perhaps indicates that physicochemical characteristics such as size, PDI and zeta potential of PEGylated PLGA nanoparticles depend highly on the preparation process and less (if any) on the amount of PEG used in nanoparticle synthesis for the formulations studied.

The similarities between empty and loaded nanoparticles demonstrated that rifampicin loading did not drastically affect the basic physicochemical properties of most of the nanoparticle formulations, as shown in **Figure 4.1**.

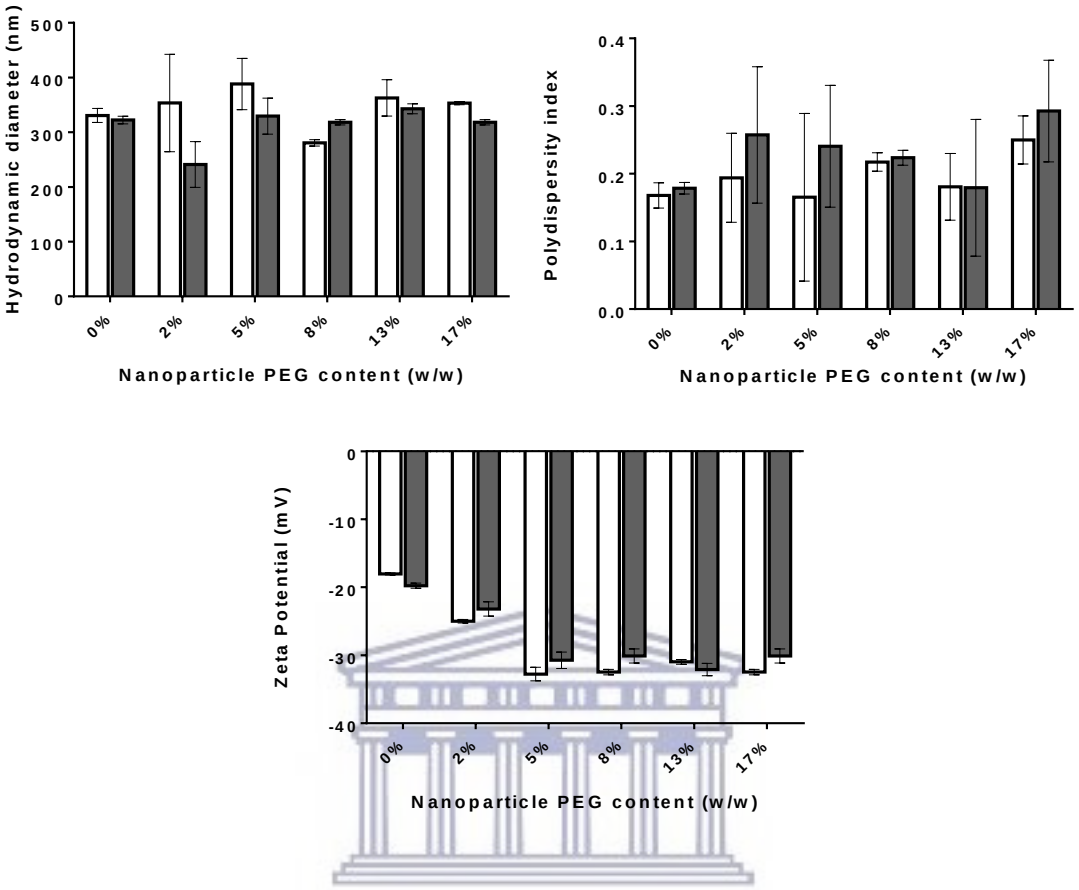

Figure 4.1 *Physicochemical properties of empty (▭) and rifampicin-loaded (▬) PLGA nanoparticle formulations with different PEG content were compared. Samples were analysed in a Malvern Zetasizer NanoZS90 (Malvern instruments, Ltd., UK) at 37 ºC. Data was obtained in triplicates and used to construct bar graphs (mean ± standard deviation, n=3 ± SD). Error bars represent calculated standard deviation from the mean.*

4.4.1.4 Characterization of nanoparticle morphology

Nanoparticle morphology was determined by SEM, which showed that all nanoparticles were spherical regardless of loading status or PEG content. This also served as confirmation of successful nanoparticle synthesis. **Figure 4.2** illustrates some of the images observed in SEM.

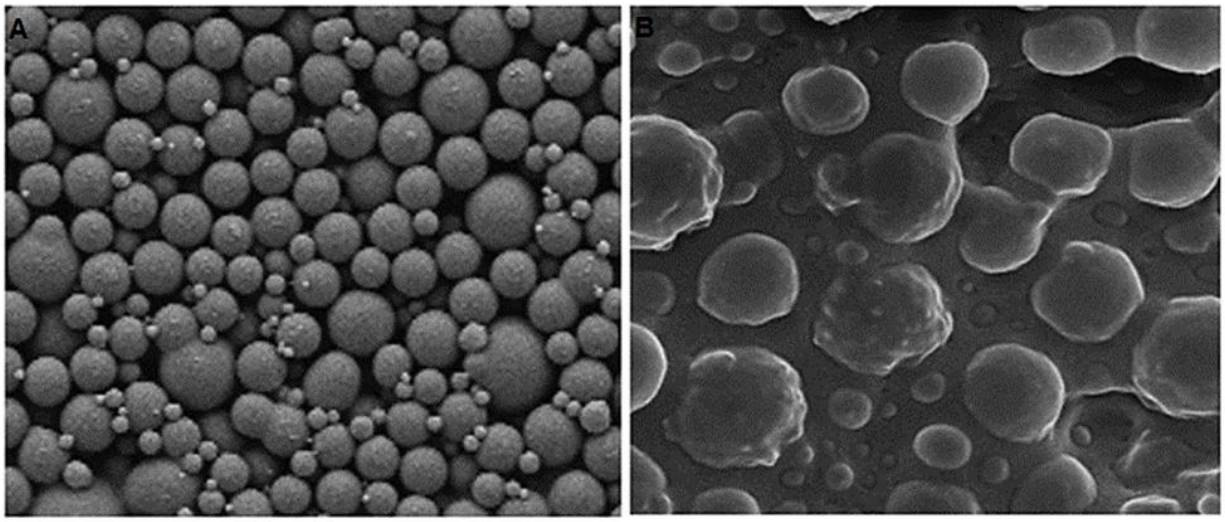

Figure 4.2 *SEM micrographs of non-PEGylated (A) and PEGylated (B) rifampicin-loaded PLGA nanoparticles (17% PEG). The nanoparticle pellet obtained from centrifuging a nanoparticle suspension was smeared onto a carbon adhesive attached to an aluminum stud and then left overnight to dry in a cupboard at room temperature. The dried nanoparticles were coated with gold palladium at 40 mA for 1 min using a sputter coater (Emitech K550X, England) and viewed with the Auriga HR-SEM F50 (Zeiss, South Africa).*

Other researchers have also synthesised spherical PEGylated and non-PEGylated PLGA nanoparticles [64, 71, 74]. However, it was interesting to notice that there was a transition from perfect smooth spheres to rough spheres with increasing PEG content, as shown in **Figure 4.3**.

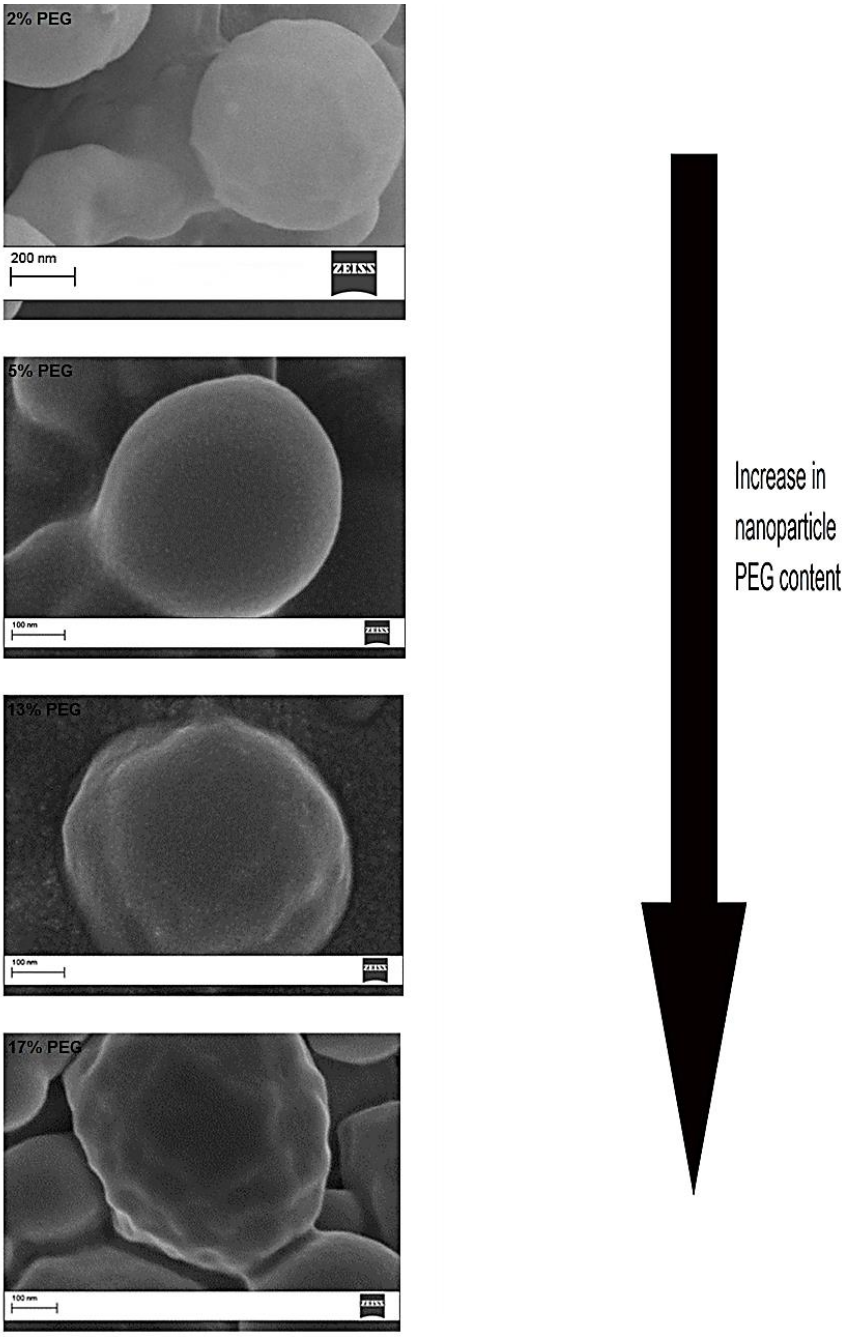

Figure 4.3 *Nanoparticle SEM images illustrating the change in nanoparticle surface smoothness as the PEG content increased (2 – 17%) on rifampicin-loaded PLGA nanoparticles. Though smoothness changed no pores were observed on nanoparticle surfaces.*

An increase in PEG content might have resulted in PEG chains collapsing onto the nanoparticle surface forming an uneven layer under the dry conditions of SEM. This

is in line with what Hrkach and co-workers reported: "*...the (PEG) polymer chains collapse onto the solid surface forming a coating layer and losing most of their mobility*…" [98]. Therefore, it would not be far-fetched to suggest that the resultant coating might not always be smooth, giving rise to the roughness observed in this study.

4.4.2 Confirmation of nanoparticle PEG content variation

Proton (^{1}H) NMR analysis of empty PEGylated PLGA nanoparticles was performed using a Bruker 400 REM instrument (400 MHz) and the data was analysed using Bruker TopSpin 3.2 software. For each of the PEGylated nanoparticles a characteristic singlet peak was observed at 3.65 ppm (**Appendix 1**). Such a peak has been attributed to the protons in the ethylene units of the PEG [98]. The peaks at 3.65 ppm were then integrated to determine the area under curve (AUC). The AUC of a peak at 3.65 ppm corresponds to the amount of PEG in a sample. As the PEG content increased from PEG 2% to 17% the AUC consequently increased from 0.1517 to 1.3000 respectively (**Figure 4.4**).

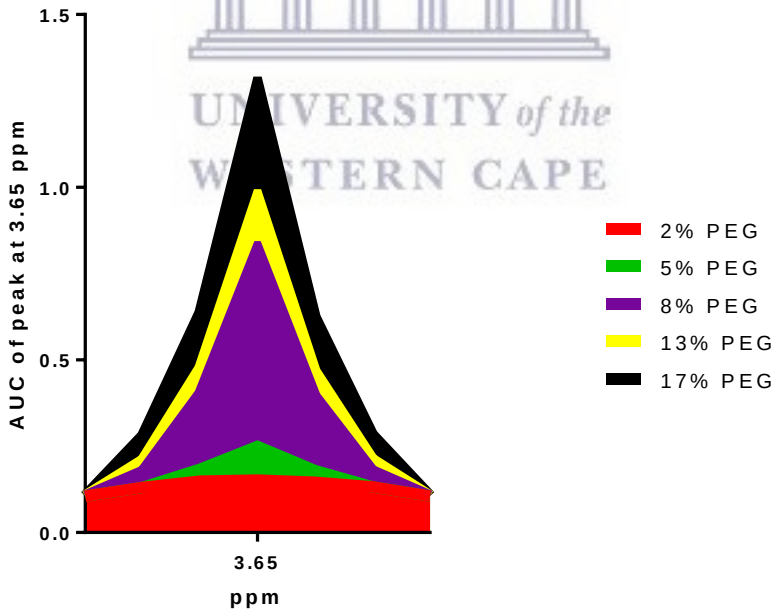

Figure 4.4 *The AUC of the ^{1}H NMR spectrum peak attributed to protons of the ethylene unit of PEG. The integral (AUC) of the peak increases as PEG content increases. Empty PEGylated nanoparticles were dissolved in deuterated chloroform and analysed on a Bruker 400 REM instrument running at 400 MHz with relaxation time set at 10 seconds and ZG at 90˚. Data was analysed using Bruker TopSpin 3.2 software.*

The detection of a peak at 3.65 ppm in the ^{1}H NMR spectra of PEGylated nanoparticles was expected as this is in line with findings from previous studies [71, 74, 98]**.** Literature suggests that PEG has a characteristic peak around 3.65 ppm which can be unambiguously detected by ^{1}H NMR [71, 74]. Blending PLGA with PEG-PLGA co-polymers allows for the easy adjustment of PEG content of the nanoparticles by simply mixing the appropriate amounts of PLGA and PLGA–PEG [8, 140]. These results confirm that polymer blending successfully produced nanoparticles with different PEG contents.

4.4.3 Drug loading and encapsulation efficiency

A validated UV-VIS method was used to quantify rifampicin loaded in nanoparticle samples. Nanoparticle mean drug loading was generally low as it ranged from 1.3% - 3.1% (w/w), whilst mean encapsulation efficiency respectively ranged from 13% - 31%. **Figure 4.5** illustrates the mean drug loading (DL) of various nanoparticle formulations. There was a statistically significant difference in nanoparticle mean drug loading as determined by one-way ANOVA ($p < 0.05$). A Tukey post hoc test revealed that the nanoparticles with 2% PEG had a statistically significantly low mean drug loading ($p < 0.05$) compared to the other nanoparticle formulations. Though 0% PEG nanoparticles had the highest drug loading, this was not statistically significantly different from drug loading of nanoparticle formulations with 5% PEG, 8% PEG, 13% and 17% PEG ($p > 0.05$).

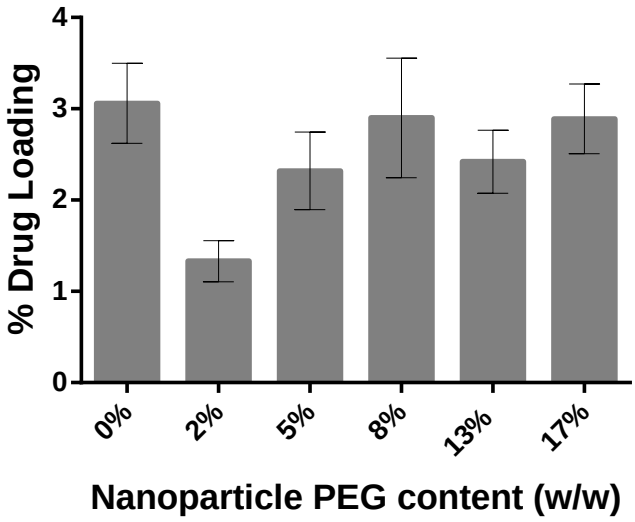

Figure 4.5 *Nanoparticle rifampicin loading. Nanoparticle samples were weighed and dissolved in chloroform, sonicated, filtered and transferred to quartz cuvettes for analysis with a UV-Visible spectrophotometer (Cintra 202, GBC Scientific Equipment, Australia).*

The statistically significantly low drug loading exhibited by nanoparticles with 2% PEG was expected as these nanoparticles had the smallest hydrodynamic size (Section **4.4.1.2**). Particle size plays a crucial role in determining drug loading. Generally, the smaller the particle size the lower the drug loading [118].

The presence of PEG reduced drug loading as non-PEGylated PLGA nanoparticles (0% PEG) had the highest drug loading and encapsulation efficiency (though not statistically significant). Inasmuch as the general assumption is that all PEG goes to the particle surface, there has been evidence suggesting that some PEG strands form part of the nanoparticle core [74]. Therefore, the lower drug loading observed for PEGylated PLGA nanoparticles can be attributed to the effects of PEG on hydrophobicity of the nanoparticle core [70, 74]. The presence of PEG lowers the hydrophobicity and hence the binding affinity for a hydrophobic drug like rifampicin, resulting in lower drug loading.

The current formula for calculating drug loading (**Equation 4.2**) has limitations. Studies by Spek and co-workers have shown that as much as 33% (w/w) of PVA (surfactant used in nanoparticle synthesis) can be found on PEGylated PLGA nanoparticle surfaces even after thorough washing [74]. The presence of PVA was shown to

increase as nanoparticle PEG content increased. As for non-PEGylated PLGA nanoparticles, residual PVA was detected but was mainly in the nanoparticle core and overall not as much as in PEGylated nanoparticles. These findings insinuate that the current formula used in calculating drug loading falls short of the necessary mathematical corrections needed to remove the contribution of PVA weight especially when comparing nanoparticles with varying PEG content.

4.4.3.1 Validation of UV-VIS assay method for rifampicin in chloroform

Rifampicin is a UV-VIS absorbing molecule with specific chromospheres in its structure that absorb at a wavelength of 475 nm [141]. This fact was successfully employed for its quantitative determination using a UV-VIS spectrophotometric method. The stock solutions and working standards were prepared in chloroform, since rifampicin is highly soluble in chloroform [141] and also because the polymers used for nanoparticle synthesis dissolve in chloroform, thereby enabling the accurate quantification of drug loaded in nanoparticles.

The standard curve of absorbance versus rifampicin concentration was found to be linear over the concentration range studied (1 – 40 µg/ml), as shown in **Figure 4.6**. The standard curve was described by the equation Y = 0.01813X + 0.001086 (where Y = absorbance, X = rifampicin concentration). The correlation coefficient (R^2) of the standard curve was 0.997.

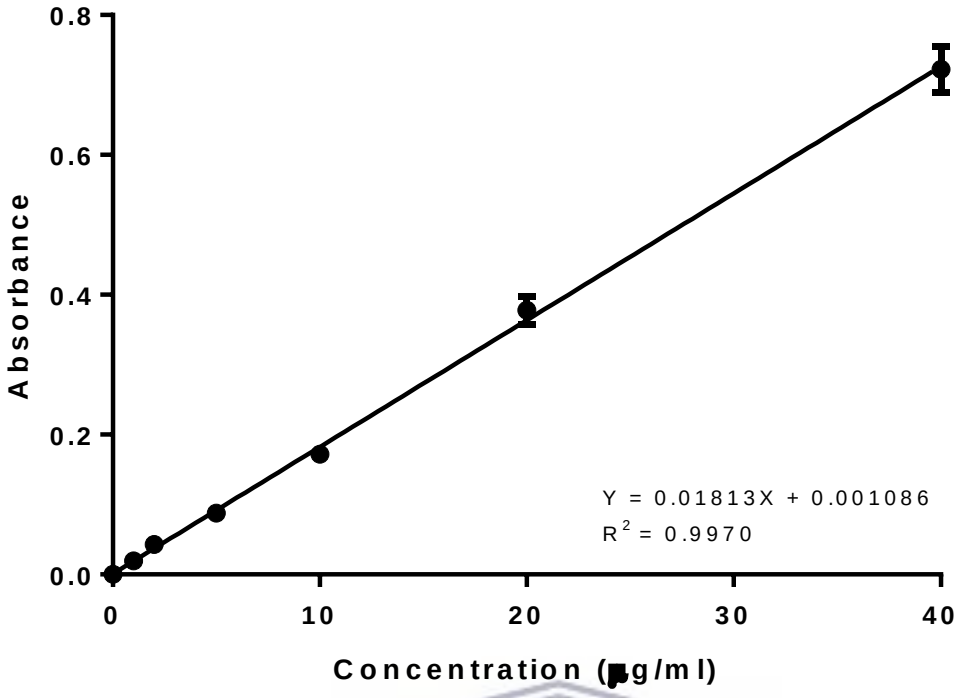

Figure 4.6 *Calibration curve of rifampicin absorbance in chloroform versus concentration at a wavelength of 475 nm. The stock solutions and working standards were prepared in chloroform. Samples were transferred to quartz cuvettes and analysed at 25ºC with a UV-Visible spectrophotometer (Cintra 202, GBC Scientific Equipment, Australia).*

The correlation coefficient (R^2) was acceptable [142] to prove linearity and was sufficient to provide accurate values for rifampicin content in the loaded nanoparticles. Therefore, using the established calibration curve, the content of rifampicin in loaded nanoparticles was established.

Replicate analyses of rifampicin standard solutions was used to assess the accuracy, precision, and repeatability of the proposed method. Three concentrations were selected within the calibration range (1, 10 and 40 µg/ml) and analysed with the established calibration curve to determine the intra and inter day variability (**Appendix 2**). Method precision had a relative standard deviation (RSD) below 9% for repeatability and below 3% for intermediate precision. Percent RSD values were found well within 10% in both instances, suggesting that the method provided reproducible results. The accuracy results were expressed as percent mean recoveries, and these fell within the range of 91.82 - 104.77%. A mean recovery of 90 – 110% is in assays, though for drug registration and quality control purposes pharmaceutical regulatory

authorities may use a narrower acceptance criteria of 98 – 102% mean recovery [142]. The study was not for quality control purposes, hence the former criterion was used, thus validity and accuracy of the proposed UV-VIS method was proved.

4.4.4 Nanoparticle colloidal stability in human serum

Empty nanoparticles were incubated for 1 h in 55% v/v human serum. Non-PEGylated nanoparticles showed a significant ($p < 0.05$) change in hydrodynamic diameter from 344 ± 3 nm to 406.7 ± 24.4 nm and a broadening of nanoparticle size distribution after 1 h of incubation. A minor increase in size ($p > 0.05$) from 357.8 ± 7.4 nm to 368.2 ± 6.98 nm and lesser broadening in size distribution was observed for nanoparticles with 2% PEG. Nanoparticles with 5% to 17% PEG were stable and retained their original hydrodynamic diameters over the 1 h incubation period. **Figure 4.7** illustrates the changes in nanoparticle size and distribution over the incubation period, for each nanoparticle formulation.

Colloidal stability of nanoparticles in the presence of proteins can be assessed by DLS studies through monitoring nanoparticle size [71]. Serum proteins interact with nanoparticles through hydrogen bonding, electrostatic forces and hydrophobic interactions, thereby forming a nanoparticle-protein complex. The absence of marked differences amongst PEGylated nanoparticles suggests that 2% PEG was sufficient to prevent protein binding.

Dynamic light scattering studies of nanoparticles in human serum were done as the technique is a useful characterization tool in nanoparticle-protein interaction studies [143]. Shifts in nanoparticle size distribution curves (Gaussian curves) are indicative of protein adsorption onto nanoparticles and aggregation. For all samples except 0% PEG there was a small shift in median particle size position after incubation with human serum, indicating the absence of observable complexing and aggregation. On the other hand, 0% PEG nanoparticles showed significant shifts of the size distribution curve to higher median size values. Other peaks were also observed in 0% and 2% PEG samples, suggestive of the formation of smaller protein mediated aggregates.

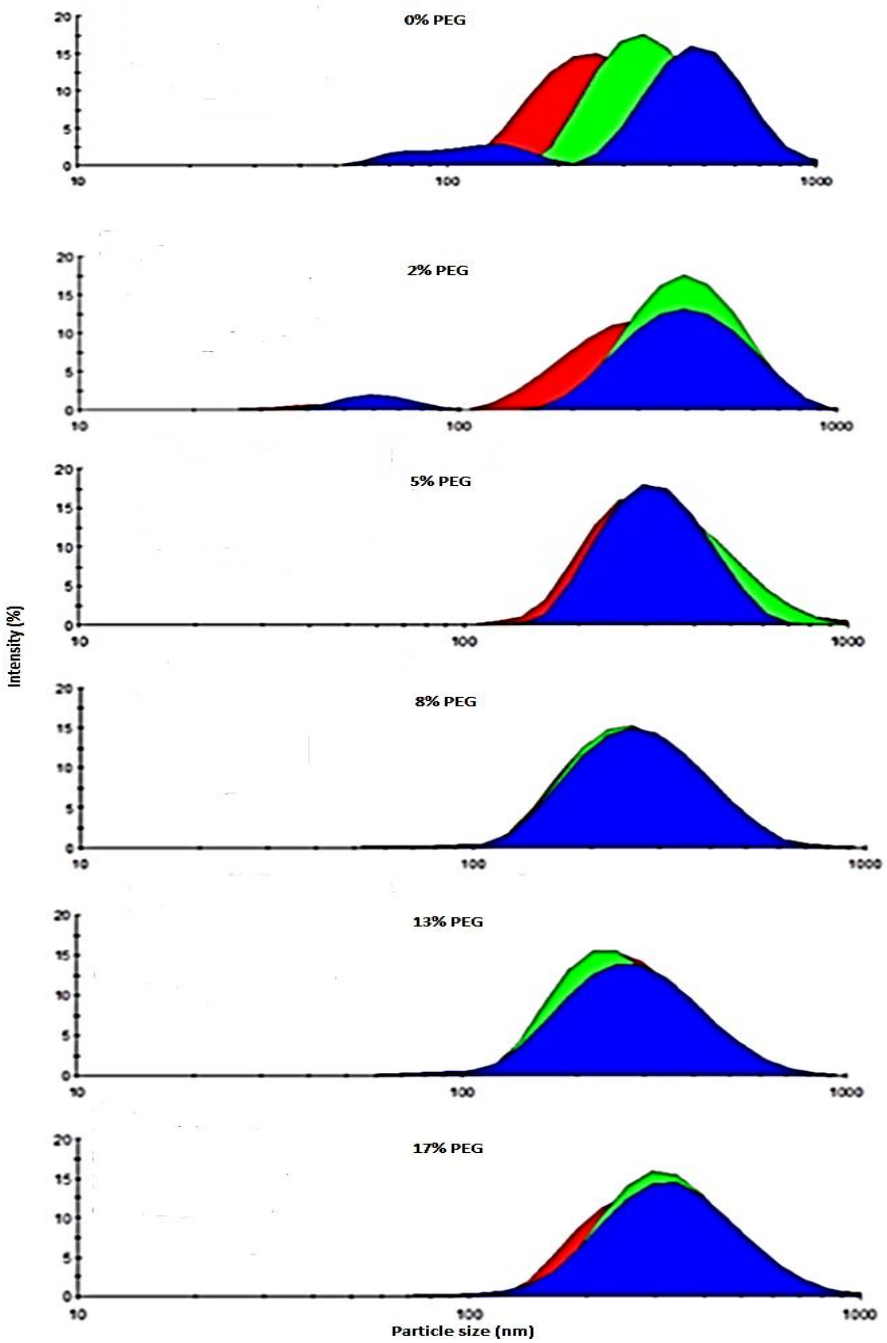

Figure 4.7 *The change in nanoparticle hydrodynamic diameter and size distribution over a 60-minute incubation period in human serum. Empty nanoparticles were incubated in 55% human serum at pH 7.4 at 37ºC. Samples were analysed in a Malvern Zetasizer NanoZS90 (Malvern instruments, Ltd., UK) at 37 ºC at time points: 0 min (■), 5 min (■), and at 60 min (■).*

A visual inspection of chromatograms from a study by Dell'Orco and co-workers show no significant differences in band intensities between protein collected from nanoparticles that were incubated for 30 seconds and those that were incubated for 6

h, thus indicating that similar amounts of human serum proteins bound to the nanoparticles regardless of the incubation time [144]. This demonstrates that all the binding takes place in a matter of nanoseconds to a few minutes as mentioned by Mahmoudi and co-workers [145] and therefore the incubation time of 1 h used in our study was adequate for the binding kinetics to reach equilibrium.

4.4.5 Nanoparticle quenching of human serum albumin fluorescence

Nanoparticles were incubated with human serum and the change in the fluorescence of HSA was assessed. After 5 minutes of incubation the largest decrease in HSA maximum fluorescence intensity was exhibited by non-PEGylated nanoparticles ($p < 0.05$). Samples of all PEGylated nanoparticles exhibited an insignificant change in HSA maximum fluorescence intensity ($p > 0.05$) as illustrated in **Figure 4.8**. No significant differences in quenching behaviour were observed between empty and loaded nanoparticles for all formulations.

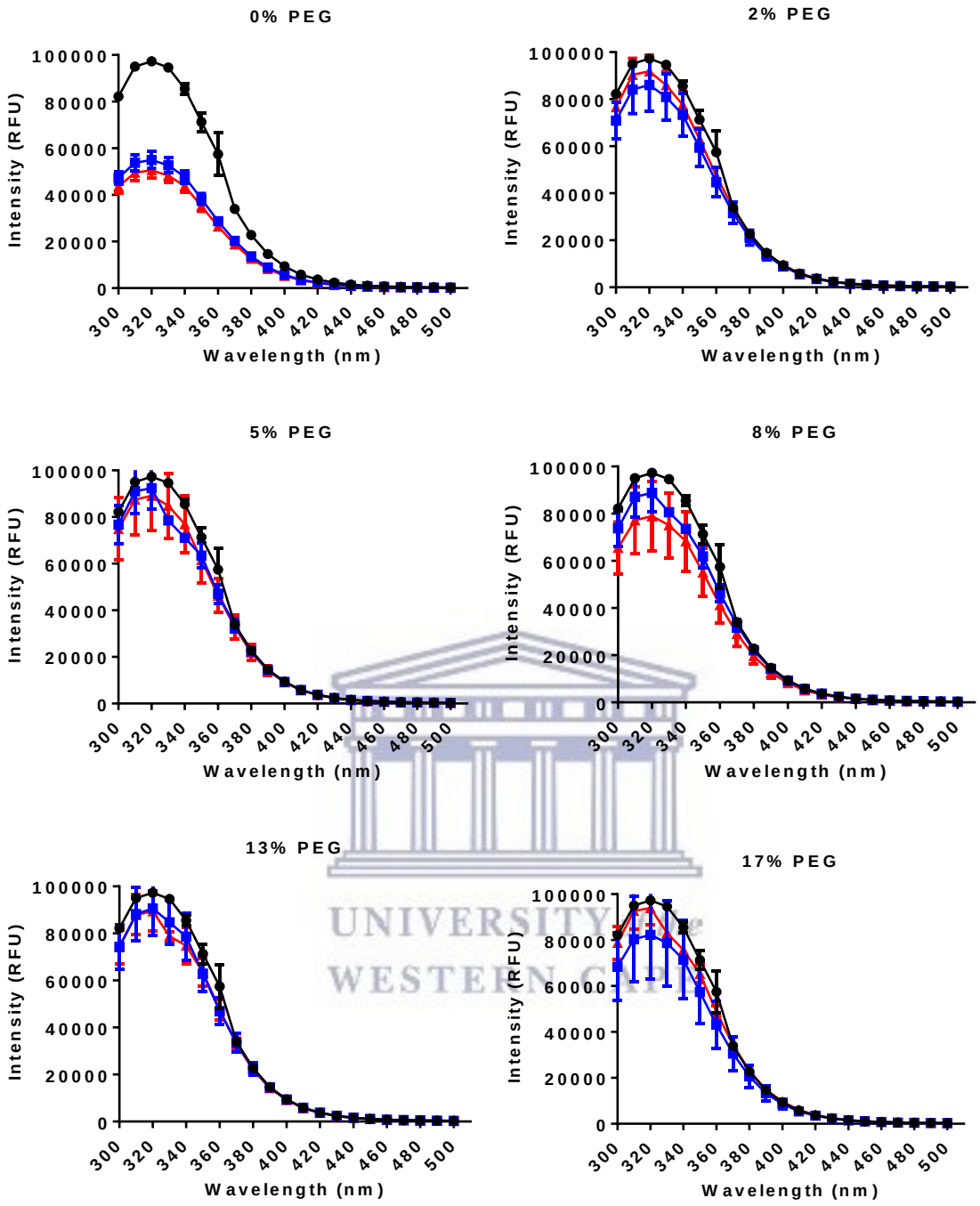

Figure 4.8 *The quenching of human serum albumin fluorescence after 5 min of incubation with nanoparticles at 37 ºC. Samples were transferred to a microplate and analysed in a Fluorescence Microplate Reader (Synergy Mx, BioTek Instruments, USA) at an excitation wavelength of 280 nm. Triplicate samples were analysed (n=3). HSA (■), rifampicin-loaded nanoparticles (■), empty nanoparticles (■).*

As the incubation time extended beyond 5 minutes the quenching of HSA fluorescence increased for all nanoparticle formulations, implying that there was continued protein binding. To quantify the interaction of nanoparticles with HSA Stern-Volmer's equation was used to calculate the quenching efficiencies of nanoparticle formulations. **Table 4.4** illustrates the mean quenching efficiencies of empty nanoparticles over the duration of the incubation.

Table 4.4 *Calculated HSA quenching efficiencies of empty nanoparticles. Nanoparticles were incubated in 55% human serum and change in human serum albumin fluorescence was determined using a Fluorescence micro-plate reader (Synergy Mx, BioTek Instruments, USA) at after 5, 20 and 60 min. Mean quenching efficiencies (n=3) were calculated using Stern-Volmer equation (Equation 4.4).*

Nanoparticle formulation	Quenching Efficiency (K_{sv}) (ml/µg)		
	5 min	**20 min**	**60 min**
0% PEG	7.70×10^{-04}	8.06×10^{-04}	1.27×10^{-03}
2% PEG	1.31×10^{-04}	1.53×10^{-04}	1.27×10^{-03}
5% PEG	5.28×10^{-05}	1.43×10^{-04}	1.21×10^{-03}
8% PEG	9.49×10^{-05}	1.35×10^{-04}	1.26×10^{-03}
13% PEG	7.29×10^{-05}	1.14×10^{-04}	1.23×10^{-03}
17% PEG	5.39×10^{-05}	1.19×10^{-04}	1.16×10^{-03}

Fluorescence intensity of HSA was quenched by the addition of nanoparticles indicating that there was binding between nanoparticles and HSA. The absence of an obvious shift in maximum emission wavelength indicated the little influence of nanoparticles on the microenvironment of the tryptophan residue in albumin [36]. As expected non-PEGylated nanoparticles quenched HSA fluorescence the most as there was no hydrated cloud around the nanoparticles to prevent protein binding, as was the case with PEGylated nanoparticles. However, unexpectedly there were no significant differences in quenching efficiency amongst PEGylated nanoparticles. This implied that 2% PEG on nanoparticles was sufficient in resisting protein binding. These results were similar to those obtained from DLS studies.

4.5 Conclusion

Overall, from the results obtained in this section of the study the following conclusions could be drawn:

- Blending of PLGA and PEG-PLGA co-polymers successfully varied PEG content on nanoparticles.
- PEGylation had a significantly greater effect on nanoparticle zeta potential and a lesser effect (if any) on nanoparticle hydrodynamic size and PDI.
- Rifampicin-loading did not significantly affect the basic physicochemical properties of PEGylated and non-PEGylated PLGA nanoparticles.
- PEGylation resulted in low rifampicin loading in PLGA nanoparticles (though not statistically significant).
- A nanoparticle PEG content of 2% (w/w) was sufficient to stabilize PLGA nanoparticles in human serum.

CHAPTER 5
DRUG RELEASE STUDIES

This chapter describes drug release studies of rifampicin-loaded PLGA nanoparticles with 0% - 17% (w/w) PEG content, using a validated UV-VIS method and the mechanism of release is elucidated using mathematical models. Firstly, an assay to quantify the amount of rifampicin released by the nanoparticles into the release media and the stability of rifampicin in the media was developed.

5.1 Materials

5.1.1 Consumables

In addition to the freeze dried rifampicin-loaded nanoparticles described in Chapter 4 the following were used:

Solvents and reagents: Ascorbic acid (99%) (Sigma Aldrich, USA); Distilled water (Millipore, Milford, MA, USA); Phosphate buffer powder (Sigma Aldrich, USA); Rifampicin powder (HPLC grade, ≥ 97%) (Sigma Aldrich, China).

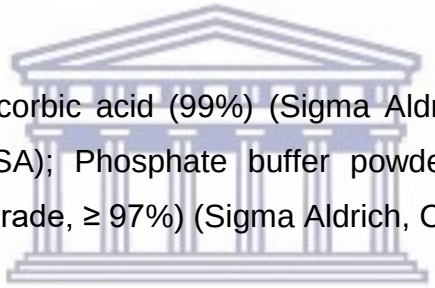

Other consumables: Centrifuge tubes (Biologix, USA); Graduated micro-tubes (SSI, USA); Hypodermic needles (Lasec, South Africa); Nylon 0.45 µm syringe filters (25 mm, StarLab Scientific); Nylon 0.22 µm syringe filters (KimLab, South Africa); Pipettes – 20, 200 & 1000 µl (Lasec, South Africa); Pipette tips - 200 & 1000 µl (Bio-smart Scientific, UK); Protein Lo Bind tubes (Eppendorf, Germany), UV quartz cuvettes 10 mm pathlength (Z276669, Sigma Aldrich, South Africa).

5.1.2 Equipment

The following equipment were used: Analytical balance (Mettler®, model PE 6000); Centrifuge (Digicen 21, Orto alresa, United Scientific); pH meter (Basic 20, Lasec, South Africa); Thermomixer (Comfort, Eppendorf, Germany); UV-Visible spectrophotometer (Cintra 202, GBC Scientific Equipment); Vortex mixer (VM-400, Gemmy Industrial Corp., Taiwan).

Computer modelling software: DDSolver (Microsoft Excel add-in program) [113].

5.2 Methods

5.2.1 Validation of UV-VIS method for assay of rifampicin in PBS pH 7.4

5.2.1.1 Preparation of calibration standards

A UV-VIS assay for rifampicin in PBS pH 7.4 spiked with ascorbic acid (500 µg/ml) was developed and validated. A stock solution of rifampicin (100 µg/ml) was prepared by dissolving a known weight of rifampicin powder (HPLC grade, ≥ 97%, Sigma Aldrich, China) in PBS pH 7.4 fortified with ascorbic acid (500 µg/ml). Standard solutions were prepared on the day of use by diluting the stock solution with PBS pH 7.4 to make concentrations of 0.1, 0.25, 0.5,1, 2.5, 5, 10, 25 and 50 µg/ml. PBS had been prepared by reconstituting phosphate buffer powder (Sigma Aldrich, USA) with 3.8 litres of distilled water to prepare a 0.1 molar solution, pH 7.4 at 25 °C, as per manufacturer's instruction.

5.2.1.2 Determination of linearity and range

For each of the rifampicin concentrations mentioned above, known volumes (2 ml) were placed in a quartz cuvette and analysed on a UV-Visible spectrophotometer (Cintra 202, GBC Scientific Equipment) at a wavelength of 475 nm. Absorbance was plotted against concentration to obtain the calibration curve. The linearity of the curve over the concentrations studied was determined by linear regression analysis. Triplicate samples were analysed.

5.2.1.3 Determination of accuracy and precision

The precision of the UV-VIS method was determined by calculating the repeatability (intra-day) and intermediate precision (inter-day). For this, three replicates of three concentrations of rifampicin (within the calibration curve concentration range) were assayed each day on three consecutive days and on each occasion the average, standard deviation and % relative standard deviation (%RSD) calculated and compared to determine the intra-day and inter-day precision. The accuracy of the method was determined by the mean concentrations obtained from the replicates and the percentage difference.

5.2.1.4 Determination of rifampicin stability in release medium

Since rifampicin undergoes oxidative degradation in aqueous media, its stability in PBS pH 7.4 containing the anti-oxidant ascorbic acid was assessed. Triplicates of three concentrations of rifampicin (10, 20 and 30 µg/ml) were incubated in conditions similar to those under which nanoparticle drug release studies were carried out (PBS pH 7.4 spiked with ascorbic acid (500 µg/ml), continuous agitation, temperature of 37°C). At set time points (15 min, 30 min, 45 min, 60 min, 6 h, 24 h, and 48 h) samples were centrifuged (13 000 rpm for 5 min) and analysed on a UV-VIS spectrophotometer (Cintra 202, GBC Scientific Equipment) at a wavelength of 475 nm.

5.2.2 *In Vitro* Drug Release

The *in vitro* drug release profiles of rifampicin-loaded nanoparticles were determined by a method previously described [133]. Rifampicin-loaded PLGA nanoparticles with 0% - 17% PEG content (1 mg/ml) were incubated in PBS pH 7.4 containing 500 µg of ascorbic acid per 1 mg of nanoparticles at 37°C in Protein Lo Bind® tubes (Eppendorf, Germany) in a Thermomixer (Comfort, Eppendorf, Germany) shaking at 100 rpm over 48 h. At set time points (15 min, 30 min, 45 min, 60 min, 2 h, 4 h, 6 h, 12 h, 24, 48 h), the tubes were removed from the Thermomixer and centrifuged at 13 000 rpm for 5 min (to separate nanoparticles from release medium) and the supernatant was collected and analysed for rifampicin at 475 nm using a validated UV-VIS method. Ascorbic acid was added to mitigate oxidative degradation of rifampicin [126, 133]. Rifampicin released was expressed as the percentage of the amount of rifampicin loaded in a given nanoparticle formulation.

5.2.3 Data analysis

Data was analysed using GraphPad® Prism 6.0 and expressed as mean ± standard deviation. One-way ANOVA was performed to establish the significance of any differences amongst means. Values were considered significant if the p-value was less than 0.05.

5.2.3.1 Mathematical modelling of drug release data

In order to determine the best mathematical model to describe the release of rifampicin from nanoparticles with varying PEG content DDSolver software (Microsoft Excel add-in program) [113] was employed. Drug release data was entered into three models, namely: Weibull, Peppas- Sahlin and Korsmeyer-Peppas models. The coefficient of determination (R^2) and the adjusted coefficient of determination (R^2_{adj}) were used as the basis for selecting the best mathematical model, with the model with the highest R^2_{adj} being selected as the best fitting model. The mechanism of release from each nanoparticle formulation was determined from the models based on the criteria previously discussed in Chapter 2.

5.3 Results and discussion

5.3.1 Validation of UV-VIS assay method for rifampicin in PBS pH 7.4

To determine linearity, various concentrations of the rifampicin standard ranging from 1 - 50 µg/ml were prepared and analysed. However, since the Beer-Lambert law seemed to be obeyed at concentrations below 50 µg/ml, an eight-point calibration curve was plotted between 1 – 25 µg/ml, as presented illustrated in **Figure 5.1**.

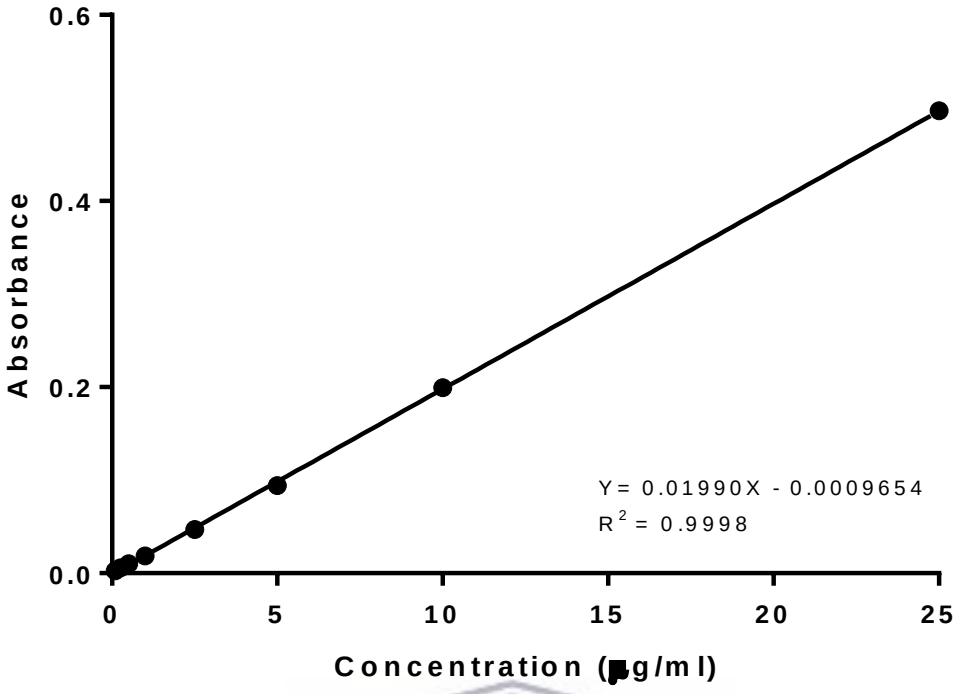

Figure 5.1 *Calibration curve of rifampicin absorbance PBS pH 7.4 versus concentration at a wavelength of 475 nm. The stock solutions and working standards were prepared in PBS pH 7.4 spiked with ascorbic acid (500 µg/ml). Samples were transferred to quartz cuvettes and analysed at 25ºC with a UV-Visible spectrophotometer (Cintra 202, GBC Scientific Equipment, Australia).*

The regression equation was Y = 0.01990X + 0.0009654, with a correlation coefficient (R^2) = 0.9998, proving a strong linear relationship between absorbance and rifampicin concentration range studied. Of all the eight concentrations that were used to construct the calibration curve the highest deviation was 2.34% RSD as shown in (**Appendix 3**), this indicated suitability of method.

Replicate analyses of rifampicin standards was used to assess the accuracy, precision, and repeatability of the proposed method. Three concentrations were selected within the calibration range (0.1, 10 and 25 µg/ml) and analysed with the illustrated calibration curve to determine the intra and inter day variability. All concentrations had a % RSD below 4% for intra-day variability and below 5% for inter-day variability. %RSD values were found well within 10% in both instances, suggesting that the method provided reproducible results. The accuracy results were expressed as percent recoveries, and these fell within the range of 102.25 - 109.07%,

demonstrating validity and accuracy of the proposed UV-VIS method. A mean recovery of 90 – 110% is acceptable when determining accuracy [142].

5.3.1.1 Stability of rifampicin in PBS pH 7.4

To determine the stability of rifampicin in release medium, three concentrations (10 µg/ml, 20 µg/ml and 30 µg/ml) of rifampicin in PBS pH 7.4 spiked with ascorbic acid were incubated at 37ºC. The %RSD of mean absorbance readings obtained after 30 min, 24 h and 48 h of incubation were determined. Absorbance readings for rifampicin concentrations: 10 µg/ml, 20 µg/ml and 30 µg/ml had %RSD values of 2.4%, 1.5% and 1.3% respectively. This is in line with acceptable assay deviations [142].

The three concentrations were chosen based on the amount of drug present in 1 mg of nanoparticles (calculated in chapter 4) and the range was 1.3 – 3.1% (w/w) for all nanoparticle formulations.

It was found that the rifampicin solutions were stable throughout the 48 h duration of the study as there was no serious deviation in absorbance of samples of known concentration analysed during the course of the study. These results reveal that the drug release data was reliable through the duration of the study. Some researchers have observed oxidative degradation of rifampicin in PBS pH 7.4 even in the presence of an anti-oxidant like ascorbic acid [133]; yet other researchers observed sustained anti-oxidant protection similar to that observed in this study [126].

5.3.2 Drug release profiles of PLGA nanoparticles with different PEG content

A comparative evaluation of the effect of PEGylation on the release of rifampicin from PLGA nanoparticles was performed. Profiles were constructed by plotting the percentage of encapsulated rifampicin released *versus* time as illustrated in **Figure 5.2**. Within 24 h of incubation all nanoparticle formulations showed a bi-phasic release profile characterized by an initial burst release followed by a plateau phase. Among the six formulations, PEGylated nanoparticles gave relatively slower release compared to non-PEGylated nanoparticles in the first 24 h. At time points 12 h and 24 h, as nanoparticle PEGylation extent increased there was a significant gradual

decrease in the percentage of rifampicin released ($p < 0.05$). The only exception to this trend were nanoparticles with 13% PEG, as illustrated in **Figure 5.2** and **Table 5.1**. However, beyond 24 h there was a reversal of the trend as is shown by the data at 48 h in **Table 5.1**, where PEGylation resulted in a significant increase in rifampicin release ($p < 0.05$). The one-way ANOVA coefficients of determination (R^2) for the trends observed ranged 0.981 to 0.985, indicating that there was a strong linear association between PEG content and rifampicin release.

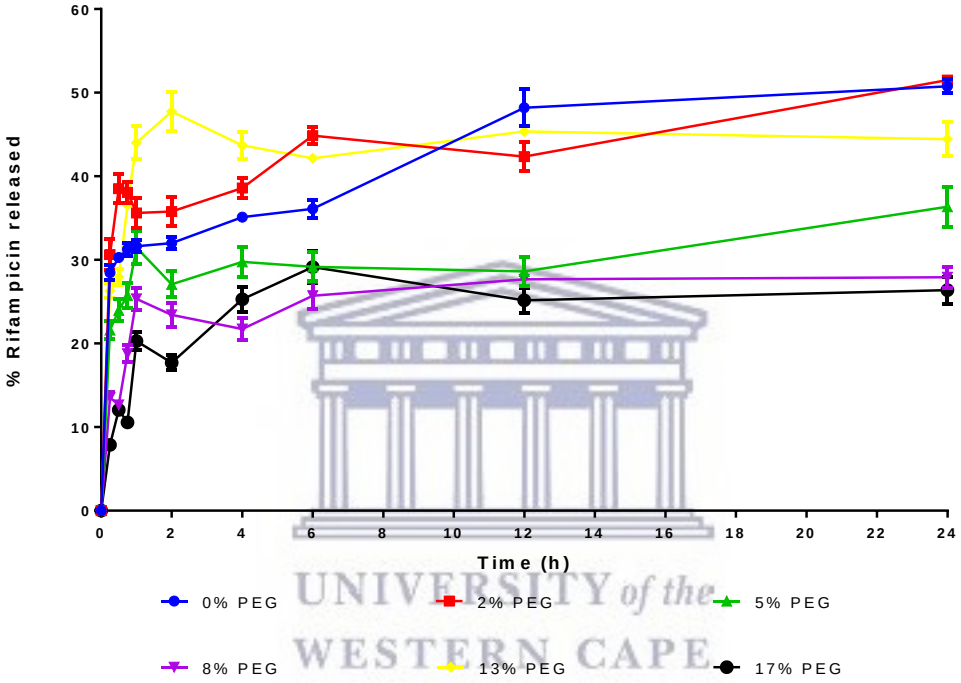

Figure 5.2 *Drug release profiles of PLGA nanoparticles with different PEG content. Nanoparticles were incubated in PBS pH 7.4 spiked with ascorbic acid at 37ºC under continuous shaking at 100 rpm for the duration of the study (n = 3).*

Table 5.1 *Comparison of the effect of nanoparticle PEG content on rifampicin release after 12 h, 24 h and 48 h of incubation in release medium (PBS pH 7.4 spiked with ascorbic acid). Data is expressed as mean ± SD (n=3). Trend outliers are highlighted in red.*

Nanoparticle formulation	Release after 12 h		Release after 24 h		Release after 48 h	
	% Rifampicin released	Effect of PEGylation	% Rifampicin released	Effect of PEGylation	% Rifampicin released	Effect of PEGylation
0% PEG	48.2 ± 2.1	Decrease in drug release as PEG content increased R^2 =0.981	50.8 ± 0.8	Decrease in drug release as PEG content increased R^2 =0.982	50.8 ± 0.9	Increase in drug release as PEG content increased R^2 = 0.985
2% PEG	42.4 ± 1.7		51.5 ± 0.3		59.0 ± 0.6	
5% PEG	28.6 ± 1.7		36.4 ± 2.4		78.9 ± 6.0	
8% PEG	27.7 ± 0.4		27.9 ± 1.2		29.6 ± 0.6	
13% PEG	45.4 ± 0.3		44.4 ± 2.0		84.4 ± 3.6	
17% PEG	25.2 ± 1.5		26.4 ± 1.6		24.7 ± 3.1	

The initial burst release phase is often attributed to the presence of drug molecules on the nanoparticle surface [102, 146]. The presence of drug molecules on the nanoparticle surface confounds the effect of PEGylation on drug release from the nanoparticle core. As a result, there was no clear trend of the effect of PEGylation on drug release in the initial burst release phase.

At 12 h and 24 h, drug release was in the plateau phase. Based on literature, the predominant activity in this phase is drug molecule diffusion from the polymer matrix into the release medium at a sustained release rate [102, 118, 133]. The effect of the hydrated cloud formed on the nanoparticle surface due to the presence of PEG could have slowed the diffusion of drug molecules from the nanoparticle core. Since rifampicin is a hydrophobic drug, as the PEG content of nanoparticles increased the hydrated cloud at the nanoparticle-release medium interface thickened. This created a repulsive aqueous barrier that could slow down the exit of rifampicin molecules from the hydrophobic PLGA nanoparticle core.

Drug release was tracked up to 48 h and at this time point the percentage of rifampicin that had been released from all nanoparticle formulations ranged from 24.7 ± 3.1% to 84.4 ± 3.6%. This suggested that significant amounts of the encapsulated drug were still present within the core of the nanoparticle and needed a longer period for complete

release [133]. This also implied that there was controlled release. The slow sustained release observed in all profiles is attributed to the diffusion of rifampicin from within the polymer matrix [72].

At 48 h there appeared to have been a sudden increase in the release of rifampicin in nanoparticles with 2% PEG, 5% PEG and 13% PEG resulting in a reversal of the trend that had been observed earlier (at 12 h and 24 h). At this point of the study there was a strong linear association (R^2 = 0.985) between PEG content and an increase in rifampicin release. It can be speculated that at this stage of the release study the effect of PEGylation on diffusion of rifampicin molecules from the nanoparticle core could have been overshadowed by polymer swelling and degradation [147, 148]. It is therefore logical to assume that PEGylation might only have a profound effect on drug release in the plateau stage of release, before polymer swelling and degradation dominate. It can also be said that PEGylation might facilitate faster swelling and degradation of PLGA nanoparticle polymer matrix, because at 48 h non-PEGylated nanoparticles had only released 50.8 ± 0.9% of the loaded drug yet 2% PEG, 5% PEG and 13% PEG nanoparticles had released significantly more of their respective payloads. Avgoustakis and co-workers also investigated the release profile of PEGylated PLGA nanoparticles with different PEG content; they found that an increase in the PEG content led to an increase in the rate of drug release [10]. This trend might be the consequence of the persistent hydrated cloud that forms on the nanoparticle surface due to the presence of PEG which might have resulted in rapid polymer matrix swelling and degradation via hydrolysis. Based on this it is logical to expect a sudden burst release in the later stages of drug release studies of PEGylated polymeric nanoparticles. However, data for 8% PEG and 17% PEG nanoparticles at 48 h does not fit into this trend.

Corrigan and co-workers argue that the duration of most drug release studies on PLGA nanoparticles do not allow enough time for polymer matrix degradation to take place [118]. Their argument was based on studies on non-PEGylated PLGA nanoparticles. The insignificant change in percentage rifampicin released at 24 h and 48 h supports that polymer degradation was not yet dominant in non-PEGylated (0% PEG) nanoparticles after 48 h of incubation. It is therefore logical to assume that the presence of PEG changes the dynamics of polymer matrix swelling and degradation.

Therefore, as for PEGylated nanoparticles, in 48 h polymer degradation might have started even though it had not reached its climax, but the effects were significant enough to cause a second burst release for nanoparticles with 2% PEG, 5% PEG and 13% PEG. Elsewhere, the degradation of PEGylated PLGA nanoparticles has been found to start immediately after immersion in release medium [10].

PEGylation therefore controls rifampicin release from PLGA nanoparticle, but its effects are not apparent in the initial stage of release and when polymer matrix swelling and degradation start.

5.3.3 Fitting of drug release data into mathematical models

The influence of PEGylation on the mechanism of rifampicin release from PLGA nanoparticles was examined by fitting drug release data into mathematical models. This was done using a peer-reviewed modelling program called DDSolver [113]. Rifampicin release data was fitted into three semi-empirical mathematical models common in literature, namely: Korsmeyer-Peppas model, Weibull model and Peppas-Sahlin model [72, 90, 117]. The adjusted coefficient of determination (R^2_{adj}) was used as the selection criteria in choosing the model of best fit, where a model with the highest R^2_{adj} value was assigned to be the best fitting model. Adjusted coefficients of determination (R^2_{adj}) enable better comparison of different models than coefficient of determination (R^2) [113].

Rifampicin release data from all samples fitted into the Korsmeyer-Peppas model except 8% PEG nanoparticle whose data best fit the Weibull model and 17% PEG nanoparticles whose release data best fit the Peppas-Sahlin model, as illustrated in **Figure 5.3**.

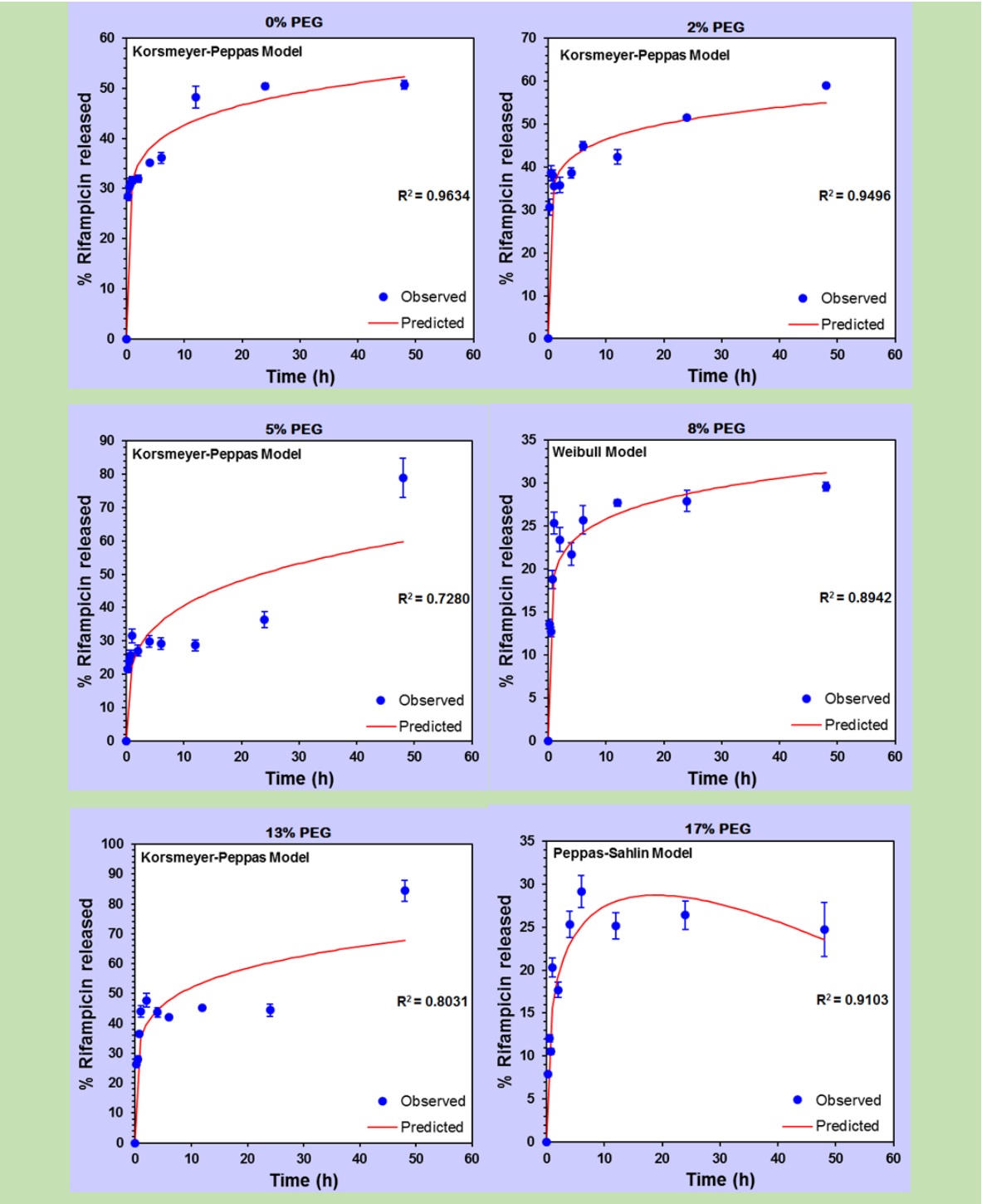

Figure 5.3 *Models of best fit for in vitro release of rifampicin from PLGA nanoparticles of different PEG content at pH 7.4. Observed results are mean ± SD (n=3). The coefficient of determination (R^2) was converted to adjusted coefficient of determination (R^2_{adj}) to allow comparison of different models and selection of the best fitting model.*

All samples had a release exponent (*n*) less than 0.43, in the Korsmeyer-Peppas model (**Table 5.2**). This indicates that the dominant mechanism of drug release was Fickian diffusion. Though data from 17% PEG NPs fit in all models the best fit was

observed in the Peppas-Sahlin model where the constant of Fickian diffusion (k_1 = 19) was greater than the constant of polymer relaxation (k_2 = - 3), which also indicated that for the duration of the study drug release was predominantly via diffusion. The value of ***b*** in Weibull model of nanoparticles with 8% PEG content was < 0.75, therefore also indicating that release was by Fickian diffusion.

Table 5.2 *Parameter values and R^2_{adj} values obtained from fitting drug release experimental data into three mathematical models. The asterisked values correspond to the highest value of R^2_{adj} obtained when the three models were compared, for each sample.*

Nanoparticle formulation	Korsmeyer-Peppas model			Weibull model			Peppas-Sahlin model			
	n	***K***	**R^2 adj**	***a***	***b***	**R^2 adj**	***k_1***	***k_2***	***m***	**R^2 adj**
0% PEG	0.13	32	0.959*	2.6	0.17	0.957	-	-	-	-
2% PEG	0.11	36	0.944*	2.2	0.14	0.939	-	-	-	-
5% PEG	0.25	23	0.698*	3.7	0.29	0.663	-	-	-	-
8% PEG	0.12	19	0.880	4.7	0.14	0.882*	-	-	-	-
13% PEG	0.17	35	0.781*	2.3	0.23	0.765	-	-	-	-
17% PEG	0.16	16	0.759	5.7	0.18	0.766	19	-3	0.38	0.888*

Modelling of drug release data demonstrated the dominant mechanism of rifampicin release for all nanoparticle formulations was by Fickian diffusion of the drug molecules from the nanoparticle core. This finding is in line with findings from a study by Dunne and co-workers, in which the time to reach maximum polymer degradation for PLGA nanoparticles with median size of 500 nm was found to be 59.7 days [146]. Therefore, the duration of drug release studies was too short for complete polymer swelling and degradation to have occurred.

However, the conclusion made by Dunne and co-workers' was based only on PLGA nanoparticles. The effect of PEGylation on the rate of PLGA degradation was not addressed and remains unknown. It is speculated that though polymer degradation had not reached its maximum rate in the time frame of the drug release studies, it

might have started though at insignificant rates to be detected in the mathematical models used.

The quantitative prediction of drug release from PLGA nanoparticles is problematic as the mechanisms of release from these composites are yet to be fully understood [118]. The effect of PLGA degradation to lactic acid and glycolic acid, nanoparticle size and drug solubility amongst other factors, complicate mathematical prediction of drug release from PLGA nanoparticles. The complication is worsened by the presence of PEG. This implies that semi-empirical models are too general and therefore not considered as accurate predictors of drug release behaviour because they overlook the influence of nanoparticle-specific properties on drug release [118]. The relatively low R^2_{adj} values confirm that semi-empirical models were not best suited for predicting the mechanism of rifampicin release from PEGylated PLGA nanoparticles.

5.4 Conclusion

From the results obtained in this section of the study the following conclusions could be drawn:

- PEGylation could be a useful tool to modulate nanoparticle drug release rates.
- Modelling of drug release data revealed a release mechanism dominated by Fickian diffusion, in spite of the differences in nanoparticle PEG content.
- It is proposed at this stage that the hydrated cloud on PEGylated nanoparticles forms a repulsive aqueous barrier that could slow down the exit of rifampicin molecules from the hydrophobic PLGA nanoparticle matrix.
- It is only within the plateau phase of release that a meaningful comparison of the effect of PEGylation on drug release can be made; beyond which the effect of polymer degradation might overshadow the effect of PEGylation.

CHAPTER 6
CONCLUSION

The overall aim of this work was to evaluate the effect of PEG incorporation on PLGA nanoparticle protein binding and drug release. It was hypothesized that the content of PEG on PLGA nanoparticles modulates serum protein binding and rifampicin release. The specific objectives were to synthesize and characterize empty and rifampicin-loaded PLGA nanoparticles with varying PEG content and evaluate their interaction with human serum proteins, as well as rifampicin release kinetics. All the objectives were met.

The presence of PEG enabled nanoparticles to resist protein binding as was seen in the instability of non-PEGylated nanoparticles in human serum and their significant quenching of albumin fluorescence. For PEGylated nanoparticles it was expected that the gradual increase in nanoparticle PEG content could translate to significantly different nanoparticle protein binding behaviour. Unfortunately, this was not the case and on this aspect the hypothesis was disapproved. However, this also implied that the lowest PEG content on those particles that were PEGylated (2% PEG) was sufficient for resistance to protein binding. Therefore, 2% PEG could be the “optimal PEG content” on PLGA nanoparticles, for maximal resistance to protein binding. These findings support our earlier argument on the “optimal PEG content” being NDDS-specific. For example, Gref and co-workers found 5% PEG content to be optimal for maximal protein resistance in PLA nanoparticles [8], but in this study we discovered that 2% PEG is also suitable, for PLGA nanoparticles. The presence of rifampicin in nanoparticles had almost no effect on the physicochemical properties of the studied formulations and as a result there were no significant differences in nanoparticle protein interactions of empty and loaded nanoparticles.

Chapter 5 addressed the other part of the hypothesis which was proved to be correct. PEGylation had an effect on the release kinetics of rifampicin from PLGA nanoparticles. It is speculated that the hydrated cloud formed by PEG on the surface of nanoparticles acts as a repulsive aqueous barrier which slows down the diffusion of rifampicin molecules out of the hydrophobic PLGA nanoparticle core in which the drug and polymer interact through hydrophobic interactions.

The presence of drug molecules on nanoparticle surfaces make it unnecessary to establish the effect of PEGylation on drug release in the early stages of drug release studies. At this stage of the study the effect of the hydrated cloud on the diffusion of drug molecules coming from within the nanoparticle core might not be apparent. This speculation was cemented by the lack of a meaningful trend in the initial burst release stage of drug release studies. It is also speculated that late stages of drug release studies are not ideal for evaluating the effect of PEGylation on polymeric nanoparticle drug release, as this effect might be overshadowed by that of polymer relaxation and degradation. In these late stages, PEGylation seemed to promote drug release, probably because the presence of a hydrated cloud on the surface of PEGylated nanoparticles facilitates the rapid degradation of PLGA by hydrolysis. However, rapid polymer degradation *in vivo* would also be desirable, as it will prevent an accumulation of polymers in cases of multiple NDDS administration [10].

The intermediate stage of the study was characterized by Fickian diffusion of drug molecules from the polymer matrix of the nanoparticle core. At this stage, neither initial burst release nor polymer relaxation and degradation significantly influenced drug release. It is at this stage that the effect of PEGylation can be determined with better accuracy.

Due to limitations highlighted in Chapter 3, we cannot conclude that the differences observed in the nanoparticle-protein interactions and release behaviours of the studied nanoparticle formulations are solely due to the differences in PEG content. However, despite the challenges and limitations of such a study, evaluating the performance of NDDS in relevant biological milieu contributes meaningfully to our understanding and prediction of NDDS *in vivo* behaviour. A holistic understanding of both *in vitro* and *in vivo* performance of NDDS is of paramount importance as NDDS research is now translating into clinical use. Such studies also assist in creation of NDDS libraries that can be used to formulate optimum delivery systems for specific therapeutic goals. For example, in cases wh

ere a certain release behaviour is required the adjustment of PEG content can be used to modulate drug release.

Overall, the results obtained showed that PEGylation stabilizes PLGA nanoparticles and 2% PEG content was sufficient to stabilize PLGA nanoparticles in human serum. Besides showing that PEGylation can modulate the release of rifampicin from PLGA nanoparticles, the other contribution to future work is that: the assessment of the effect of PEGylation in NDDS is best done in the intermediate stages (plateau phase) of drug release. Based on these findings, future studies on PEGylated PLGA nanoparticles could verify if indeed 2% PEG content is the optimal PEG content for maximal resistance to serum protein binding in these NDDS. In addition to verification studies, future work could also assess the *in vivo* performance of the NDDS assessed in this study.

Bibliography

[1] K.K. Jain, Drug delivery systems-an overview, in: K.K. Jain, J.M. Walker (Eds.), Drug delivery systems, Humana Press, New Jersey, 2008, pp.1-50.

[2] D. Bobo, K.J. Robinson, J. Islam, K.J. Thurecht, S.R. Corrie, Nanoparticle-based medicines: a review of FDA-approved materials and clinical trials to date, Pharm. Res. 33 (2016) 2373-2387.

[3] S. Tenzer, D. Docter, J. Kuharev, A. Musyanovych, V. Fetz, R. Hecht, F. Schlenk, D. Fischer, K. Kiouptsi, C. Reinhardt, Rapid formation of plasma protein corona critically affects nanoparticle pathophysiology, Nat. Nanotechnol. 8 (2013) 772-781.

[4] D.E. Owens III, N.A. Peppas, Opsonization, biodistribution, and pharmacokinetics of polymeric nanoparticles, Int. J. Pharm. 307 (2006) 93-102.

[5] A.L. Klibanov, K. Maruyama, V.P. Torchilin, L. Huang, Amphipathic polyethyleneglycols effectively prolong the circulation time of liposomes, FEBS Lett. 268 (1990) 235-237.

[6] M.T. Peracchia, E. Fattal, D. Desmaële, M. Besnard, J.P. Noël, J.M. Gomis, M. Appel, J. d'Angelo, P. Couvreur, Stealth® PEGylated polycyanoacrylate nanoparticles for intravenous administration and splenic targeting, J. Controlled Release 60 (1999) 121-128.

[7] A. Gabizon, H. Shmeeda, Y. Barenholz, Pharmacokinetics of pegylated liposomal doxorubicin, Clin. Pharmacokinet. 42 (2003) 419-436.

[8] R. Gref, M. Lück, P. Quellec, M. Marchand, E. Dellacherie, S. Harnisch, T. Blunk, R.H. Müller, 'Stealth' corona-core nanoparticles surface modified by polyethylene glycol (PEG): influences of the corona (PEG chain length and surface density) and of the core composition on phagocytic uptake and plasma protein adsorption, Colloids Surf. B: Biointerfaces 18 (2000) 301-313.

[9] A.E. Nel, L. Mädler, D. Velegol, T. Xia, E.M.V. Hoek, P. Somasundaran, F. Klaessig, V. Castranova, M. Thompson, Understanding biophysicochemical interactions at the nano–bio interface, Nat. Mater. 8 (2009) 543-557.

[10] K. Avgoustakis, A. Beletsi, Z. Panagi, P. Klepetsanis, A. Karydas, D. Ithakissios, PLGA–mPEG nanoparticles of cisplatin: *in vitro* nanoparticle degradation, *in vitro* drug release and *in vivo* drug residence in blood properties, J. Controlled Release 79 (2002) 123-135.

[11] D. Luo, K.A. Carter, A. Razi, J. Geng, S. Shao, D. Giraldo, U. Sunar, J. Ortega, J.F. Lovell, Doxorubicin encapsulated in stealth liposomes conferred with light-triggered drug release, Biomaterials 75 (2016) 193-202.

[12] International Organization for Standardization, ISO/TS 80004-1:2015(en), Nanotechnologies — Vocabulary — Part 1: Core terms, Available at https://www.iso.org/obp/ui/#iso:std:iso:ts:80004:-1:ed-2:v1:en (17 October 2016).

[13] International Organization for Standardization, ISO/TS 80004-2:2015(en), Nanotechnologies — Vocabulary — Part 2: Nano-objects, Available at https://www.iso.org/obp/ui/#iso:std:iso:ts:80004:-2:ed-1:v1:en (17 October (2016).

[14] HORIBA Scientific, What is a nanoparticle? Available at http://www.horiba.com/scientific/products/particle-characterization/applications/what-is-a-nanoparticle/ (15 October 2016).

[15] European Commission Scientific Committee on Emerging and Newly Identified Health Risks, Scientific Basis for the Definition of the Term “Nanomaterial”, (2010), ISSN 1831-4783 ISBN 978-92-79-12757-1, doi:10.2772/39703 ND-AS-09-004-EN-N.

[16] Malvern, Zetasizer Nano ZS90, Available at http://www.malvern.com/en/products/product-range/zetasizer-range/zetasizer-nano-range/zetasizer-nano-zs90/ (13 May 2016).

[17] M. Elsabahy, G.S. Heo, S. Lim, G. Sun, K.L. Wooley, Polymeric nanostructures for imaging and therapy, Chem. Rev. 115 (2015) 10967-11011.

[18] K. Park, Facing the truth about nanotechnology in drug delivery, ACS Nano 7 (2013) 7442-7447.

[19] W.X. Mai, H. Meng, Mesoporous silica nanoparticles: a multifunctional nano therapeutic system, Integr. Biology 5 (2013) 19-28.

[20] W. Gao, S. Thamphiwatana, P. Angsantikul, L. Zhang, Nanoparticle approaches against bacterial infections, Wires Nanomed. Nanobiotechnol. 6 (2014) 532-547.

[21] C.M. Dawidczyk, C. Kim, J.H. Park, L.M. Russell, K.H. Lee, M.G. Pomper, P.C. Searson, State-of-the-art in design rules for drug delivery platforms: lessons learned from FDA-approved nanomedicines, J. Controlled Release 187 (2014) 133-144.

[22] R. Berges, Eligard®: Pharmacokinetics, Effect on Testosterone and PSA Levels and Tolerability, Eur. Urol. Suppl. 4 (2005) 20-25.

[23] R. Amarnath Praphakar, M.A. Munusamy, K.K. Sadasivuni, M. Rajan, Targeted delivery of rifampicin to tuberculosis-infected macrophages: design, in-vitro, and in-vivo performance of rifampicin-loaded poly(ester amide)s nanocarriers, Int. J. Pharm. 513 (2016) 628-635.

[24] R.A. Jain, The manufacturing techniques of various drug loaded biodegradable poly (lactide-co-glycolide)(PLGA) devices, Biomaterials 21 (2000) 2475-2490.

[25] E. Locatelli, M. Comes Franchini, Biodegradable PLGA- b-PEG polymeric nanoparticles: synthesis, properties, and nanomedical applications as drug delivery system, J. Nanopart. Res. 14 (2012) 1-17.

[26] B. Devrim, A. Kara, İ Vural, A. Bozkır, Lysozyme-loaded lipid-polymer hybrid nanoparticles: Preparation, characterization and colloidal stability evaluation, Drug Dev. Ind. Pharm. (2016) 1-36.

[27] B. Mandal, N.K. Mittal, P. Balabathula, L.A. Thoma, G.C. Wood, Development and *in vitro* evaluation of core–shell type lipid–polymer hybrid nanoparticles for the delivery of erlotinib in non-small cell lung cancer, Eur. J. Pharm. Sci. 81 (2016) 162-171.

[28] R. Gref, Y. Minamitake, Biodegradable long-circulating polymeric nanospheres, Science 263 (1994) 1600.

[29] A. Albanese, P.S. Tang, W.C. Chan, The effect of nanoparticle size, shape, and surface chemistry on biological systems, Annu. Rev. Biomed. Eng. 14 (2012) 1-16.

[30] K. Mohr, M. Sommer, G. Baier, S. Schöttler, P. Okwieka, S. Tenzer, K. Landfester, V. Mailänder, M. Schmidt, R.G. Meyer, Aggregation behavior of polystyrene-nanoparticles in human blood serum and its impact on the *in vivo* distribution in mice, J. Nanomed. Nanotechnol. 5 (2014). doi:10.4172/2157-7439.1000193

[31] J.S. Suk, Q. Xu, N. Kim, J. Hanes, L.M. Ensign, PEGylation as a strategy for improving nanoparticle-based drug and gene delivery, Adv. Drug Deliv. Rev. 99 (2016) 28-51.

[32] D. Vllasaliu, R. Fowler, S. Stolnik, PEGylated nanomedicines: recent progress and remaining concerns, Expert Opin. Drug Deliv. 11 (2014) 139-154.

[33] M. Mahmoudi, I. Lynch, M.R. Ejtehadi, M.P. Monopoli, F.B. Bombelli, S. Laurent, Protein− nanoparticle interactions: opportunities and challenges, Chem. Rev. 111 (2011) 5610-5637.

[34] C. Fornaguera, G. Calderó, M. Mitjans, M.P. Vinardell, C. Solans, C. Vauthier, Interactions of PLGA nanoparticles with blood components: protein adsorption, coagulation, activation of the complement system and hemolysis studies, Nanoscale 7 (2015) 6045-6058.

[35] S.M. Moghimi, A.C. Hunter, J.C. Murray, Long-circulating and target-specific nanoparticles: theory to practice, Pharmacol. Rev. 53 (2001) 283-318.

[36] Z. Xu, Q. Yang, J. Lan, J. Zhang, W. Peng, J. Jin, F. Jiang, Y. Liu, Interactions between carbon nanodots with human serum albumin and γ-globulins: the effects on the transportation function, J. Hazard. Mater. 301 (2016) 242-249.

[37] M.P. Monopoli, C. Åberg, A. Salvati, K.A. Dawson, Biomolecular coronas provide the biological identity of nanosized materials, Nat. Nanotechnol. 7 (2012) 779-786.

[38] S.R. Saptarshi, A. Duschl, A.L. Lopata, Interaction of nanoparticles with proteins: relation to bio-reactivity of the nanoparticle, J. Nanobiotechnol. 11 (2013). doi: 10.1186/1477-3155-11-26

[39] B. Kharazian, N. Hadipour, M. Ejtehadi, Understanding the nanoparticle–protein corona complexes using computational and experimental methods, Int. J. Biochem. Cell Biol. 75 (2016) 162–174.

[40] I. Lynch, K.A. Dawson, Protein-nanoparticle interactions, Nano Today 3 (2008) 40-47.

[41] D. Walczyk, F.B. Bombelli, M.P. Monopoli, I. Lynch, K.A. Dawson, What the cell “sees” in bionanoscience, J. Am. Chem. Soc. 132 (2010) 5761-5768.

[42] C.C. Fleischer, C.K. Payne, Nanoparticle–cell interactions: molecular structure of the protein corona and cellular outcomes, Acc. Chem. Res. 47 (2014) 2651-2659.

[43] T. Cedervall, I. Lynch, S. Lindman, T. Berggard, E. Thulin, H. Nilsson, K.A. Dawson, S. Linse, Understanding the nanoparticle-protein corona using methods to quantify exchange rates and affinities of proteins for nanoparticles, Proc. Natl. Acad. Sci. U. S. A. 104 (2007) 2050-2055.

[44] L. Treuel, S. Brandholt, P. Maffre, S. Wiegele, L. Shang, G.U. Nienhaus, Impact of protein modification on the protein corona on nanoparticles and nanoparticle–cell interactions, ACS Nano 8 (2014) 503-513.

[45] J. Yoo, E. Chambers, S. Mitragotri, Factors that control the circulation time of nanoparticles in blood: challenges, solutions and future prospects, Curr. Pharm. Des. 16 (2010) 2298-2307.

[46] A. Verma, F. Stellacci, Effect of Surface Properties on Nanoparticle?Cell Interactions, Small 6 (2010) 12-21.

[47] S. H. De Paoli Lacerda, J.J. Park, C. Meuse, D. Pristinski, M.L. Becker, A. Karim, J.F. Douglas, Interaction of gold nanoparticles with common human blood proteins, ACS Nano 4 (2009) 365-379.

[48] C. Fang, B. Shi, Y. Pei, M. Hong, J. Wu, H. Chen, *In vivo* tumor targeting of tumor necrosis factor-α-loaded stealth nanoparticles: Effect of MePEG molecular weight and particle size, Eur. J. Pharm. Sci. 27 (2006) 27-36.

[49] A.C. Anselmo, M. Zhang, S. Kumar, D.R. Vogus, S. Menegatti, M.E. Helgeson, S. Mitragotri, Elasticity of nanoparticles influences their blood circulation, phagocytosis, endocytosis, and targeting, ACS Nano 9 (2015) 3169-3177.

[50] J.A. Champion, S. Mitragotri, Role of target geometry in phagocytosis, Proc. Natl. Acad. Sci. U. S. A. 103 (2006) 4930-4934.

[51] A. Arnida, M.M. Janát-Amsbury, A. Ray, C.M. Peterson, H. Ghandehari, Geometry and surface characteristics of gold nanoparticles influence their biodistribution and uptake by macrophages, Eur. J. Pharm. Biopharm. 77 (2011) 417-423.

[52] M.S. Ehrenberg, A.E. Friedman, J.N. Finkelstein, G. Oberdörster, J.L. McGrath, The influence of protein adsorption on nanoparticle association with cultured endothelial cells, Biomaterials 30 (2009) 603-610.

[53] A. Kondo, S. Oku, F. Murakami, K. Higashitani, Conformational changes in protein molecules upon adsorption on ultrafine particles, Colloids Surf. B: Biointerfaces 1 (1993) 197-201.

[54] J. Buijs, C.C. Vera, E. Ayala, E. Steensma, P. Håkansson, S. Oscarsson, Conformational stability of adsorbed insulin studied with mass spectrometry and hydrogen exchange, Anal. Chem. 71 (1999) 3219-3225.

[55] C. Li, S. Wallace, Polymer-drug conjugates: Recent development in clinical oncology, Adv. Drug Deliv. Rev. 60 (2008) 886-898.

[56] K. Knop, R. Hoogenboom, D. Fischer, U.S. Schubert, Poly (ethylene glycol) in drug delivery: pros and cons as well as potential alternatives, Angew. Chem. Int. Ed. 49 (2010) 6288-6308.

[57] A. Abuchowski, T. van Es, N.C. Palczuk, F.F. Davis, Alteration of immunological properties of bovine serum albumin by covalent attachment of polyethylene glycol, J. Biol. Chem. 252 (1977) 3578-3581.

[58] A.S. Hoffman, The early days of PEG and PEGylation (1970s–1990s), Acta Biomater. 40 (2016) 1-5.

[59] Sigma Aldrich, Polyethylene glycol 6000, United States Pharmacopeia (USP) Reference Standard, Available at http://www.sigmaaldrich.com/catalog/product/usp/1546580?lang=en&region=ZA (21 November 2015).

[60] S. Moghimi, J. Szebeni, Stealth liposomes and long circulating nanoparticles: critical issues in pharmacokinetics, opsonization and protein-binding properties, Prog. Lipid Res. 42 (2003) 463-478.

[61] M. Yang, S.K. Lai, Y. Wang, W. Zhong, C. Happe, M. Zhang, J. Fu, J. Hanes, Biodegradable nanoparticles composed entirely of safe materials that rapidly penetrate human mucus, Angew. Chem. Int. Ed. 50 (2011) 2597-2600.

[62] J.M. Chan, L. Zhang, K.P. Yuet, G. Liao, J. Rhee, R. Langer, O.C. Farokhzad, PLGA–lecithin–PEG core–shell nanoparticles for controlled drug delivery, Biomaterials 30 (2009) 1627-1634.

[63] H. Wang, P. Zhao, W. Su, S. Wang, Z. Liao, R. Niu, J. Chang, PLGA/polymeric liposome for targeted drug and gene co-delivery, Biomaterials 31 (2010) 8741-8748.

[64] L.L.I.J. Booysen, L. Kalombo, E. Brooks, R. Hansen, J. Gilliland, V. Gruppo, P. Lungenhofer, B. Semete-Makokotlela, H.S. Swai, A.F. Kotze, A. Lenaerts, L.H. du Plessis, *In vivo*/*in vitro* pharmacokinetic and pharmacodynamic study of spray-dried poly-(dl-lactic-co-glycolic) acid nanoparticles encapsulating rifampicin and isoniazid, Int. J. Pharm. 444 (2013) 10-17.

[65] C.D. Walkey, J.B. Olsen, H. Guo, A. Emili, W.C. Chan, Nanoparticle size and surface chemistry determine serum protein adsorption and macrophage uptake, J. Am. Chem. Soc. 134 (2012) 2139-2147.

[66] S.K. Lai, D.E. O'Hanlon, S. Harrold, S.T. Man, Y.Y. Wang, R. Cone, J. Hanes, Rapid transport of large polymeric nanoparticles in fresh undiluted human mucus, Proc. Natl. Acad. Sci. U. S. A. 104 (2007) 1482-1487.

[67] Y. Wang, S.K. Lai, J.S. Suk, A. Pace, R. Cone, J. Hanes, Addressing the PEG mucoadhesivity paradox to engineer nanoparticles that “slip” through the human mucus barrier, Angew. Chem. Int. Ed. 47 (2008) 9726-9729.

[68] K. Bouchemal, S. Briançon, E. Perrier, H. Fessi, Nano-emulsion formulation using spontaneous emulsification: solvent, oil and surfactant optimisation, Int. J. Pharm. 280 (2004) 241-251.

[69] N. Anton, J. Benoit, P. Saulnier, Design and production of nanoparticles formulated from nano-emulsion templates—a review, J. Controlled Release 128 (2008) 185-199.

[70] A. Beletsi, Z. Panagi, K. Avgoustakis, Biodistribution properties of nanoparticles based on mixtures of PLGA with PLGA–PEG diblock copolymers, Int. J. Pharm. 298 (2005) 233-241.

[71] Q. Xu, L.M. Ensign, N.J. Boylan, A. Schön, X. Gong, J. Yang, N.W. Lamb, S. Cai, T. Yu, E. Freire, Impact of Surface Polyethylene Glycol (PEG) Density on Biodegradable Nanoparticle Transport in Mucus ex vivo and Distribution in vivo, ACS Nano 9 (2015) 9217 - 9227.

[72] I. Khan, A. Gothwal, A.K. Sharma, A. Qayum, S.K. Singh, U. Gupta, Biodegradable nano-architectural PEGylated approach for the improved stability and anticancer efficacy of bendamustine, Int. J. Biol. Macromol. 92 (2016) 1242-1251.

[73] Sigma Aldrich, Poly(ethylene glycol) methyl ether-block-poly(L-lactide-co-glycolide), Available at http://www.sigmaaldrich.com/catalog/product/aldrich/799041?lang=en&region=ZA (21 November 2016).

[74] S. Spek, M. Haeuser, M. Schaefer, K. Langer, Characterisation of PEGylated PLGA nanoparticles comparing the nanoparticle bulk to the particle surface using UV/vis spectroscopy, SEC, ^{1}H NMR spectroscopy, and X-ray photoelectron spectroscopy, Appl. Surf. Sci. 347 (2015) 378-385.

[75] W. Gombotz, W. Guanghui, A. Hoffman, Immobilization of poly (ethylene oxide) on poly (ethylene terephthalate) using a plasma polymerization process, J. Appl. Polym. Sci. 37 (1989) 91-107.

[76] W.R. Gombotz, W. Guanghui, T.A. Horbett, A.S. Hoffman, Protein adsorption to and elution from polyether surfaces, in: J. Milton Harris (Ed.), Poly (Ethylene Glycol) Chemistry, Springer US, New York, 1992, pp. 247-261.

[77] K.P. Antonsen, A.S. Hoffman, Water structure of PEG solutions by differential scanning calorimetry measurements, in: J. Milton Harris (Ed.), Poly (Ethylene Glycol) Chemistry, Springer US, New York, 1992, pp. 15-28.

[78] N. Graham, Poly (ethylene glycol) gels and drug delivery, in: J. Milton Harris (Ed.), Poly (ethylene glycol) Chemistry, Springer US, New York, 1992, pp. 263-281.

[79] P. Harder, M. Grunze, R. Dahint, G. Whitesides, P. Laibinis, Molecular conformation in oligo (ethylene glycol)-terminated self-assembled monolayers on gold and silver surfaces determines their ability to resist protein adsorption, J. Phys. Chem. B 102 (1998) 426-436.

[80] Q. Yang, S.K. Lai, Anti-PEG immunity: emergence, characteristics, and unaddressed questions, Wires Nanomed. Nanobiotechnol. 7 (2015) 655-677.

[81] X. Wang, T. Ishida, H. Kiwada, Anti-PEG IgM elicited by injection of liposomes is involved in the enhanced blood clearance of a subsequent dose of PEGylated liposomes, J. Controlled Release 119 (2007) 236-244.

[82] H. Koide, T. Asai, K. Hatanaka, S. Akai, T. Ishii, E. Kenjo, T. Ishida, H. Kiwada, H. Tsukada, N. Oku, T cell-independent B cell response is responsible for ABC phenomenon induced by repeated injection of PEGylated liposomes, Int. J. Pharm. 392 (2010) 218-223.

[83] K. Shiraishi, K. Kawano, Y. Maitani, T. Aoshi, K.J. Ishii, Y. Sanada, S. Mochizuki, K. Sakurai, M. Yokoyama, Exploring the relationship between anti-PEG IgM behaviors and PEGylated nanoparticles and its significance for accelerated blood clearance, J. Controlled Release 234 (2016) 59-67.

[84] H. Ma, K. Shiraishi, T. Minowa, K. Kawano, M. Yokoyama, Y. Hattori, Y. Maitani, Accelerated blood clearance was not induced for a gadolinium-containing PEG-poly (L-lysine)-based polymeric micelle in mice, Pharm. Res. 27 (2010) 296-302.

[85] S. Prabhu, S. Mutalik, S. Rai, N. Udupa, B.S.S. Rao, PEGylation of superparamagnetic iron oxide nanoparticle for drug delivery applications with decreased toxicity: an *in vivo* study, J. Nanopart. Res. 17 (2015) 1-22.

[86] E.A. Nance, G.F. Woodworth, K.A. Sailor, T.Y. Shih, Q. Xu, G. Swaminathan, D. Xiang, C. Eberhart, J. Hanes, A dense poly(ethylene glycol) coating improves penetration of large polymeric nanoparticles within brain tissue, Sci. Transl. Med. 4 (2012) 149ra119.

[87] J.A. Loureiro, B. Gomes, G. Fricker, M.A.N. Coelho, S. Rocha, M.C. Pereira, Cellular uptake of PLGA nanoparticles targeted with anti-amyloid and anti-transferrin receptor antibodies for Alzheimer's disease treatment, Colloids Surf. B: Biointerfaces 145 (2016) 8-13.

[88] N. Kamaly, Z. Xiao, P.M. Valencia, A.F. Radovic-Moreno, O.C. Farokhzad, Targeted polymeric therapeutic nanoparticles: design, development and clinical translation, Chem. Soc. Rev. 41 (2012) 2971-3010.

[89] J. Hrkach, D. Von Hoff, M. Mukkaram Ali, E. Andrianova, J. Auer, T. Campbell, D. De Witt, M. Figa, M. Figueiredo, A. Horhota, S. Low, K. McDonnell, E. Peeke, B. Retnarajan, A. Sabnis, E. Schnipper, J.J. Song, Y.H. Song, J. Summa, D. Tompsett, G. Troiano, T. Van Geen Hoven, J. Wright, P. LoRusso, P.W. Kantoff, N.H. Bander, C. Sweeney, O.C. Farokhzad, R. Langer, S. Zale, Preclinical development and clinical translation of a PSMA-targeted docetaxel nanoparticle with a differentiated pharmacological profile, Sci. Transl. Med. 4 (2012) 128ra39.

[90] N. Kamaly, B. Yameen, J. Wu, O.C. Farokhzad, Degradable controlled-release polymers and polymeric nanoparticles: Mechanisms of controlling drug release, Chem. Rev. 116 (2016) 2602-2663.

[91] A. Salvati, A.S. Pitek, M.P. Monopoli, K. Prapainop, F.B. Bombelli, D.R. Hristov, P.M. Kelly, C. Åberg, E. Mahon, K.A. Dawson, Transferrin-functionalized nanoparticles lose their targeting capabilities when a biomolecule corona adsorbs on the surface, Nat. Nanotechnol. 8 (2013) 137-143.

[92] W.R. Gombotz, W. Guanghui, T.A. Horbett, A.S. Hoffman, Protein adsorption to poly (ethylene oxide) surfaces, J. Biomed. Mater. Res. 25 (1991) 1547-1562.

[93] K. Beroström, E. Österberg, K. Holmberg, A.S. Hoffman, T.P. Schuman, A. Kozlowski, J.M. Harris, Effects of branching and molecular weight of surface-bound poly (ethylene oxide) on protein rejection, J. Biomater. Sci. Polym. Ed. 6 (1995) 123-132.

[94] N. Silveira, M.M. Longuinho, S.G. Leitão, R.S.F. Silva, M.C. Lourenço, P.E.A. Silva, M.d.C.F.R. Pinto, L.G. Abraçado, P.V. Finotelli, Synthesis and characterization of the antitubercular phenazine lapazine and development of PLGA and PCL nanoparticles for its entrapment, Mat. Sci. Eng. C 58 (2016) 458-466.

[95] P.J. Flory, Principles of polymer chemistry, Cornell University Press, New York,1953.

[96] Y. Liu, Y. Hu, L. Huang, Influence of polyethylene glycol density and surface lipid on pharmacokinetics and biodistribution of lipid-calcium-phosphate nanoparticles, Biomaterials 35 (2014) 3027-3034.

[97] N. Dos Santos, C. Allen, A. Doppen, M. Anantha, K.A. Cox, R.C. Gallagher, G. Karlsson, K. Edwards, G. Kenner, L. Samuels, Influence of poly (ethylene glycol) grafting density and polymer length on liposomes: relating plasma circulation lifetimes to protein binding, Biochim. Biophys. Acta Biomembr. 1768 (2007) 1367-1377.

[98] J.S. Hrkach, M.T. Peracchia, A. Bomb, N. Lotan, R. Langer, Nanotechnology for biomaterials engineering: structural characterization of amphiphilic polymeric nanoparticles by ^{1}H NMR spectroscopy, Biomaterials 18 (1997) 27-30.

[99] S.K. Bharti, R. Roy, Quantitative ^{1}H NMR spectroscopy, Trends Analyt. Chem. 35 (2012) 5-26.

[100] R. Murthy, *In Vitro* Evaluation of NPDDS, in: Y. Pathak, D. Thassu (Eds.), Drug Delivery Nanoparticles Formulation and Characterization, Informa Healthcare USA, Inc. New York, 2009, pp.156-168.

[101] L. Xie, S. Beyer, V. Vogel, M.G. Wacker, W. Mäntele, Assessing the drug release from nanoparticles: Overcoming the shortcomings of dialysis by using novel optical techniques and a mathematical model, Int. J. Pharm. 488 (2015) 108-119.

[102] M.A. Shetab Boushehri, A. Lamprecht, Nanoparticles as drug carriers: current issues with *in vitro* testing, Nanomedicine 10 (2015) 3213-3230.

[103] V. Forest, J. Pourchez, The nanoparticle protein corona: The myth of average, Nano Today (2016). http://dx.doi.org/10.1016/j.nantod.2015.10.007 (in press).

[104] S.P. Boulos, T.A. Davis, J.A. Yang, S.E. Lohse, A.M. Alkilany, L.A. Holland, C.J. Murphy, Nanoparticle–protein interactions: a thermodynamic and kinetic study of the adsorption of bovine serum albumin to gold nanoparticle surfaces, Langmuir 29 (2013) 14984-14996.

[105] V. Mirshafiee, R. Kim, M. Mahmoudi, M.L. Kraft, The importance of selecting a proper biological milieu for protein corona analysis *in vitro*: Human plasma versus human serum, Int. J. Biochem. Cell Biol. 75 (2016) 188-195.

[106] P. Aggarwal, J.B. Hall, C.B. McLeland, M.A. Dobrovolskaia, S.E. McNeil, Nanoparticle interaction with plasma proteins as it relates to particle biodistribution, biocompatibility and therapeutic efficacy, Adv. Drug Deliv. Rev. 61 (2009) 428-437.

[107] C. Salvador-Morales, E. Flahaut, E. Sim, J. Sloan, M.L. H. Green, R.B. Sim, Complement activation and protein adsorption by carbon nanotubes, Mol. Immunol. 43 (2006) 193-201.

[108] S.S. D'Souza, P.P. DeLuca, Methods to assess *in vitro* drug release from injectable polymeric particulate systems, Pharm. Res. 23 (2006) 460-474.

[109] Y. Zambito, E. Pedreschi, G. Di Colo, Is dialysis a reliable method for studying drug release from nanoparticulate systems? - A case study, Int. J. Pharm. 434 (2012) 28-34.

[110] S. Modi, B.D. Anderson, Determination of drug release kinetics from nanoparticles: overcoming pitfalls of the dynamic dialysis method, Mol. Pharm. 10 (2013) 3076-3089.

[111] A. Lamprecht, P. Saulnier, F. Boury, C. Passirani, J. Proust, J. Benoit, A quantitative method for the determination of amphiphilic drug release kinetics from nanoparticles using a Langmuir balance, Anal. Chem. 74 (2002) 3416-3420.

[112] T. Kumeria, K. Gulati, A. Santos, D. Losic, Real-time and in situ drug release monitoring from nanoporous implants under dynamic flow conditions by reflectometric interference spectroscopy, ACS Appl. Mater. Interfaces 5 (2013) 5436-5442.

[113] Y. Zhang, M. Huo, J. Zhou, A. Zou, W. Li, C. Yao, S. Xie, DDSolver: an add-in program for modeling and comparison of drug dissolution profiles, AAPS J. 12 (2010) 263-271.

[114] M. Barzegar-Jalali, K. Adibkia, H. Valizadeh, M.R.S. Shadbad, A. Nokhodchi, Y. Omidi, G. Mohammadi, S.H. Nezhadi, M. Hasan, Kinetic analysis of drug release from nanoparticles, J. Pharm. Pharm. Sci. 11 (2008) 167-177.

[115] L. Zeng, L. An, X. Wu, Modeling drug-carrier interaction in the drug release from nanocarriers, J. Drug Deliv. 2011 (2011) 370308.

[116] Y. Agata, Y. Iwao, A. Miyagishima, S. Itai, Novel mathematical model for predicting the dissolution profile of spherical particles under non-sink conditions, Chem. Pharm. Bull. 58 (2010) 511-515.

[117] P.I. Soares, A.I. Sousa, I.M. Ferreira, C.M. Novo, J.P. Borges, Towards the development of multifunctional chitosan-based iron oxide nanoparticles: Optimization and modelling of doxorubicin release, Carbohydr. Polym. 153 (2016) 212-221.

[118] O.I. Corrigan, X. Li, Quantifying drug release from PLGA nanoparticulates, Eur. J. Pharm. Sci. 37 (2009) 477-485.

[119] E.P.B. George, Science and Statistics, J. Am. Stat. Assoc. 71 (1976) 791-799.

[120] G.E. Box, Robustness in the strategy of scientific model building, in: R.L Launer, G.N Wilkinson (Eds.), Robustness in statistics, Academic Press Inc., London, 1979, pp.201-236.

[121] World Health Organization, Global tuberculosis report 2016, (2016) 1-3.

[122] P. Couvreur, C. Vauthier, Nanotechnology: intelligent design to treat complex disease, Pharm. Res. 23 (2006) 1417-1450.

[123] R. Pandey, Z. Ahmad, Nanomedicine and experimental tuberculosis: facts, flaws, and future, Nanomedicine: NBM 7 (2011) 259-272.

[124] A. Dube, Y. Lemmer, R. Hayeshi, M. Balogun, P. Labuschagne, H. Swai, L. Kalombo, State of the art and future directions in nanomedicine for tuberculosis, Expert Opin. Drug Deliv. 10 (2013) 1725-1734.

[125] S. Xie, Y. Tao, Y. Pan, W. Qu, G. Cheng, L. Huang, D. Chen, X. Wang, Z. Liu, Z. Yuan, Biodegradable nanoparticles for intracellular delivery of antimicrobial agents, J. Controlled Release 187 (2014) 101-117.

[126] P. Vijayaraj Kumar, H. Agashe, T. Dutta, N.K. Jain, PEGylated dendritic architecture for development of a prolonged drug delivery system for an antitubercular drug, Curr. Drug Deliv. 4 (2007) 11-19.

[127] Y. Anisimova, S. Gelperina, C. Peloquin, L. Heifets, Nanoparticles as antituberculosis drugs carriers: effect on activity against Mycobacterium tuberculosis in human monocyte-derived macrophages, J. Nanopart. Res. 2 (2000) 165-171.

[128] R. Pandey, G.K. Khuller, Solid lipid particle-based inhalable sustained drug delivery system against experimental tuberculosis, Tuberculosis 85 (2005) 227-234.

[129] W. Mehnert, K. Mäder, Solid lipid nanoparticles: Production, characterization and applications, Adv. Drug Deliv. Rev. 47 (2001) 165-196.

[130] H. Kaur, V. Kumar, K. Kumar, S. Rathor, P. Kumari, J. Singh, Polymer particulates in drug delivery, Curr. Pharm. Des. 22 (2016) 2761-2787.

[131] H. Swai, B. Semete, L. Kalombo, P. Chelule, Potential of treating tuberculosis with a polymeric nano-drug delivery system, J. Controlled Release 132 (2008) e48.

[132] A. Dube, J.L. Reynolds, W. Law, C.C. Maponga, P.N. Prasad, G.D. Morse, Multimodal nanoparticles that provide immunomodulation and intracellular drug delivery for infectious diseases, Nanomedicine: NBM 10 (2014) 831-838.

[133] M. Tukulula, R. Hayeshi, P. Fonteh, D. Meyer, A. Ndamase, M.T. Madziva, V. Khumalo, P. Lubuschagne, B. Naicker, H. Swai, Curdlan-Conjugated PLGA Nanoparticles Possess Macrophage Stimulant Activity and Drug Delivery Capabilities, Pharm. Res. (2015) 1-14.

[134] H. Xie, K.L. Gill-Sharp, D.P. O'Neal, Quantitative estimation of gold nanoshell concentrations in whole blood using dynamic light scattering, Nanomedicine: NBM 3 (2007) 89-94.

[135] Z. Yu, G. Kastenmüller, Y. He, P. Belcredi, G. Möller, C. Prehn, J. Mendes, S. Wahl, W. Roemisch-Margl, U. Ceglarek, Differences between human plasma and serum metabolite profiles, PloS one 6 (2011) e21230.

[136] Laerd Statistics, One-way ANOVA - How to report the significance, Lund Research Ltd (2013), Available at https://statistics.laerd.com/statistical-guides/one-way-anova-statistical-guide 4.php (24 February 2016).

[137] R. Pandey, A. Zahoor, S. Sharma, G. Khuller, Nanoparticle encapsulated antitubercular drugs as a potential oral drug delivery system against murine tuberculosis, Tuberculosis 83 (2003) 373-378.

[138] M. Kale, P. Suruse, R. Singh, G. Malhotra, P. Raut, Effect of size reduction techniques on doxorubicin hydrochloride loaded liposomes, Int J Biol Pharm Res 3 (2012) 308-316.

[139] B. Sabeti, M.I. Noordin, S. Mohd, R. Hashim, A. Dahlan, H.A. Javar, Development and characterization of liposomal doxorubicin hydrochloride with palm oil, Biomed. Res. Int. 2014 (2014) 765426.

[140] M. Zambaux, F. Bonneaux, R. Gref, E. Dellacherie, C. Vigneron, MPEO-PLA nanoparticles: Effect of MPEO content on some of their surface properties, J. Biomed. Mater. Res. 44 (1999) 109-115.

[141] British Pharmacopoeia Commission, British Pharmacopoeia 2015, (2014).

[142] G.A. Shabir, Step-by-step analytical methods validation and protocol in the quality system compliance industry, JVT 10 (2005) 314-325.

[143] B.A. Aguilar-Castillo, J.L. Santos, H. Luo, Y.E. Aguirre-Chagala, T. Palacios-Hernández, M. Herrera-Alonso, Nanoparticle stability in biologically relevant media: influence of polymer architecture, Soft matter 11 (2015) 7296-7307.

[144] D. Dell'Orco, M. Lundqvist, C. Oslakovic, T. Cedervall, S. Linse, Modeling the time evolution of the nanoparticle-protein corona in a body fluid, PloS one 5 (2010) e10949.

[145] M. Mahmoudi, M.A. Shokrgozar, S. Sardari, M.K. Moghadam, H. Vali, S. Laurent, P. Stroeve, Irreversible changes in protein conformation due to interaction with superparamagnetic iron oxide nanoparticles, Nanoscale 3 (2011) 1127-1138.

[146] M. Dunne, O. Corrigan, Z. Ramtoola, Influence of particle size and dissolution conditions on the degradation properties of polylactide-co-glycolide particles, Biomaterials 21 (2000) 1659-1668.

[147] S.N. Rothstein, W.J. Federspiel, S.R. Little, A simple model framework for the prediction of controlled release from bulk eroding polymer matrices, J. Mater. Chem. 18 (2008) 1873-1880.

[148] R.P. Batycky, J. Hanes, R. Langer, D.A. Edwards, A theoretical model of erosion and macromolecular drug release from biodegrading microspheres, J. Pharm. Sci. 86 (1997) 1464-1477.

Appendices

Appendix 1: Proton NMR spectra of empty PEGylated PLGA nanoparticles

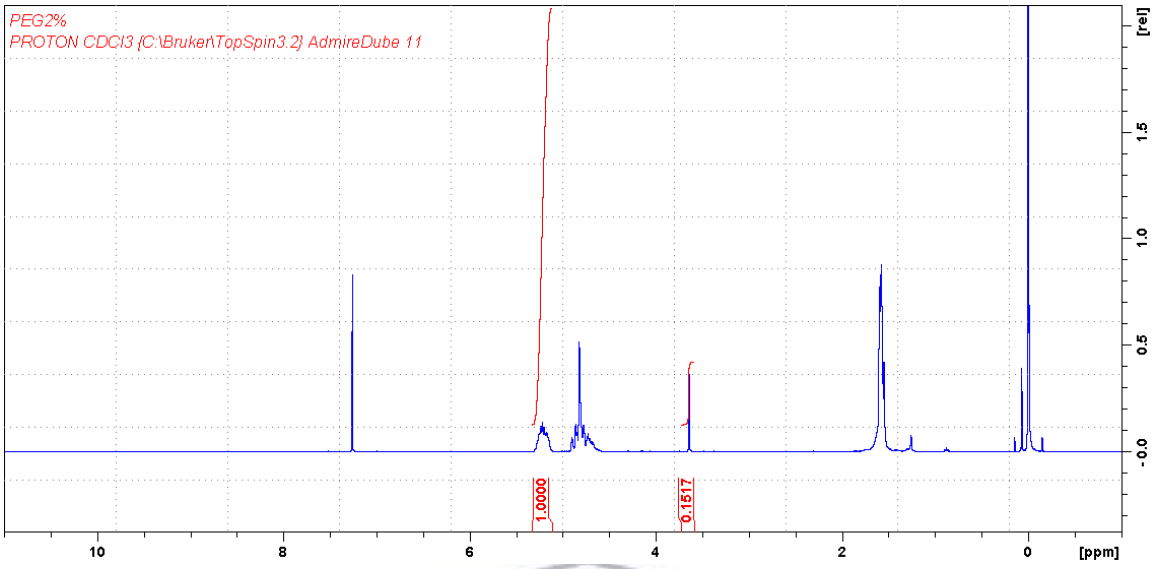

Figure A1.1 *H^1 NMR spectrum of PLGA nanoparticles with PEG content of 2% (w/w)*

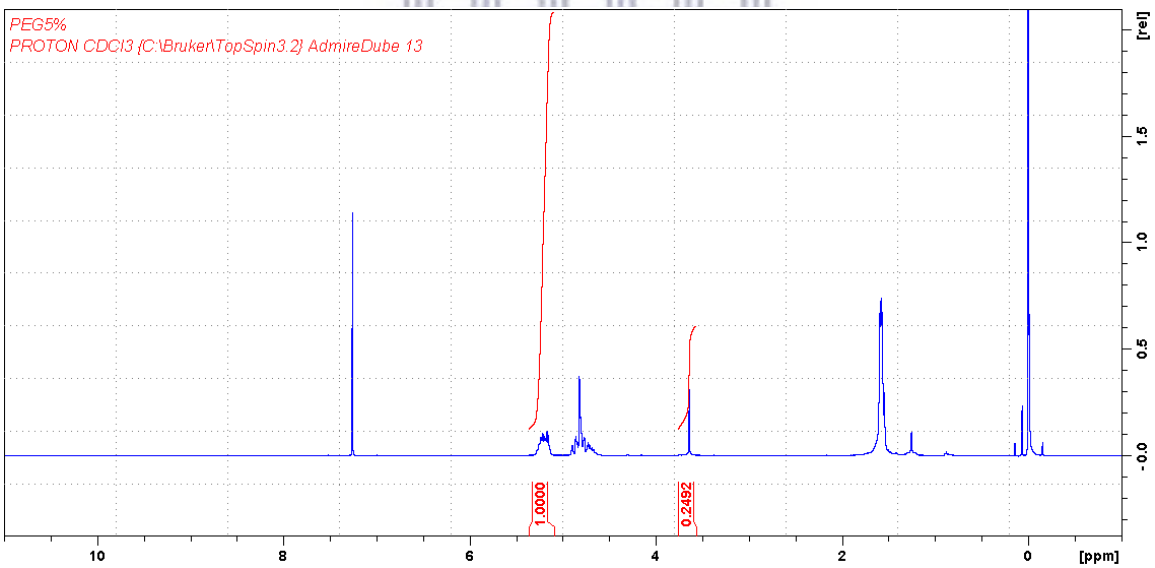

Figure A1.2 *H^1 NMR spectrum of PLGA nanoparticles with PEG content of 5% (w/w)*

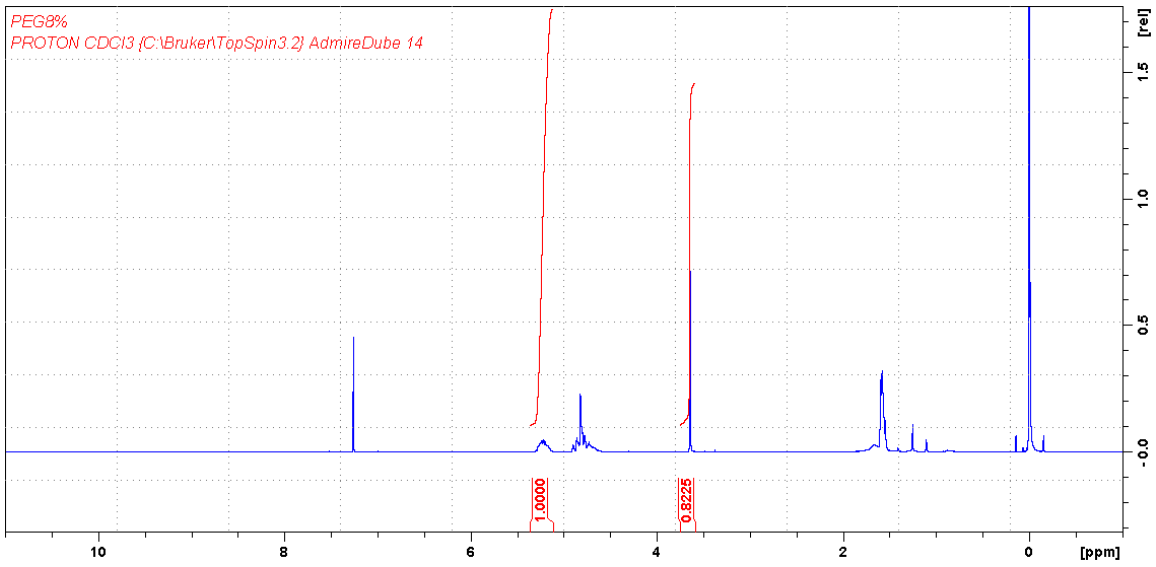

Figure A1.3 *H^1 NMR spectrum of PLGA nanoparticles with PEG content of 8% (w/w)*

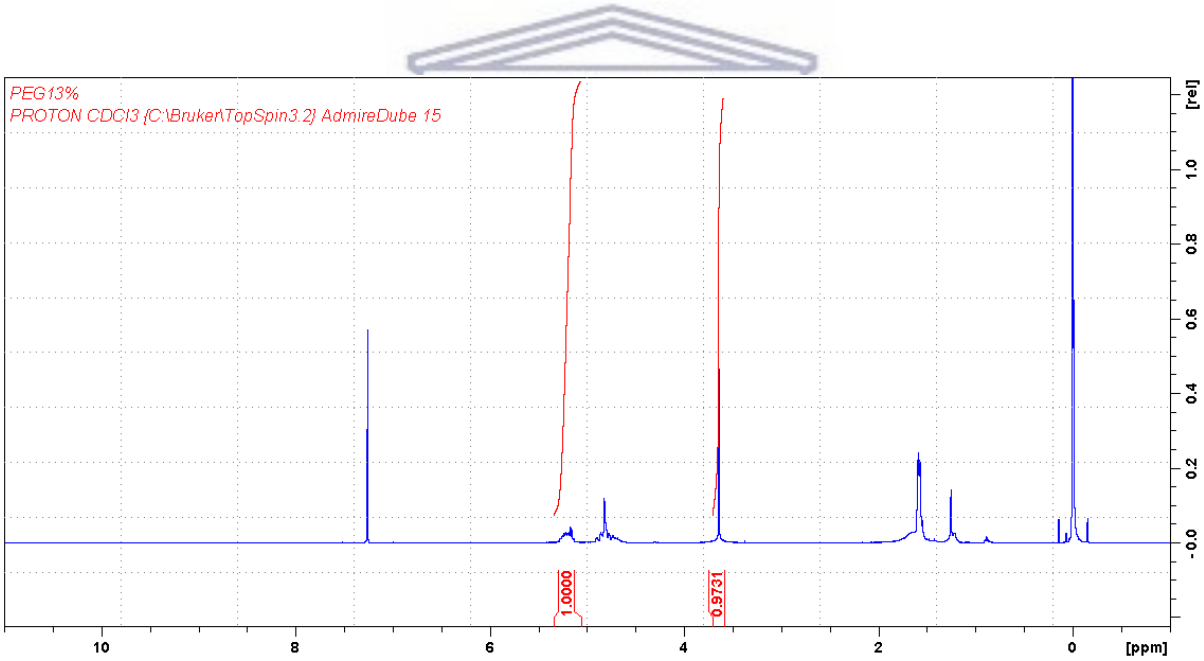

Figure A1.4 *H^1 NMR spectrum of PLGA nanoparticles with PEG content of 13% (w/w)*

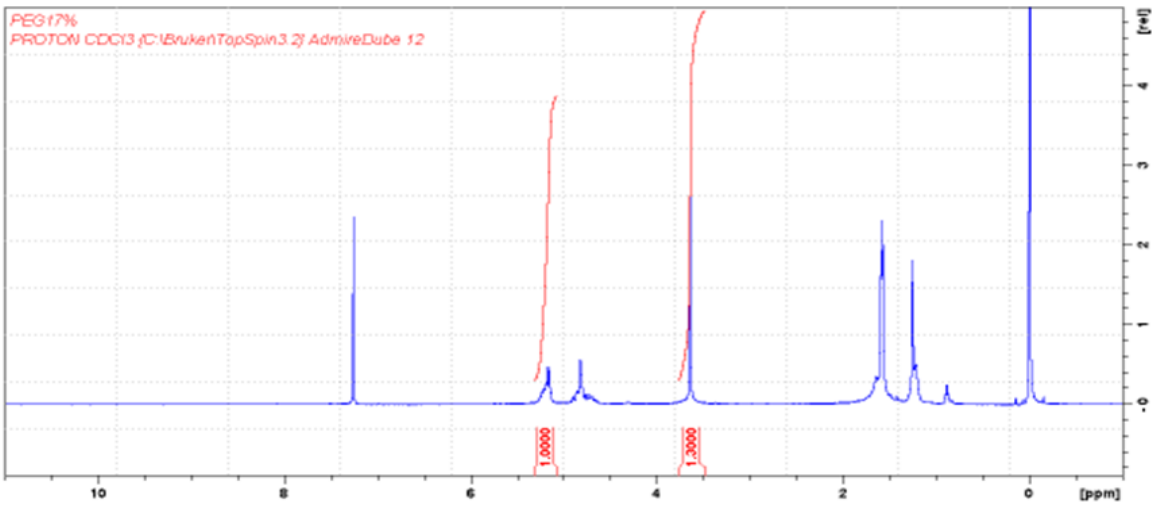

Figure A1.5 *H^1 NMR spectrum of PLGA nanoparticles with PEG content of 17% (w/w)*

Appendix 2: Validation data of UV-VIS assay method for rifampicin in chloroform

Table A2.1 *Concentration versus absorbance of rifampicin at 475 nm*

Concentration (µg/ml)	Mean Absorbance (n = 3)	%RSD
0	0.0002	0
1	0.0193	5.2
2	0.0428	6.3
5	0.0878	8.5
10	0.1718	5.9
20	0.3777	5.3
40	0.7222	4.6

Table A2.2 *Intra-day variations of UV-VIS method for determination of rifampicin*

Concentration (µg/ml)	Mean Absorbance (n = 3)	%RSD	Mean Determined Concentration (µg/ml)
1	0.0189	2.945906	0.98257
10	0.1731333	0.61217	9.489649
40	0.7275667	1.263393	40.07064

Table A2.3 *Inter-day variations of UV-VIS method for determination of rifampicin*

Concentration (µg/ml)	Mean Absorbance (n = 3)	%RSD	Mean Determined Concentration (µg/ml)	% Recovery
1	0.0177	8.82	0.91822	91.82
10	0.1745	1.66	9.563192	95.63
40	0.7609	4.28	41.90921	104.77

Appendix 3: Validation of data of UV-VIS assay method for rifampicin in PBS pH 7.4 spiked with ascorbic acid

Table A3.1 *Concentration versus absorbance of rifampicin in PBS (pH 7.4) at 475 nm*

Concentration (µg/ml)	Mean Absorbance (n = 3)	%RSD
0.1	0.0025	2.34
0.25	0.0059	0.97
0.5	0.0101	0.00
1	0.0187	0.54
2.5	0.0470	0.33
5	0.0941	0.22
10	0.1996	0.05
25	0.4969	0.07

Table A3.2 *Intra-day variations of UV-VIS method for determination of rifampicin*

Concentration (µg/ml)	Mean Absorbance (n = 3)	%RSD	Mean Determined Concentration (µg/ml)
1	0.019	3.19	1.01
10	0.201	1.60	10.17
25	0.492	0.96	24.76

Table A3.3 *Inter-day variations of UV-VIS method for determination of rifampicin*

Concentration (µg/ml)	Mean Absorbance (n = 3)	%RSD	Mean Determined Concentration (µg/ml)	% Recovery
1	0.021	4.79	1.09	109.07
10	0.209	3.92	10.53	105.31
25	0.508	0.85	25.56	102.25